Neurophysiology of the Subthalamic Nucleus

Jeremy Francis Atherton

A thesis submitted for the degree of Ph.D.

The University of Edinburgh

January 2001

For

Stuart Gambles

1975 - 2000

Declaration

I have composed this thesis myself and it reports original research that has been conducted by myself unless otherwise acknowledged in the text.

The work described in chapter 6 from page 129 to page 141 was carried out by A.K. Wright and K.E. McLaughlin. However, the experiments were conceived and designed under my supervision.

Edinburgh, 29 January 2001

Jeremy Atherton

Acknowledgements

I would like to thank the following people for their help and guidance during the course of my Ph.D. studies.

My supervisor Professor Gordon Arbuthnott. He has always been there to answer questions or discuss ideas. His knowledge of, and enthusiasm for science has been a continual source of inspiration which has kept me going through the days when it seemed like the experiments might never work.

My assistant supervisor Professor David Willshaw, who has provided valuable support at many key points throughout my project.

The amount of help that Dr. Andrew Gillies has been willing to provide has never ceased to amaze me. Without his initial work this project would never have been possible. He is able to explain his models in a way that a neuroscientist can understand and is tolerant of all the silly questions that I ask.

Ann Wright has generously passed on many of her technical skills to me, teaching me surgical and histological techniques. She has put up with me in the lab when many others wouldn't have and has always been willing to lend a helping hand.

I would like to thank the other (past and present) members of Professor Arbuthnott and Dr Ingham's research group for their help, friendship, and support. In particular Dr. Cali Ingham, Linda Norrie, Dr. Andrew Shering, Pat Taggart, Sue Hood, Sankari Ramanathan and Ben Stephens. I would also like to thank the technical staff of the Department of Preclinical Veterinary Sciences many of whom have provided me with valuable technical support.

This project was backed by the financial support of the Medical Research Council who I would particularly like to thank for providing me with an extra three months of support at the end of my project.

Finally, I would like to thank my wife, Jan.

Contents

List of Figures

Abstract

Possibly as many as half the neurones in the STN have axon collaterals that branch off from the main axon and re-innervate the nucleus. This suggests that rather than working autonomously as was previously thought, the neurones of the STN can operate together as a network. Computer models of the STN showed that the level of interconnectivity within the STN would be huge, even if each axon collateral only contacted a small number of the total neurones with dendritic fields that overlapped with it. A network model showed that such a system was capable of switch-like behaviour. At low levels of activity the neurones would act autonomously. However, excitatory inputs could increase the degree of non-synchronous correlation between the activity of neurones in the STN leading them all to enter a high activity state. A single cell model was then developed in order to look at how this high activity state could be terminated. An interesting problem arose in the construction of this model; no known kinetics for the voltage-gated sodium and potassium channels could replicate the high frequency (500Hz) firing rates that are obtained by STN neurones.

Intracellular recordings were made *in vitro* to investigate the mechanisms underlying high-frequency firing in the STN. Using a two-pulse protocol the speed of recovery from inactivation was measured giving an estimate of the inactivation characteristics of the ion channels in these neurones. These experiments showed that the neurones have very slow inactivation kinetics suggesting that STN neurones may have a much shortened refractory period, enabling high frequency firing. Such a mode of operation requires a large, fast potassium current. A potential candidate for this current is the Kv3.1 potassium channel, which is strongly expressed by STN neurones.

Extracellular recordings were used to look for evidence of functional interconnections between cells within the STN. These experiments showed that blocking any interconnections with a glutamatergic antagonist had no effect on the resting firing pattern or rate of STN neurones. However, when the neurones were depolarised using increased levels of potassium in the perfusing solution, the normally regular firing pattern of the neurones was disrupted and became irregular. The glutamatergic antagonist attenuated this disruption showing that it was at least partially mediated through glutamatergic synapses, the best candidate for which are those at the interconnections between the STN neurones.

Having investigated high frequency firing in the STN, and how such increased levels of activity could influence co-ordinated firing within the STN, the effects of one of the STNs targets was assessed. Lesions of the globus pallidus have been shown to create a chronic increase in the levels of STN activity *in vivo*. At three and six weeks after such lesions a marked reduction was found in the number of neurones in the substantia nigra that stained positive for tyrosine hydroxylase (marking them as dopaminergic cells). These data provide evidence supporting the excitotoxic hypothesis for the progressive loss of dopaminergic cells that is seen in Parkinson's Disease.

1 Introduction

The basal ganglia are a network of subcortical nuclei that have long been associated with the control of movement. Amongst these nuclei, the *subthalamic nucleus* (STN) is the only one to contain excitatory, glutamate-containing neurones. In the past the STN had been regarded as a relay, or accessory nucleus, passively passing information along the, so-called, indirect pathway through the basal ganglia (Albin *et al.*, 1989). In recent years it has been recognised that the STN plays a more important role, particularly in many of the disorders that are associated with basal ganglia dysfunction (Chesselet & Delfs, 1996). Because of this an increasing body of research has been aimed at discovering the true role of the STN.

Up to 50% of STN neurones have axon collaterals, which branch off from their main axon and terminate within the nucleus itself (Kita & Kitai, 1987). Should these intranuclear axon collaterals make functional interconnections between the neurones in the STN, they could form a large positive feedback system. Geometric computer modelling, using data relating to the size of the dendritic fields of STN neurones and the length of their axon collaterals, revealed the potential for a single neurone to make contacts with up to a quarter of the other neurones in the STN. Subsequent modelling of the electrophysiological properties of these neurones revealed that such interconnectivity could lead to the development of switch-like behaviour within the nucleus (Gillies & Willshaw, 1998b). Under the right conditions the neurones could exist in two states; either all would be firing action potentials at their resting rate or all at their maximum rate. The predictions of these modelling experiments have

important implications for our understanding of the role of the STN within the basal ganglia.

Further computer modelling experiments have revealed that this switch-like property of the STN has implications for the way in which it interacts with the *globus pallidus* (GP; *external segment of the globus pallidus* (GPe) in primates). These two nuclei are reciprocally connected to each other (Smith *et al.*, 1998) and, under certain conditions, oscillations may form between them (Gillies & Willshaw, 1998a; Plenz & Kitai, 1999; Magill *et al.*, 2000). It is thought that these oscillations may be an important factor in the genesis of the symptoms of *Parkinson's Disease* (PD). Neurones of the STN in the PD brain have been shown to have a faster resting firing rate and to have a more irregular or even bursty firing pattern (Rodriguez *et al.*, 1998a; Magnin *et al.*, 2000). Surgical interventions aimed at suppressing altered firing patterns in the GP and STN have proven relatively successful in alleviating some of the symptoms of PD (Bergman *et al.*, 1990). This oscillatory behaviour can only emerge in the computer model if there are functional interconnections between the neurones of the STN, further implicating the STN in the pathophysiology of PD. Thus, determining if the neurones do indeed make functional connections with each other would represent an important step towards understanding the STN and its role within the genesis of disorders of the basal ganglia.

The high frequency firing of STN neurones that could occur in these pathological states has been suggested to be a contributing factor in the aetiology of PD (Rodriguez *et al.*, 1998b). These neurones send excitatory projections to the

substantia nigra pars compacta (SNc) (Chergui *et al.*, 1994; Benazzouz *et al.*, 2000). This nucleus is the source of the dopaminergic neurones of the nigrostriatal pathway, which degenerate in PD patients. The excitatory nature of the STN projection to these neurones leads to the possibility that some of the cell death in the SNc could be mediated through an excitotoxic mechanism due to the hyperactivity of the STN neurones (Rodriguez *et al.*, 1998b). This implicates the STN not just in the genesis of the symptoms of the PD but also in its progression, and as a potential primary cause of the disease.

1.1 Overview of the Thesis

The research presented in this thesis takes the form of a conversation between 'wet' experimental research and the theoretical computer modelling. Some of the assumptions and conclusions of the earlier models are tested in an *in vitro* slice preparation. The data gained from these experiments is then used to provide feedback to the models in order to develop them further. The conclusions reached from these new models are then used in the design of further experiments. Chapters 2 reviews the current state of basal ganglia research whilst chapter 3 looks at the role that models can play in this research. The experiments described in chapter 4 were an attempt to discover the processes underlying the fast firing of STN neurones. Chapter 5 details an experiment aimed at discovering if there are functional interconnections between the neurones of the STN. Chapter 6 looks at the implications of this research for clinical research into the aetiology of PD. Finally, in Chapter 7, the results from all of this research are summarised and some conclusions drawn.

Table 1.1 A List of Abbreviations

6-OHDA	-	6-hydroxydopamine
aCSF	-	artificial cerebrospinal fluid
AMPA	-	α-amino-3-hydroxy-5-methyl-3-isoxazolepropionate
Ca(T)Ch	-	low voltage activated calcium T channel
ChAT	-	choline acetyl transferase
CNQX	-	6-cyano-7-nitroquinoxaline-2,3-dione
CV	-	coefficient of variation
DAB	-	3,3' diaminobenzodine substrate
DOPA	-	dihydroxyphenylalanine
EP	-	entopeduncular nucleus
GABA	-	γ-amino butyric acid
GFAP	-	glial fibrillary acidic protein
GP	-	globus pallidus
GPe	-	external segment of the globus pallidus
HRP	-	horseradish peroxidase
HVA	-	high voltage activated
ISI	-	interspike interval
K(Ca)Ch	-	calcium activated potassium channel
KCh	-	voltage-gated potassium channel
LVA	-	low voltage activated

MSN - medium sized densely spiny neurone

MEA - midbrain extrapyramidal area

Nacc - Nucleus Accumbens

NaCh - voltage-gated sodium channel

NMDA - *N*-methyl-*D*-aspartate

PBS - sodium phosphate buffered saline

PBS-TX - PBS containing 0.3% Triton-X100

PD - Parkinson's Disease

PPN - pedunculopontine tegmental nucleus

PHA-L - *phaseolus vulgaris*-leucoagglutinin

SN - substantia nigra

SNc - substantia nigra pars compacta

SNr - substantia nigra pars reticulata

STN - subthalamic nucleus

TH - tyrosine hydroxylase

TH+ve - tyrosine hydroxylase immunopositive

TTB - time to block

VP - ventral pallidum

WGA-HRP - horseradish peroxidase conjugated with wheatgerm agglutini

2 The Basal Ganglia

'*Basal ganglia*' is the collective name used to describe a closely interconnected group of subcortical nuclei that are thought to operate as a single system. Classically these are the *striatum* (caudate nucleus and putamen in primates), the GP and the *entopeduncular nucleus* (EP). The *substantia nigra* (SN) and STN have been included more recently, as they have also been found to have roles in the functioning of the basal ganglia. Figure 2.1 shows the anatomical locations these nuclei in a parasagittal section of the rat brain.

2.1 Neurobiology of the Basal Ganglia

2.1.1 GABAeric Nuclei

2.1.1.1 The Striatum

The majority (96%; Kemp and Powell (1971)) of neurones in the striatum are *Medium Sized Densely Spiny Neurones* (MSN). These neurones use GABA (γ-amino butyric acid) as their primary neurotransmitter (Graybiel, 1990). Their dendrites are densely covered in spines and receive inputs from the cortex, SNc (Hauber & Fuchs, 2000), other MSNs, and some thalamic nuclei. They also receive inputs from the other neurones in the striatum, these are mainly cholinergic or GABAergic interneurones. The MSNs can be subdivided into two groups by the

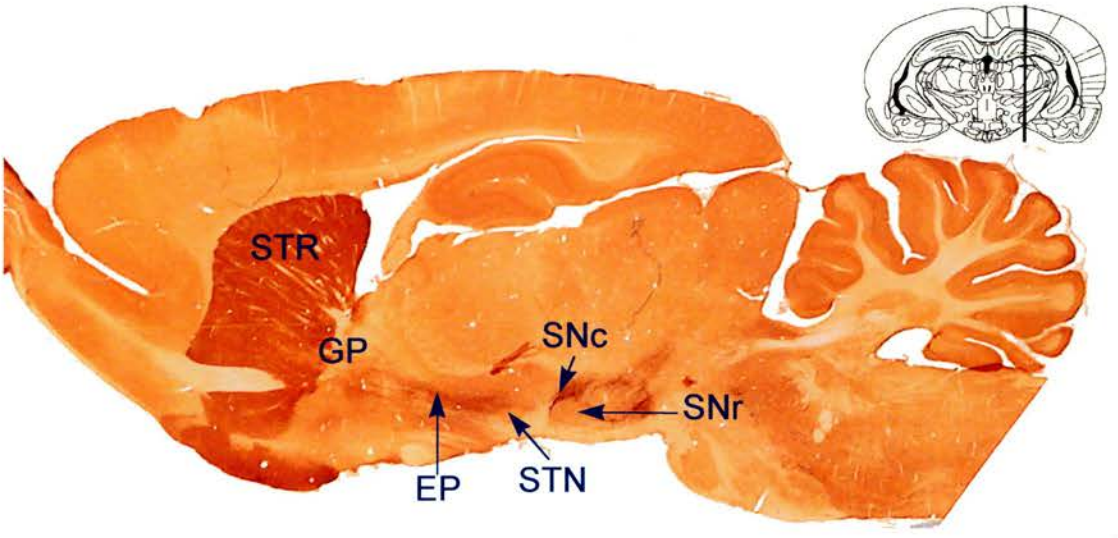

Figure 2.1 The anatomical locations of the main nuclei of the basal ganglia in the rat brain. The photomicrograph shows a sagittal section of the rat brain stained with an antibody raised against tyrosine hydroxylase. The anatomical location of the main nuclei of the basal ganglia are marked. The coronal section shows the plane in which the sagittal section was cut. EP = entopeduncular nucleus; GP = globus pallidus; SNc = substantia nigra pars compacta; SNr = substantia nigra pars reticulata; STN = subthalamic nucleus; STR = striatum.

neurotransmitters that they use as co-transmitters with GABA (Graybiel, 1990). One group uses dynorphin and substance P. These neurones send projections to the substantia nigra pars reticulata (SNr) and EP (Smith *et al.*, 1998). The other group contains enkephalin and sends projections to the GP (Smith *et al.*, 1998).

2.1.1.2 The Globus Pallidus

The GABAergic neurones of the GP receive their main inputs from the striatum (Parent & Hazrati, 1995) and the STN (Canteras *et al.*, 1990), although there is also evidence of inputs from the cortex and from some thalamic nuclei (Mouroux *et al.*, 1997). They send projections to the STN, EP, SNr, and reticular thalamic nucleus (Parent & Hazrati, 1995). The neuronal population of the GP is heterogeneous with evidence for at least three different types of cell (Cooper & Stanford, 2000).

2.1.1.3 The Entopeduncular Nucleus

Neurones in the EP receive inputs from the striatum, GP and STN (Albin *et al.*, 1989). They are GABAergic and send projections to the thalamus (Bevan *et al.*, 1994), and *pedunculopontine nucleus* (PPN) (Jackson & Crossman, 1983).

2.1.1.4 The Substantia Nigra

The substantia nigra is divided into two parts; SNr and SNc (Paxinos & Watson, 1986). The SNr contains mostly GABAergic neurones that receive inputs from and

send projections to the same nuclei as the EP (Albin *et al.*, 1989). The SNc contains mostly dopaminergic neurones that project to the striatum along the nigrostriatal pathway. These neurones receive inputs from the SNr (GABA), GP (GABA) (Celada *et al.*, 1999), STN (glutamate) (Chergui *et al.*, 1994), PPN (acetyl choline and glutamate) (Scarnati *et al.*, 1986; Bolam *et al.*, 1991; Di Loreto *et al.*, 1992; Futami *et al.*, 1995).

2.1.2 The Subthalamic Nucleus

In 1865 Luys described a 'band of grey matter that is an accessory to the thalamus, swollen in the middle and tapered at the edges' (Luys (1865); authors translation). This *corpus Luysi* has more recently become known as the STN. Cajal (1911) provided a more detailed description of the mouse STN. In this he described an ovoid or lens-shaped group of cells, rostral to the substantia nigra, which had a similar morphology across many species of mammal. In Nissl-stained sections he saw abundant fusiform to polygonal, medium-sized neurones. With Golgi stained sections, Cajal saw that these neurones were embedded in a dense axonal plexus that he described as:

"...one of the richest and densest axonal plexuses in the diencephalon."

This axonal plexus was formed mainly of collaterals arising at right angles from the peduncular fibres ventral to the nucleus. Cajal suggested that the nucleus receives from two afferent pathways: One pathway formed by collaterals of fibres in the

internal capsule that originate in the cerebral cortex and another arising in the striatum. He thought that efferent fibres emerged from the STN and projected along only one pathway to the motor nuclei of the brainstem and spinal cord.

Afsharpour (1985) provides us with a more contemporary description of the morphology of STN neurones. Using the Golgi staining technique to visualise the morphology of individual cells, he described the STN as a disk-shaped nucleus lying obliquely on the dorsomedial surface of the cerebral peduncle. Many of the dendrites of the STN neurones crossed into the cerebral peduncle and there were also cells, similar to STN neurones, embedded there. The STN neurones were found to have two to six primary dendrites (most had three or four) which varied from 140 to 440 μm in length. Afsharpour felt, on the basis of morphology, that the neurones fell into two groups. The largest group, neurones with a bipolar dendritic tree, had one of the primary dendrites emerging from the midsection of the cell body with the remaining dendrites emerging from opposite poles of the cell. There was however another group, these neurones had radiating dendrites that emerged from all over the cell body without displaying any specific polar orientation. Figure 2.2 shows examples of neurones that exemplify these two different morphologies.

Kita *et al.* (1983b) also made a division of the STN neurones into two populations based on their morphology. They distinguished the two populations by looking at axonal morphology and dendritic branching. Approximately 50% of the neurones had axons that had collateral branches, which terminated within the nucleus itself. Figure 2.3 shows an example of such a neurone with three axon collaterals. These

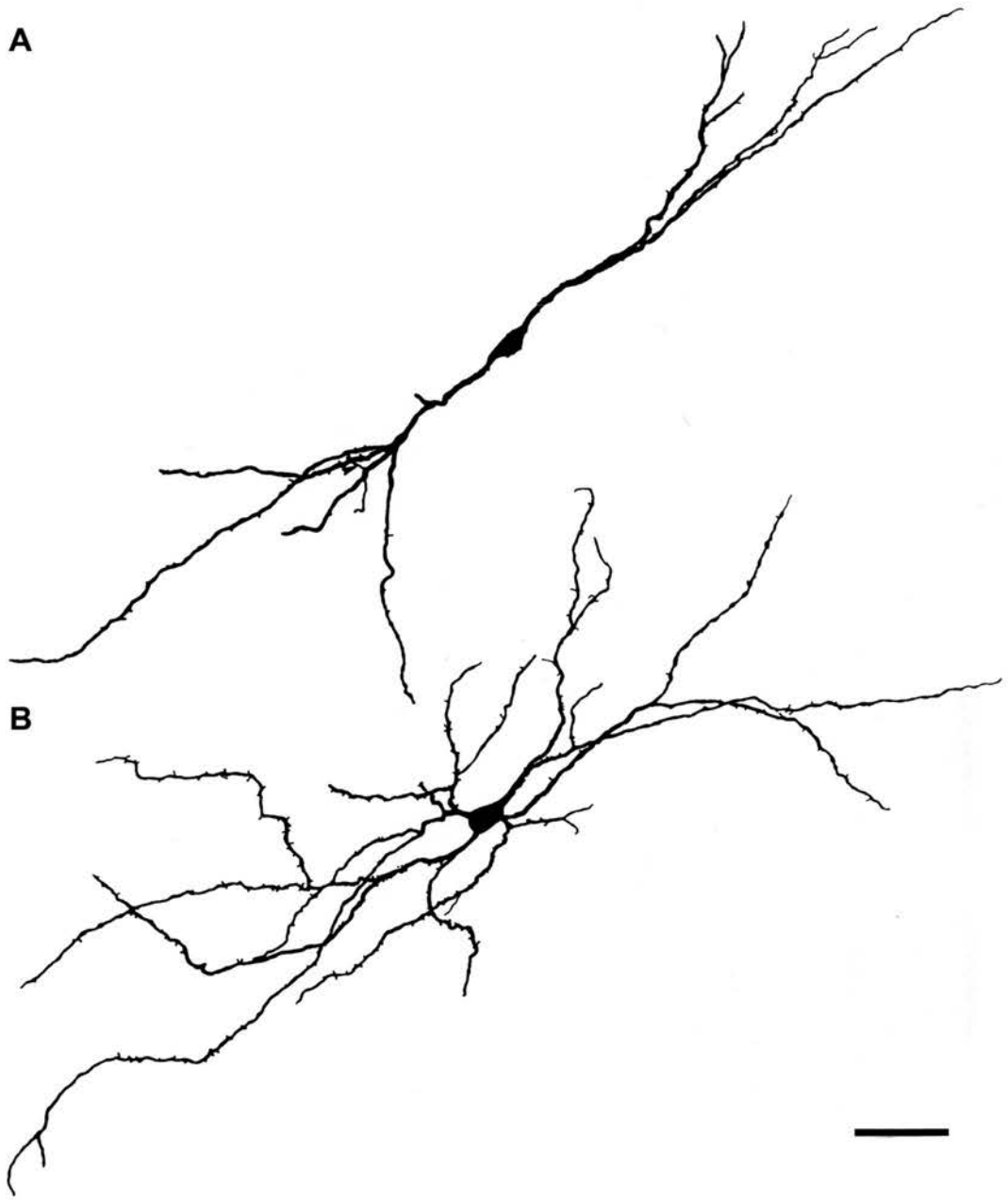

Figure 2.2 The morphology of Golgi stained neurones in the rat subthalamic nucleus. **A** shows a bipolar neurone with dendrites emerging from either end of the soma. **B** shows a neurone with radiating dendrites emerging from the cell body without displaying any polarity. The scale bar represents 50 μm. Adapted from Afsharpour (1985).

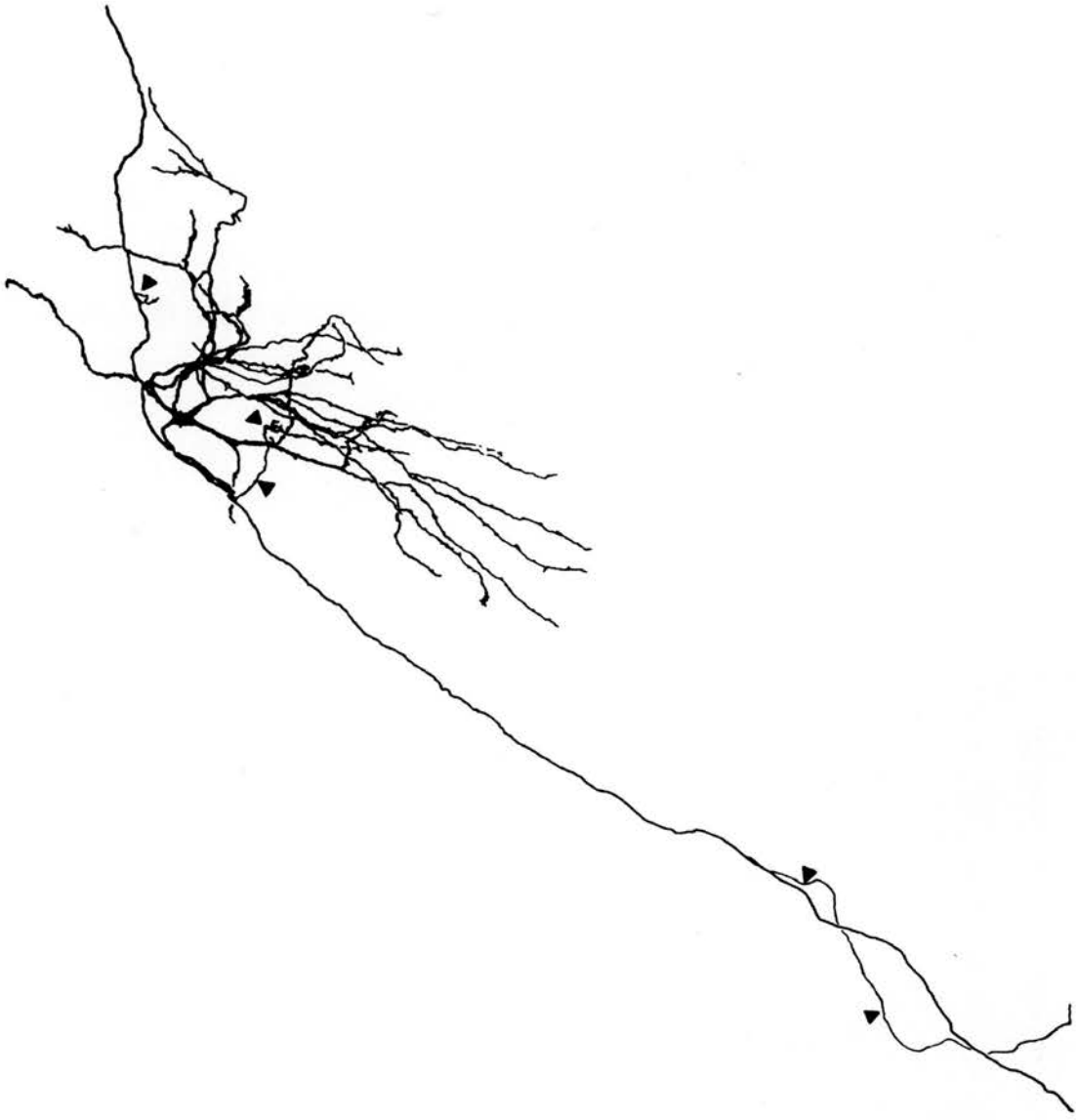

Figure 2.3 Drawing of a subthalamic nucleus neurone filled intracellularly with Horseradish Peroxidase. Arrowheads mark intranuclear axon collaterals. Adapted from Kita *et al.* (1983).

neurones also had a higher level of dendritic branching. Whether these divisions into two groups described by Afsharpour (1985) and Kita *et al.* (1983b) represent the same two distinct populations of neurones or not is unclear.

Generally, in rats, the neurones of the STN are treated as being of only one type - the STN projection neurone, of which there are approximately 13,600 (Oorschot, 1996). The nucleus is lens shaped and is situated on the dorsomedial surface of the internal capsule, at the point where the internal capsule merges with the cerebral peduncle. Fingers of groups of neurones appear to spread from the STN into both the internal capsule and cerebral peduncle. The longest axes of the nucleus are roughly equal in length at around 1.0-1.5 mm and are aligned rostrocaudally and dorsolateral-ventromedially. The shortest axis is 250-300 μm in the dorsomedial-ventrolateral plane. Dorsal to the STN lies the *zona incerta*, ventral is the meeting point of the internal capsule and cerebral peduncle, to the rostral end the EP lies embedded in the internal capsule, whilst the substantia nigra lies close to the caudal end. In some species it is difficult to define the caudal boundary between the STN and the SNc (Overton *et al.*, 1995). The STN is the only nucleus within the basal ganglia whose neurones use glutamate as their neurotransmitter (Smith *et al.*, 1998).

2.1.2.1 The connections of STN neurones

The afferent and efferent connections of the STN have been extensively studied using both retrograde and anterograde tracing techniques. The large number of axons of passage, which pass through the STN and could take up the tracer, complicate the

interpretation of tracing experiments that use injections of a marker into the STN. For this reason it is important to verify a connection with any given nucleus with two sets of experiments, one using injections into the STN, and one using injections into the nuclei that are proposed to connect to the STN. Using these techniques Canteras *et al.* (1990) have described the afferent projections to the STN. First they made injections of horseradish peroxidase (HRP) or HRP conjugated with wheatgerm agglutinin (WGA-HRP) into the STN. Then they made injections of WGA-HRP into the areas of the brain in which they had seen filled cell bodies after the first series of injections. Only structures that had shown labelled cell bodies in the first experiment and that had also shown terminals in the STN in the second experiments were considered as having a definite projection to the STN. These areas included; ipsilaterally, the cortex - in particular the primary motor and somatosensory cortex, the medial precentral areas and the anterior cingulate area, both the dorsal and ventral pallidum (GP), the thalamic parafascicular nucleus, and bilaterally, the dorsal raphé nucleus and pedunculopontine tegmental nucleus (PPN). This study also noted possible projections to the STN from the ipsilateral EP and SN; in particular it was noted that there is a possible dopaminergic projection from the SNc. The existence of connections from these nuclei to the STN is difficult to verify due to the numerous axons of passage. In addition, tracer picked up by axon terminals can travel first retrogradely and then anterogradely along collateral branches of the axon (Shink *et al.*, 1996).

It is generally accepted that the STN receives input from the ipsilateral cortex, in particular the frontal areas of the cortex (Kitai & Kita, 1986; Canteras *et al.*, 1990;

Fujimoto & Kita, 1993; Bevan *et al.*, 1995; Beurrier *et al.*, 2000; Deniau *et al.*, 2000). This projection is glutamatergic and mostly takes the form of axon collaterals from descending pathways (Bevan *et al.*, 1995). There are also glutamatergic, excitatory projections to the STN from the parafascicular nucleus of the thalamus (Féger *et al.*, 1994; Orieux *et al.*, 2000). Many reports have confirmed the existence of a GABAergic, inhibitory projection to the STN from the GP (Rouzaire-dubois *et al.*, 1980; Kita *et al.*, 1983a; Bevan *et al.*, 1997). Figure 2.4 shows all the connections of STN discussed both here and below.

Stimulation of those areas of cortex that project to the STN leads to a characteristic response from the STN neurones (Fujimoto & Kita, 1993; Maurice *et al.*, 1998). This takes the form of two peaks of excitation separated by a short period of inhibition and followed by a longer inhibitory period (figure 2.5A). This response was observed in all neurones recorded in the STN after stimulation of the same area of cortex. This means that the cortical stimulus must be spreading, there are a variety of ways in which it is possible for this to happen:

(i) Through cortico-cortical interconnections.

(ii) Through collateralisation of the cortico-subthalamic axons.

(iii) Through interconnections between the neurones of the STN.

(iv) Or a combination of these three explanations.

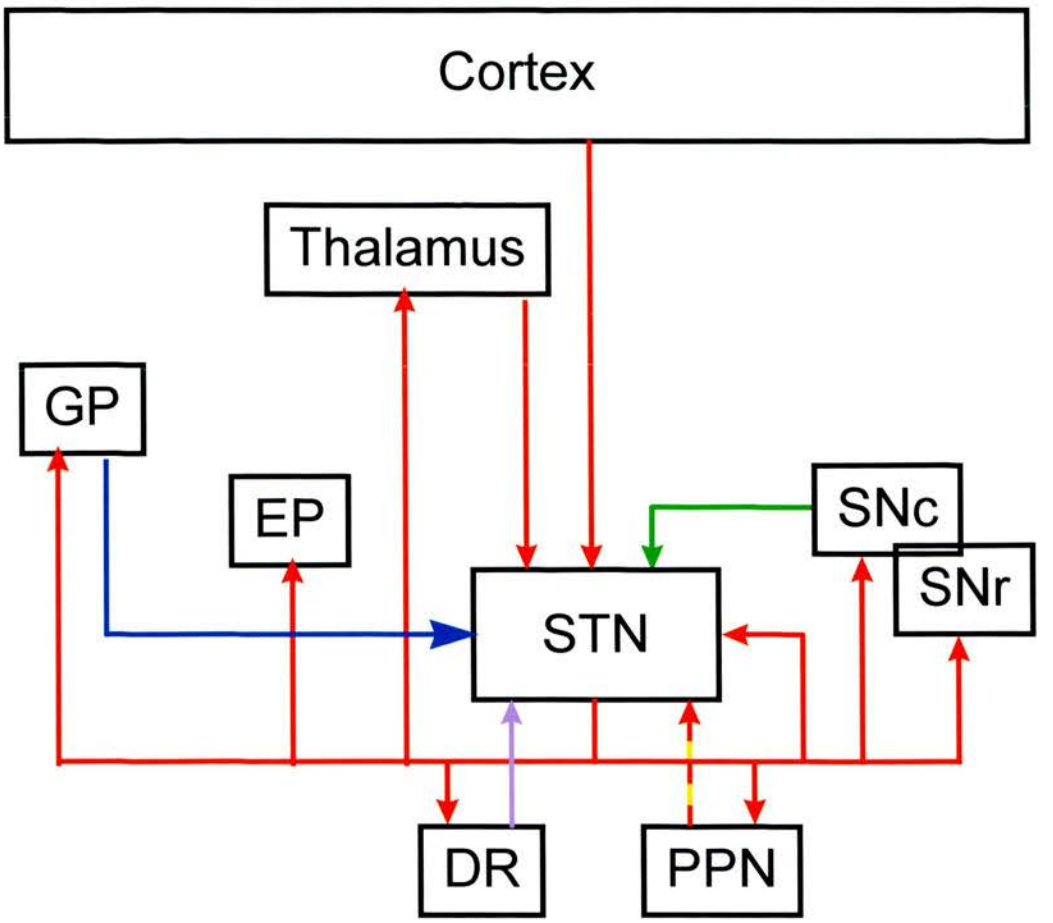

Figure 2.4 The main connections of the rat subthalamic nucleus. Red lines indicate excitatory glutamatergic connections. The blue line indicates an inhibitory GABAergic connection. The Green line indicates a dopaminergic connection. The lilac line indicated a serotonergic connection. The red/orange hatched line indicated a connection that may be glutamatergic, cholinergic, or both. DR = dorsal raphe nucleus; EP = entopeduncular nucleus; GP = globus pallidus; PPN = pedunculopontine tegmental nucleus; SNc = substantia nigra pars compacta; SNr = substantia nigra pars reticulata; STN = subthalamic nucleus.

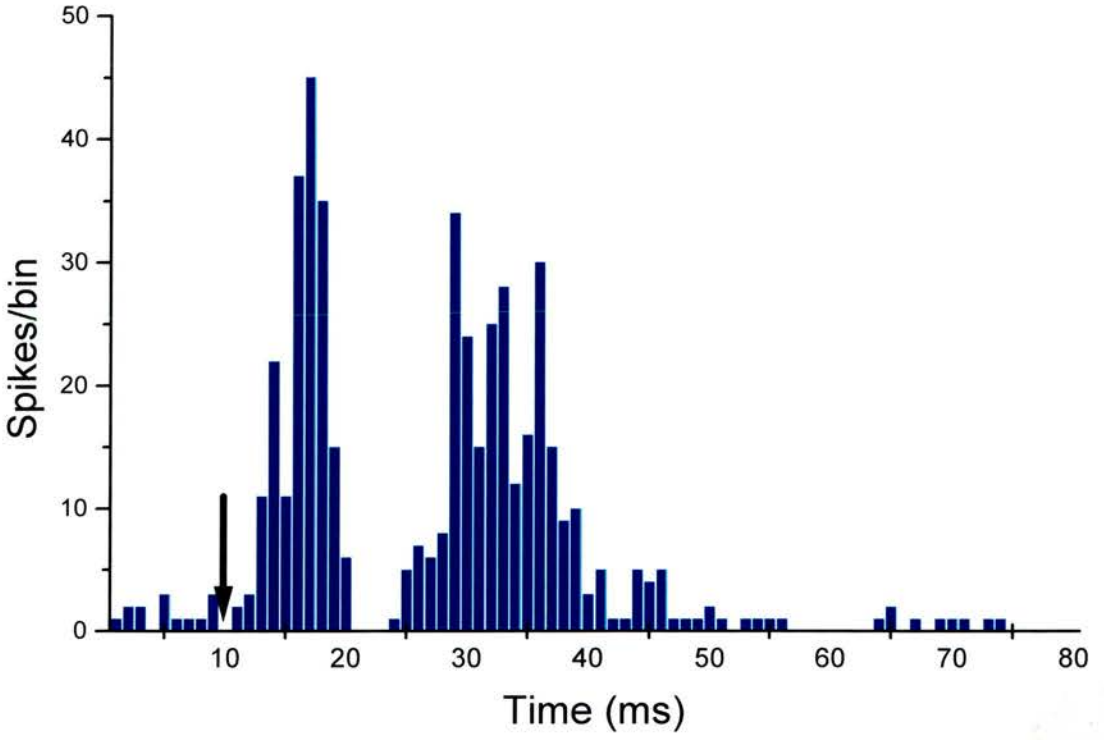

Figure 2.5 The response of a neurone in the rat subthalamic nucleus to stimulation of the motor cortex. The arrow marks the point of stimulation. The neurone responds with a characteristic double wave of excitation divided by a short inhibitory period. Adapted from Fujimoto and Kita (1993).

Of these possibilities the second is the most unlikely as many authors have shown that the cortico-subthalamic projection maintains a degree of the topographical organisation that is seen in the cortex (Bevan *et al.*, 1995). Evidence for this also comes from cortical stimulation studies that used the immediate early gene c-fos as a marker of activation of STN neurones rather than electrophysiology (Westby *et al.*, 2000). These studies showed that, after stimulation protocols that led to c-fos expression in STN neurones, the c-fos positive cell bodies were all grouped together in discrete clusters. This seems to be contrary to the electrophysiological evidence. However, it is worth noting that c-fos expression is thought to be in proportion to the level of synaptic activation (and in particular the opening of NMDA (*N-methyl-D-aspartate*) receptors) rather than the number of action potentials fired. This difference, though subtle, could explain the apparent discrepancy between the molecular and electrophysiological data.

As well as the cortical and GP inputs to the STN, there are inputs that are thought to have a modulatory role on the behaviour of STN neurones. There are inputs to the STN from the PPN (Canteras *et al.*, 1990; Bevan & Bolam, 1995; Orieux *et al.*, 2000), these are mainly cholinergic but there are also some glutamatergic fibres. In other basal ganglia nuclei glutamatergic and cholinergic inputs are thought to work together to enhance the opening of NMDA receptors (implying an involvement of synaptic plasticity) and this is possibly the role that the PPN plays here (Kitai *et al.*, 1999). There are also serotonergic inputs from the dorsal raphé nucleus (Canteras *et al.*, 1990; Flores *et al.*, 1995). The existence of this input is difficult to prove conclusively because some of the axons of passage through the STN have their origin

in the dorsal raphé. Flores *et al* (1995) have, however, found functional evidence for the existence of such a projection. They measured the spontaneous activity of STN neurones in an *in vitro* slice preparation. Of the neurones tested, 84% increased their firing rate during the application of serotonin. Out of the remaining neurones, some showed a brief increase in firing rate followed by a decrease, others showed a decrease in firing rate, whilst others were unaffected. The possibility that the effects of serotonin seen in this experiment could be mediated through an intermediate nucleus cannot be ruled out. On the other hand, neither can the suggestion that this is a direct effect of serotonin. The functional significance of such a projection is unknown but the possibility of recurrent connections between the STN and the dorsal raphé allows for the STN to have some level of feedback control over this pathway.

There is also an increasing body of evidence that dopaminergic projections play an important role in the STN. In the rat tyrosine hydroxylase (TH; an enzyme in the dopamine synthesis pathway) stained sections show only a very sparse dopaminergic innervation of the STN (figure 2.6). However, Hassani *et al.* (1997) showed retrograde labelling of cell bodies in the SNc following injection of fluorogold into the STN. These cells were also found to be positive for TH labelling. They also found terminals in the STN following injections of biocytin into the SNc. Campbell *et al* (1985) made extracellular recordings from STN neurones *in vivo* both before and after the application of dopamine or dopamine agonists/antagonists by microiontophoresis. Of the STN neurones studied, 46% responded to dopamine with a decrease in their firing rate. 15% responded with an increase in firing, 11% showed an initial depression in firing rate followed by a delayed increase, whilst the

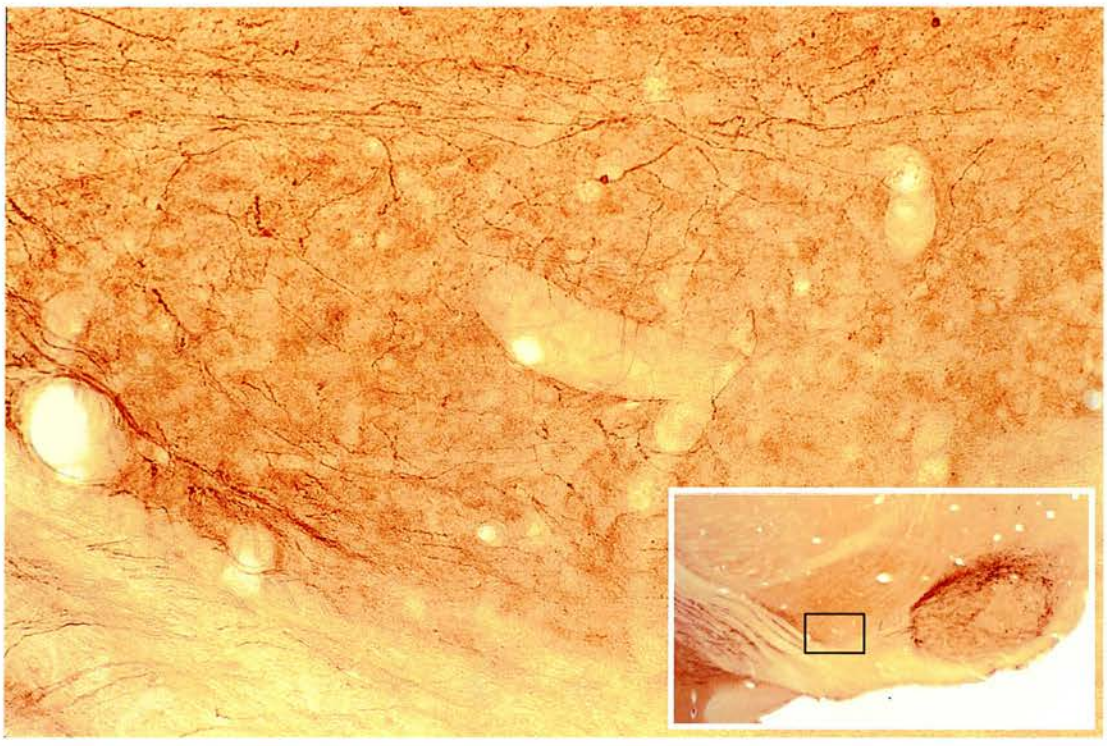

Figure 2.6 Photomicrograph of a parasagittal section of rat brain stained with an antibody against tyrosine hydroxylase. The low power inset shows the location of the high magnification photograph. Fibres from the substantia nigra pars compacta can be seen traversing the dorsal border of the subthalamic nucleus (STN). There are a number of fibres that leave this fibre bundle and enter the STN. These fibres show varicosities within the STN indicating that they are making synaptic contacts with STN neurones. Tissue courtesy of A.K. Wright.

remaining 28% showed no response. These responses were mimicked by the application of the dopaminergic agonist apomorphine and to a lesser extent by noradrenaline. Flores *et al* (1993) made injections of the dopaminergic neurotoxin 6-hydroxydopamine (6-OHDA) into the STN in order to lesion any dopaminergic innervation that may be present. Following this, dopamine levels were measured and found to have fallen only in the injected STN, and not in the striatum or the contralateral STN. This lesion also led to the appearance of EMG activity in the gastrocnemius-soleus muscle on the lesioned side, but not on the intact side. As well as this, injections of methamphetamine induced rotation behaviour in the lesioned animals but not in sham operated controls.

Kita and Kitai (1987) have studied the efferent projections of the STN using anterograde transport of PHA-L (*phaseolus vulgaris-leucoagglutinin*) injected into the STN. Single cell fills with HRP had already shown that STN neurones all send projections to the GP, EP, and SNr (Kita *et al.*, 1983b). PHA-L tracing confirmed this and also showed moderate projections to the striatum, frontal cortex, substantia innominata, SNc, PPN, dorsal raphé nucleus and the mesencephalic and pontine reticular formation (Kita & Kitai, 1987). It is worth noting however that the injections in this study almost all included some of the zona incerta, which could account for some of the more sparse projections that were seen. Ultrastructural examination of the STN terminals in the GP and SNr showed that these formed asymmetric synapses that contained small pleomorphic vesicles. These terminals were mostly onto dendritic shafts although some were onto the cell bodies.

2.1.2.2 The electrophysiology of STN neurones

How the cells of the STN behave electrophysiologically depends on the type of preparation used. When *in vitro* slices are used the cells fire regularly at rest at around 4 - 40 Hz (Nakanishi *et al.*, 1987; Bevan & Wilson, 1999; Beurrier *et al.*, 2000). This firing has been shown to be spontaneous and independent of any excitatory input to the STN (Bevan & Wilson, 1999). Increasing levels of hyperpolarisation slows and eventually stops the firing of action potentials, when this is released the cells display a rebound depolarisation which is often accompanied by a short burst of action potentials (Nakanishi *et al.*, 1987). Figure 2.7A shows an example of rebound firing from one of the STN neurones used in the experiments described in chapter 4. Depolarising the cells increases their firing rate up to a maximum of around 500 Hz (figure 2.7B). The relationship between firing frequency and increasing amounts of depolarisation produces a sigmoidal I-f curve (Nakanishi *et al.*, 1987). The gradient at the linear part of this curve is about 900 Hz/nA indicating that within this narrow range the neurones are extremely sensitive to small changes of current. Repetitive firings are followed by a long, calcium dependent, period of hyperpolarisation (Nakanishi *et al.*, 1987; Gillies, 1996) (figure 2.7C). Occasionally a cell displays burst firing behaviour (figure 2.7D) which, it has been reported, can be induced by small amounts of hyperpolarising current (Beurrier *et al.*, 1999).

In vivo recordings show the STN neurones to fire irregularly at 6 to 16 Hz (Ryan *et al.*, 1992). Some cells show bursting activity which is increased in animals with 6-

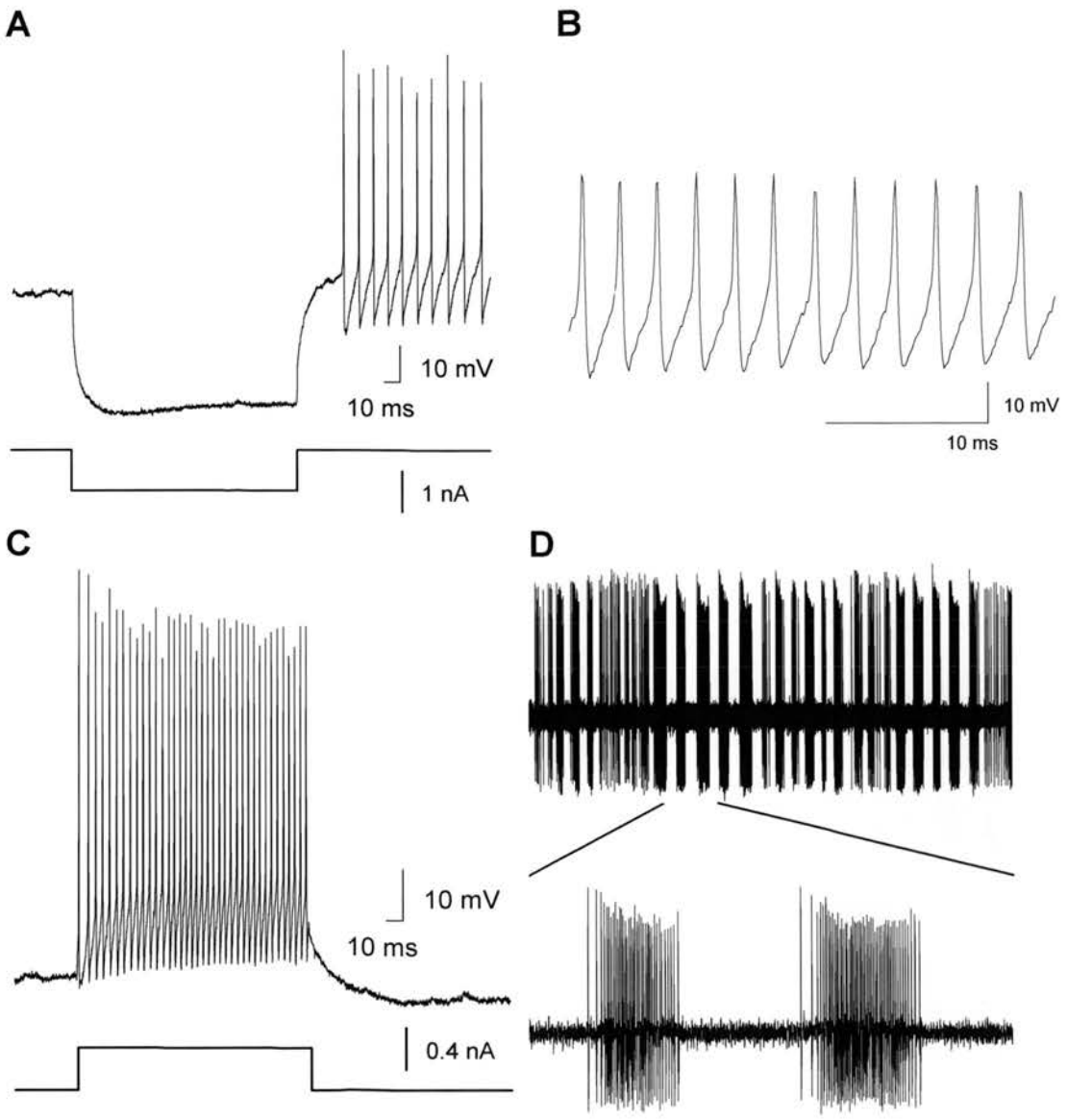

Figure 2.7 Characteristics of the electrophysiology of subthalamic nucleus neurones. **A** Following hyperpolarisation the neurone displays a rebound depolarisation leading to the generation of action potentials. **B** When sufficiently depolarised the neurone can fire action potentials at rates up to 500 Hz. This trace shows an intracellular recording from a neurone being driven to fire at nearly 500 Hz **C** Following a train of action potentials, induced by a small pulse of depolarising current, there is a relatively long period of hyperpolarisation (full extent not shown). **D** Sometimes neurones exhibit bursting behaviour. The ten second extracellular trace shows a neurone switching between burst firing and continuous firing modes. 1000 ms of this trace has been amplified to show detail from two consecutive bursts.

OHDA lesions of the dopaminergic neurones of the nigrostriatal pathway. Stimulation of the somatosensory cortex elicits a stereotyped 'double-pulse' in nearly all of the cells in the STN (figure 2.3). This consists of two peaks of excitation separated by a short period of inhibition. This response is often followed by a long period of inhibition, which can last for many seconds (Fujimoto & Kita, 1993; Maurice *et al.*, 1998). In order to try to dissect out the various elements of this response, lesions or cuts were made in various places (Fujimoto & Kita, 1993). Lesioning the striatum or cutting the input from the brainstem (PPN) to the STN had no effect on the double-pulse. However, a lesion of the GP, which increased the resting firing rate of the STN neurones by approximately 20%, also changed the nature of their response to cortical stimulation. The cells now responded with a much longer single peak of excitation. This was slightly longer than the entire double-pulse response observed in control animals and was still followed by a long-lasting period of inhibition. An explanation for this data is that the cortical stimulation elicits a long-lasting excitation of the STN neurones. This may occur because the response is lengthened by the activation of NMDA (*N*-methyl *D*-aspartate) receptors. Another explanation given by the authors is that the prolongation of the response might be due to activation of the intranuclear connections within the STN. Under normal circumstances this period of excitation is broken by a brief period of inhibition due to negative feedback following the activation of the GP by the STN neurones.

This explanation has now been questioned following the results of similar experiments using stimulation of other areas of the cortex (Maurice *et al.*, 1998). Prefrontal cortex, like somatosensory cortex has both a direct and an indirect

projection to the STN. Stimulation of prefrontal cortex induces a very similar response from STN neurones, to that induced by stimulation of the somatosensory cortex. However, unlike the pathway from somatosensory cortex, the indirect projection from prefrontal cortex through the basal ganglia to the STN does not pass through the striatum and GP. Instead it follows a slightly different, but parallel, pathway. The structures in this pathway are thought to be functionally homologous to the striatum and GP allowing a direct comparison between these two sets of experiments. Chemical manipulation of the nuclei in this indirect pathway was used to alter the nature of the STN response to stimulation of the prefrontal cortex. Infusion of the AMPA/kainate glutamatergic antagonist CNQX (*6-Cyano-7-nitroquinoxaline-2,3-dione*) into the *nucleus accumbens* (Nacc; c/f striatum) led to an increase in the duration of the inhibitory period that separated the two excitatory peaks (or the appearance of an inhibitory period, if none existed). This treatment also led to a decrease in the size (52-96% decrease) of the second excitatory peak. Infusion of the GABAergic antagonist bicuculline into the *ventral pallidum* (VP; read GP) led to similar alterations in the STN response. Finally, infusion of CNQX into the VP led to an increase in the size of the second excitatory peak and a decrease in size (or disappearance) of the short inhibitory period. Figure 2.8 shows all of the changes found by Maurice *et al.* (1998). These data were used to produce an alternative explanation for the double-pulse response of STN neurones to cortical stimulation. Maurice *et al.* (1998) argued that this response does really consist of two separate excitatory waves. The first as a result of direct excitation of STN neurones by projections from the cortex, the second as a result of disinhibition of the STN neurones due to the inhibition of GP neurones by projections from the striatum.

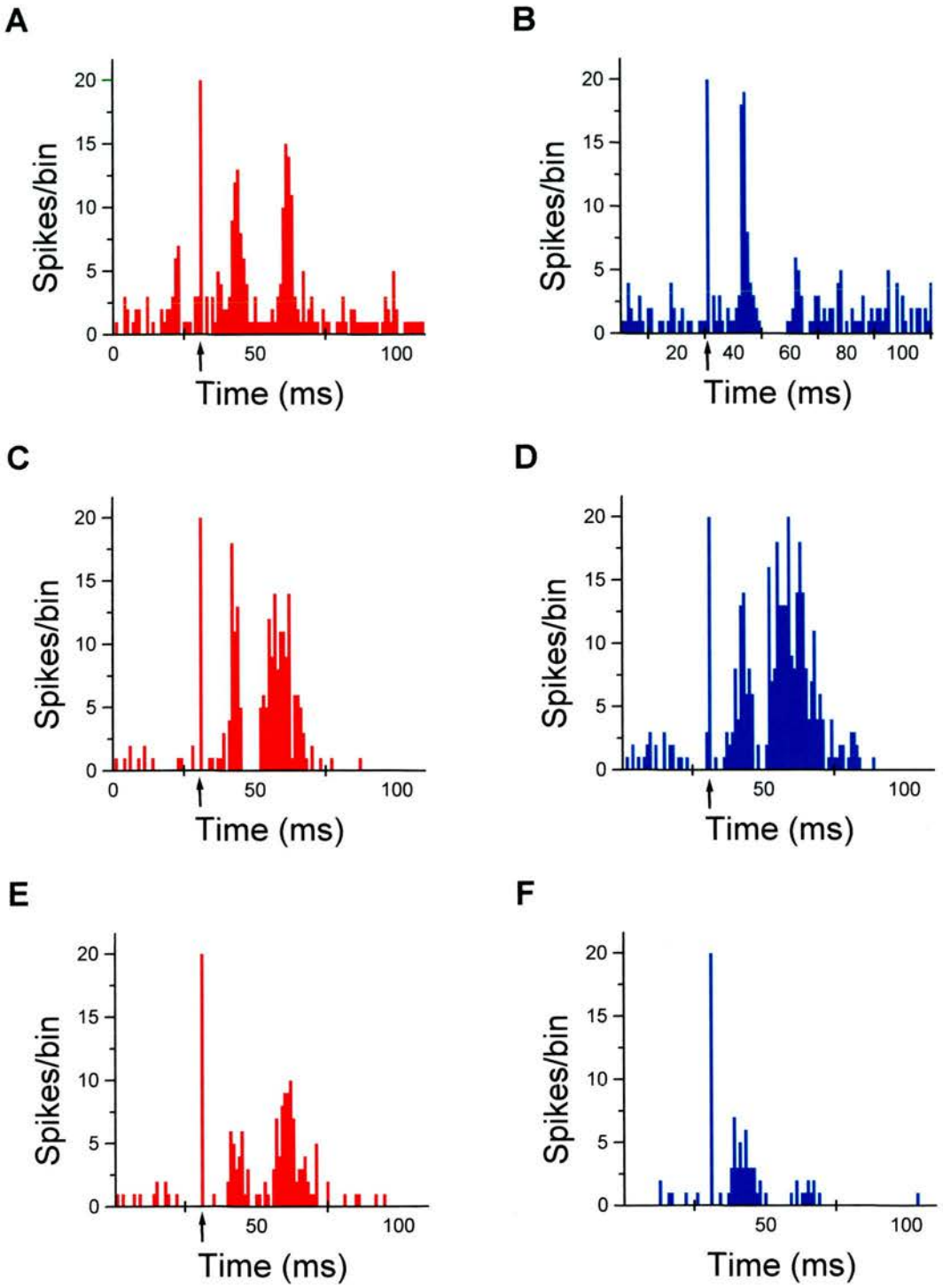

Figure 2.8 Modulation of the response of neurones in the subthalamic to stimulation of the prefrontal cortex. **A** and **B** show the response before and during the application of bicuculline (500 μM; 2 μl/min) in to the ventral pallidum. **C** and **D** show the response before and during the application of CNQX (500 μM; 2 μl/min) in to the ventral pallidum. **E** and **F** show the responses before and during the application of CNQX (500 μM; 2 μl/min) into the nucleus accumbens. In all the graphs an arrow shows the time point at which prefrontal cortex was stimulated. Adapted from Maurice *et al.* (1998)

Figure 2.9 compares these two differing explanations. Whilst this explanation adequately fits the data of Maurice *et al.* (1998) it fails to explain the finding that a GP lesion results in the merging of the two excitatory peaks into one long peak (Fujimoto & Kita, 1993). They disregarded these experiments, on the grounds that reorganisation of the synaptic inputs to the STN cells could have occurred in the three weeks following the GP lesions, or that the lesion could have changed their excitability. However, Fujimoto and Kita (1993) had shown that the gap between the two excitatory peaks coincided with IPSPs, which are most likely to have originated from the GP. This suggests that the initial peak of excitation is indeed followed by a short wave of inhibition. This evidence favours the earlier explanation of this STN response.

Recent data has shown that stimulation of the auditory cortex only evokes the late part of the STN response (Deniau *et al.*, 2000). The early excitatory peak and the middle inhibitory period are missing. This suggests that possibly a combination of the two explanations can be formulated. The early peak may only be present if the area of cortex stimulated has a direct projection to the STN. This wave of excitation might be terminated by feedback inhibition from the GP, as suggested by the coincidence of the middle inhibitory period with IPSPs. If the GP is lesioned, then this inhibitory period does not occur and the first wave of excitation is amplified, hiding the second excitatory peak. This second peak may be due to disinhibition due to the release of the STN from a tonic level of inhibition by the GP as the GP is inhibited by the striatal neurones that have also been excited by the cortical

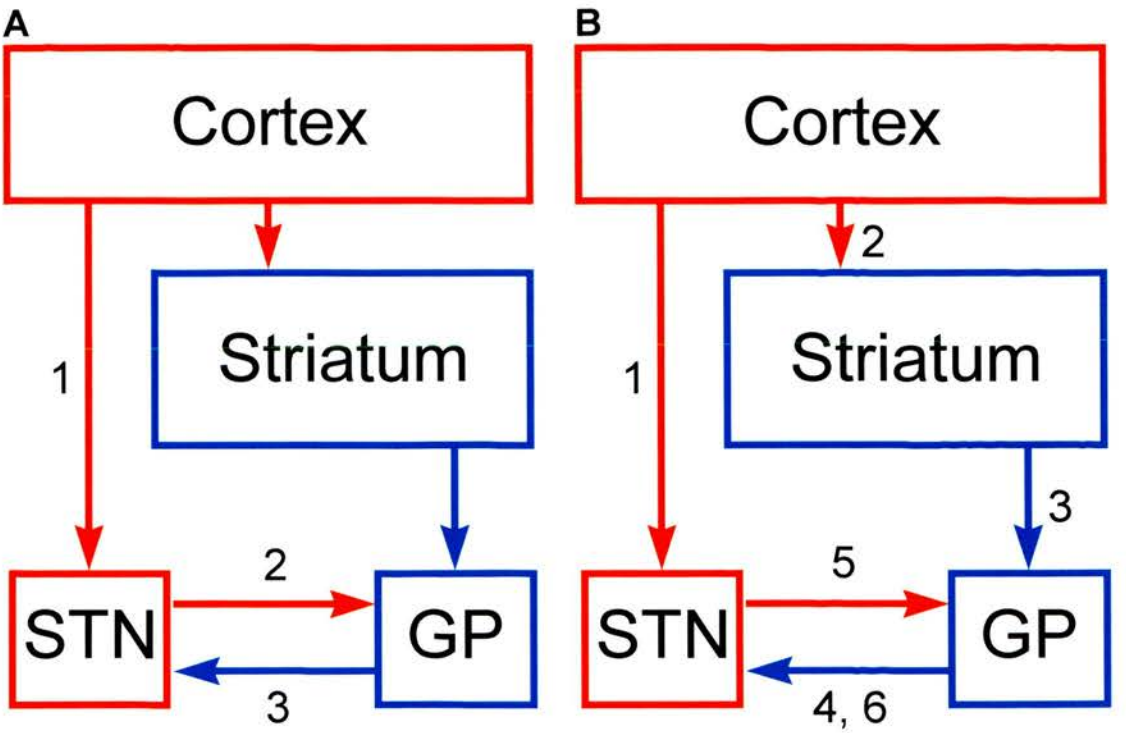

Figure 2.9 Alternate explanations for the generation of the 'double pulse' response of subthalamic nucleus (STN) neurones to cortical stimulation (see figure 2.6). **A** Fujimoto & Kita's (1993) explanation. The direct cortical projection to the STN (1) causes a long lasting excitation of the neurones, this is interrupted by a period of inhibition from feedback through the globus pallidus (GP; 2 & 3). **B** Maurice *et al.*'s (1998) explanation. The direct cortical projection to the STN (1) causes the first excitatory peak, whilst an indirect, disinhibitory cortical projection through striatum and globus pallidus (GP; 3 & 4) causes the second excitatory peak. These two peaks are interrupted by a period of inhibition from the feedback circuit *via* the globus pallidus (5 & 6). Red arrows = excitatory connections (glutamatergic); blue arrows = inhibitory connections (GABAergic); For striatum and GP also read nucleus accumbens and ventral pallidum respectively.

stimulation. Indeed, it has now been shown that such rebound excitation can occur in physiological situations (Bevan *et al.*, 2000).

The influence of the projections from the STN on the nuclei of the basal ganglia that they contact has been extensively studied. It was originally thought that the neurones of the STN used GABA as their neurotransmitter. This was based on the discovery that lesions of the STN lead to ballism (as described in section 2.3.2) and led to the idea that the STN suppresses unwanted movements by inhibiting neurones in the GP and EP (Whittier & Mettler, 1949a; Whittier & Mettler, 1949b). Apparent confirmation of this came from experiments using injections of ^{3}H-GABA into the GP or EP of the cat (Nauta & Cuenod, 1982). Following these injections labelled neurones were observed in the STN. That these neurones were able to take up GABA at their axon terminals and transport it retrogradely to the soma was taken as evidence that they use GABA as their neurotransmitter. Other studies both in the cat (Larsen & Sutin, 1978) and rat (Perkins & Stone, 1980; Rouzaire-dubois *et al.*, 1983; Rouzaire-dubois *et al.*, 1984) found that electrical stimulation of the STN led to the inhibition of GP or EP neurones. The inhibition in the EP could be blocked by microiontophoretic injections of the GABA antagonists bicuculline or picrotoxin into the EP. However, the conclusions drawn from these data was questioned by experiments showing that electrical stimulation of antidromically identified STN neurones lead to excitatory responses in both the SNc and the SNr (Hammond *et al.*, 1978). In addition, STN terminals in the pallidum were found to form asymmetrical synapses containing round vesicles, a characteristic that is usually associated with glutamatergic terminals (Kitai & Kita, 1986; Kita & Kitai, 1987). The neurones of

the STN have been shown to display immunoreactivity against glutamate and not GABA (Smith & Parent, 1988). Finally, evidence from chemical stimulation or inhibition of the STN has shown that the STN neurones are excitatory to neurones in the GP, EP, and SNr (Robledo & Feger, 1990; Feger & Robledo, 1991). When the GABAergic agonist muscimol was injected into the STN, inhibiting its neurones, the firing rate, and local cerebral glucose utilisation (LCGU; as measured by the 2-deoxyglucose technique) of neurones in the ipsilateral SNr, EP, and GP were reduced. Conversely, injections into the STN of bicuculline, a GABA antagonist that excites its neurones, led to corresponding increases of firing and LCGU in these nuclei. Figure 2.10 shows the changes in the firing rates of neurones in the STN, SNr, EP, and GP found following these pharmacological manipulations. Thus the STN is able to exert an excitatory influence on its target nuclei and its tonic level of activity is, at least in part, responsible for the tonic activity levels in these nuclei. In an interesting development, recent data from human *post-mortem* tissue has shown that neurones in the human STN are enriched in mRNA encoding GAT-1, a brain specific high-affinity GABA uptake protein (Augood *et al.*, 1999). This data is in agreement with the data from the cat showing that STN neurones can actively accumulate GABA (Nauta & Cuenod, 1982). This same study showed that the human STN neurones also expressed mRNA for the calcium binding proteins parvalbumin and calretinin (Augood *et al.*, 1999). These are proteins that are normally associated with GABAergic neurones. Thus, in the human at least, either some STN cells do utilise GABA as their neurotransmitter or the glutamatergic neurones of the STN for some reason express mRNA encoding proteins that are normally associated with GABAergic neurones.

A

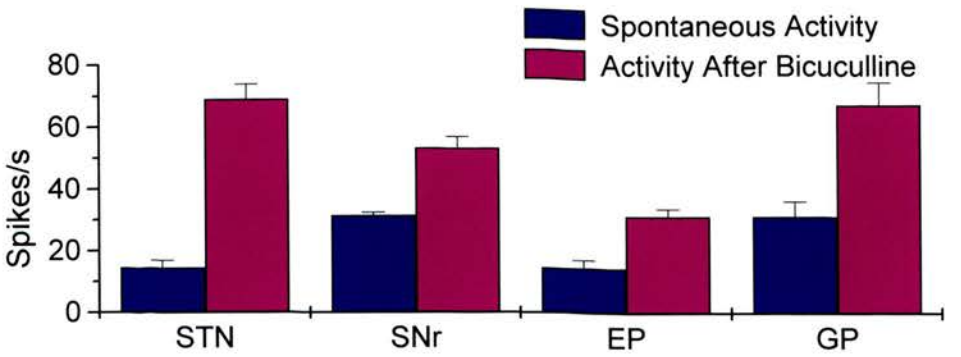

B

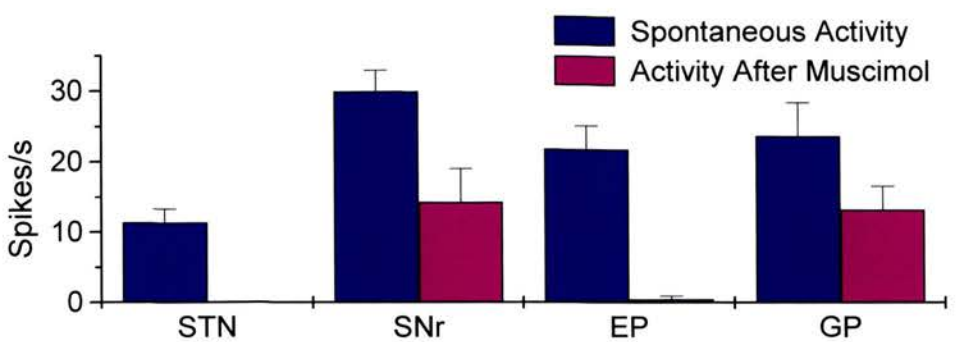

Figure 2.10 Histograms showing the effects of injections of either **A** bicuculline (0.39 mM) or **B** muscimol (0.95 mM) into the subthalamic nucleus (STN) on the activity of neurones in the STN, substantia nigra pars reticulata (SNr), entopeduncular nucleus (EP), and the globus pallidus (GP). Adapted from Robledo & Féger (1990).

2.2 The Direct/Indirect Pathway Hypothesis

In order to try to understand the functioning of the basal ganglia, both in its normal and its pathological states, Albin *et al* (1989) proposed a theoretical model. This model is constructed around two parallel pathways that information travelling through the basal ganglia could take. For this reason it is known as the 'direct/indirect pathway hypothesis'. According to this model, the cortex provides the major input pathway to the basal ganglia through the striatum. MSNs in the striatum are divided into two populations according to the route they use to project to the output nuclei of the basal ganglia (EP/SNr). These two routes are called the direct pathway and the indirect pathway. The two populations of neurones can be further distinguished by the peptides used by the MSNs as co-transmitters with GABA. The MSNs projecting along the direct pathway connect directly to the EP/SNr, these neurones contain substance P and dynorphin co-localised with GABA. The MSNs projecting to the indirect pathway contain enkephalin. Information travelling through this pathway is relayed to the EP/SNr through the GP and STN. Neurones in the EP/SNr are GABAergic (inhibitory) and have a tonic level of activity, which can be raised or lowered by their inputs. Thus, the basal ganglia can control the levels of activity in their target structures (thalamus, brainstem/spinal cord) through increasing or decreasing the level of inhibition of these structures by the EP/SNr. Increased activity in those striatal neurones that project *via* the direct pathway leads to direct inhibition of the EP/SNr and a consequent disinhibition of their target neurones. Activation of the striatal neurones of the indirect pathway leads to inhibition of the neurones in the GP. The GP exerts a tonic level of inhibition over the STN and so its

inhibition leads to excitation of the neurones in the STN. As the STN projects to the EP/SNr activation of this pathway leads to excitation of the output neurones, further inhibiting their targets. It is this balance of increased inhibition/disinhibiting the target neurones of the basal ganglia that is thought to underlie its normal function. By inhibiting undesired motor programs and disinhibiting the desired one, normal movement is allowed to proceed unhindered. Figure 2.11 shows a diagram of the direct/indirect pathways from the Albin *et al.* (1989) model.

This delicate balance of inhibition/disinhibition is thought to be under the control of dopamine. The dopaminergic neurones of the SNc send projections to the MSNs in the striatum. Here they make synapses onto the necks of the spines of these neurones. Dopamine does not affect all MSNs in the same manner. The neurones that project to the direct pathway preferentially express the dopamine D1 receptor. The result of activation of this type of dopamine receptor is stimulation of the postsynaptic neurone. The neurones that project along the indirect pathway mostly express the dopamine D2 receptor. These neurones are inhibited by increased levels of dopamine. Thus increases in the activity of the dopaminergic neurones in the SNr facilitate movement whilst decreased activity of these neurones leads to the inhibition of movements.

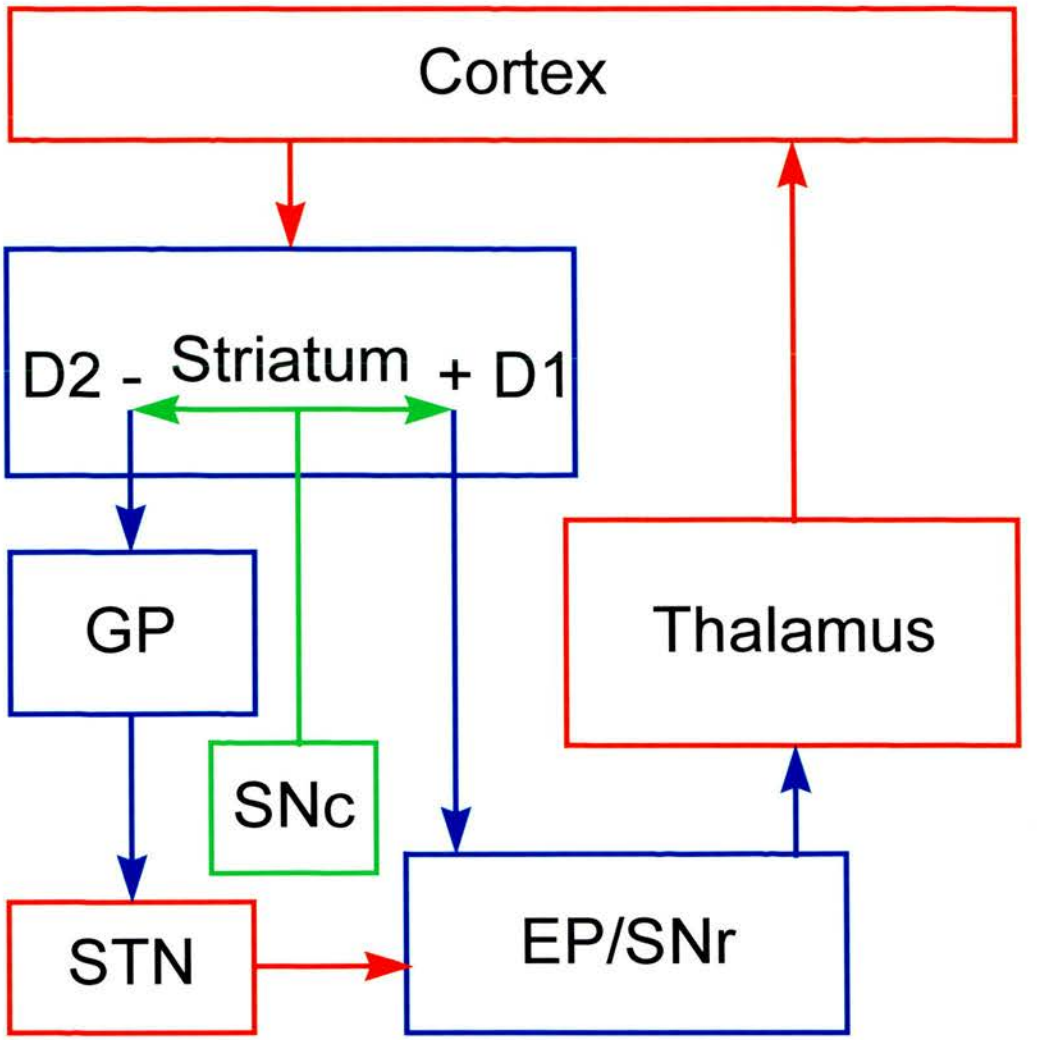

Figure 2.11 The direct/indirect pathways model of basal ganglia function. Excitatory nuclei and their projections are shown in red. Inhibitory nuclei and their projections are shown in blue. The dopaminergic nigrostriatal pathway is shown in black. The cortex provides excitatory input to the striatum. From the striatum information can be passed along one of two pathways. The direct pathway is formed by the projection from the striatum to the entopeduncular nucleus (EP) and the substantia nigra pars reticulata (SNr). The indirect pathway also ends up at these two output nuclei but passes *en route* through the globus pallidus (GP) and the subthalamic nucleus (STN). The substantia nigra pars compacta (SNc) provides dopaminergic input to the striatum where information flow along the direct and indirect pathways can be controlled *via* the differential effects of dopamine on the striatal neurones that project to each pathway.

2.3 Diseases of the Basal Ganglia

There are a number of neurological disorders that follow or damage to one (or more) of the nuclei of the basal ganglia. Amongst these are *Parkinson's Disease* (PD), *Huntington's Disease* and *hemiballism*.

2.3.1 Parkinson's Disease

PD is the commonest disease of the basal ganglia. It was first described by James Parkinson (Parkinson, 1817):

> *"SHAKING PALSY. (Paralysis Agitans.)*
> *Involuntary tremulous motion, with lessened muscular power, in parts not in action and even when supported; with a propensity to bend the trunk forward, and to pass from a walking to a running pace; the senses and intellects being uninjured."*

It is a hypokinetic disorder characterised by rigidity, resting tremor, slowness (bradykinesia), gait disturbance, and postural instability. These symptoms are a consequence of the degeneration of dopaminergic neurones, in particular those neurones that form the nigrostriatal pathway. Coupled with this neurodegeneration is presence of intracytoplasmic inclusions, called Lewy bodies, in the remaining neurones. Neurodegeneration and Lewy bodies are seen elsewhere but are most profound in the SNc. The disease is progressive, with the first symptoms arising

when there is a 60 to 80% loss of SNc dopamine neurones. The specific causes of the loss of dopaminergic neurones are unknown. Epidemiological studies have implicated a number of factors in its aetiology (Olanow & Tatton, 1999). These include exposure to well water, pesticides, herbicides, industrial chemicals, wood pulp mills, farming, and living in a rural environment. There is also some evidence for the involvement of genetic factors particularly in cases of the disease with an early onset. Of particular interest are mutations in the gene that codes for the protein α-synuclein (Olanow & Tatton, 1999). A fragment of this protein called the non-β amyloid component has been isolated from senile plaques in the brains of Alzheimer's Disease patients and α-synuclein is an abundant component of Lewy bodies.

According to the direct/indirect pathway model the symptoms of PD arise as a consequence of increased output from the EP/SNr (Albin *et al.*, 1989). The model predicts that this increased output will occur following the loss of the dopaminergic neurones that project to the striatum and the consequent lowering of levels of dopamine in the striatum. This lowering of dopamine levels in the striatum reduces the influence of excitatory projections to those MSNs that project along the direct pathway rendering them hypoactive. Conversely, the influence of excitatory projections to those MSNs that project along the indirect pathway is increased, causing them to be hyperactive. These changes in activity lead to an increase in the levels of inhibition to the neurones in the GP and consequently a lowering of the GP's inhibition of neurones in the STN. Thus the neurones of the EP/SNr receive

less inhibition from the MSNs of the striatum and more excitation from the STN rendering them hyperactive. Figure 2.12A details all of these changes.

2.3.2 Huntington's Disease and Ballism

Huntington's disease is a genetic disorder that results in the degeneration of neurones in the striatum. Ballism (Hemiballism) is also a hyperkinetic disorder that usually occurs following strokes that lesion the STN. The Albin *et al.* (1989) model predicts that the symptoms of both these conditions occur following the decrease (or complete loss) of excitatory output from the STN. This will result in the hypoactivity of the neurones in the EP/SNr which results in the loss of the usual inhibition of undesired movements (see figure 2.12B & C).

2.3.3 Evaluation of the Albin Model

Initially the Albin *et al.* (1989) model was very successful. As a consequence of the predicted changes in activity in the various nuclei of the basal ganglia there has been an upsurge of research into the use of surgical intervention to treat PD.

The major treatment for PD is a dopamine replacement strategy using the dopamine precursor levodopa. This therapy, whilst extremely successful in the short term (5-10 years), gradually loses efficacy resulting in the need for higher doses. Eventually the majority of patients develop severe side effects, which include dyskinesia and hallucinations (Crossman, 2000; Benabid *et al.*, 2000). For this reason there has been

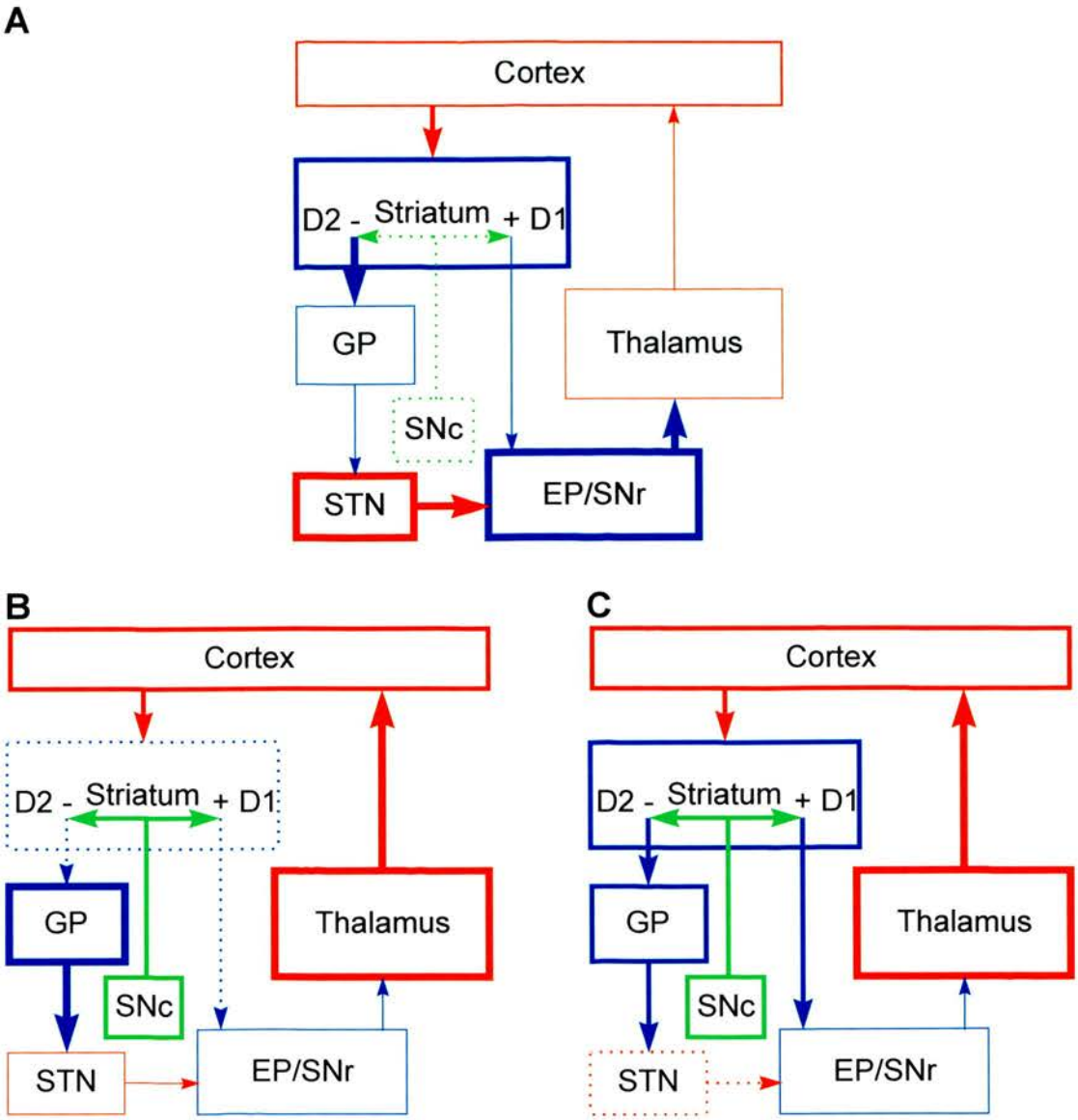

Figure 2.12 The pathological changes in information flow through the basal ganglia as predicted by the direct/indirect pathway model. **A** Parkinson's Disease. **B** Huntington's Disease. **C** Ballism. The thickness of the lines in these diagrams represents the relative levels of activity. These various changes in activity in each of these disorders is described in the main text. Red lines = glutamatergic neurones; blue lines = GABAergic neurones; green lines = dopaminergic neurones. EP = entopeduncular nucleus; GP = globus pallidus; SNc = substantia nigra pars compacta; SNr = substantia nigra pars reticulata; STN = subthalamic nucleus.

a large amount of interest in research aimed at the development of novel therapeutic strategies for the treatment of PD. The Albin *et al.* (1989) model was used to make the prediction that surgical intervention in the indirect pathway would reduce the dysfunctional output from this pathway and maybe lead to a restoration of normal movement. In particular the STN provides an attractive target for lesioning as the model predicts that many of the symptoms of the disease are due to hyperactivity of the neurones in this nucleus. Unfortunately, the STN is a very small nucleus and is highly vasculated. This makes it a difficult nucleus to lesion without the risk of causing damage to other nuclei. For this reason attention turned to lesioning other nuclei. Remarkably, lesions in either the thalamus or the GPi are successful in the treatment of many of the symptoms of PD (Vitek & Bakay, 1997; Tasker *et al.*, 1997). This is counter-intuitive, as the thalamus is an area that is predicted by the model to be hypoactive in the brains of PD patients. That these treatments are successful has lead to the suggestion that the symptoms of PD are due not so much to changes in the absolute firing rates of neurones in the basal ganglia nuclei. Rather, they are due to abnormal firing patterns and changes in the degree of temporal and spatial synchronisation between these neurones (Obeso *et al.*, 2000). A lesion such as a pallidotomy might remove this abnormal output allowing some normal function to be restored.

Instead of lesioning the STN, it was discovered that implanting stimulating electrodes delivering current pulses at around 100Hz can successfully alleviate many of the symptoms of PD (Gao *et al.*, 1898; Henderson & Dunnett, 1998; Limousin *et al.*, 1998; Rodriguez *et al.*, 1998a; Bejjani *et al.*, 2000). This is a less dangerous

procedure and has been tried successfully in many patients. However, it is uncertain how this works. It has been suggested that stimulating the neurones in the STN may cause the appearance of depolarisation block that will effectively behave like a reversible lesion. This idea is disputed, as a depolarisation block would not necessarily reduce glutamate release from STN axon terminals[1]. In support of this are recent results showing that STN stimulation in the rat, using the same parameters that are used therapeutically in humans, induces an increase in extracellular levels of glutamate in the SN and GP (Windels *et al.*, 2000a; Windels *et al.*, 2000b). These authors also showed increased extracellular levels of GABA in the SN. This suggests that in the GP (which sends direct projections to the SN) not only were there increased extracellular levels of glutamate but the neurones were also being driven by this increased excitation. These increases in levels of glutamate and GABA release have been shown to be proportional to the frequency of STN stimulation and a corresponding increase of dopamine release in the striatum has been observed (Savasta *et al.*, 2000; Bruet *et al.*, 2000). These results agree with data from the GP and thalamic lesions in PD patients. Both suggest that the emphasis that the direct/indirect pathway hypothesis places on changes in firing rates in the basal ganglia in the genesis of the symptoms of PD is incorrect. Rather, it is changes in the firing patterns and synchrony of neurones that are probably the important factors in the genesis of these symptoms.

---

[1] In fact, depolarization block may not stop the generation and conduction of action potentials. Instead, the site of generation may be moved along the axon away from the cell body.

The role of the indirect pathway in this model has also had to be re-evaluated in the light of new data concerning the anatomy and physiology of the GP and the STN. The importance of the direct projection from the cortex to the STN has already been discussed. This projection (along with a thalamo-subthalamic projection) provides a second input stage to the basal ganglia providing a quicker path for information travelling through than the route through the striatum. There is evidence that the recurrent connection from the STN to the GP is very important. Indeed, much of the tonic activity of GP neurones seems to be under the control of the STN (Robledo & Feger, 1990; Feger & Robledo, 1991). The tight interconnection between these two nuclei has come under an increasing degree of scrutiny. Changes in the behaviour of either nucleus can potentially drive feedback in the opposite direction through the other. This means that left alone the activity of the two nuclei will reach an equilibrium with each other. However, inputs that disturb this equilibrium could cause over-compensations that have the potential to set the two nuclei oscillating against each other (Plenz & Kitai, 1999). Complicating this further is the possible influence of dopaminergic projections on the neurones of the STN (and the GP). As reviewed above, there is a mounting body of evidence that the STN receives a direct innervation from the dopaminergic cells of the SNc. Loss of dopamine can lead to an increase in the firing rate and burstiness of STN cells *in vivo* in 6-OHDA lesioned rats (Hassani *et al.*, 1996) (but compare with Kreiss *et al.* (1997)). These changes are not totally due to knock-on effects of changes in dopamine levels in the striatum. This is evidenced by experiments showing that whilst lesions of the GP lead to approximately a 20% increase in the firing rate of STN neurones, 6-OHDA lesions of the nigrostriatal pathway lead to a 106% increase (Hassani *et al.*, 1996). The authors

take this as evidence for a direct effect of the dopamine cell loss on STN neurones. However, it could be argued that the changes in firing pattern seen in the GP following the 6-OHDA lesion might cause STN cells to fire faster than would happen following a simple GP lesion.

2.4 Alternative Models of Basal Ganglia Function

A number of alternatives to the Albin *et al.* (1989) model have been proposed (Gillies & Arbuthnott, 2000). Of particular interest are those models that place the basal ganglia as the seat of reinforcement learning for the generation of complex sequences of movements (Schultz, 1997; Suri & Schultz, 1998; Suri & Schultz, 1999). Wickens *et al.* (1998) have shown that a discrete, localised dopamine signal can promote long-term potentiation in the cortico-striatal pathway. Schultz (1997) has found that dopamine neurones exhibit a short increase in their activity in response to an unpredicted reward. If such a reward predictably follows an external stimulus then the dopamine signal moves to follow that stimulus. In this way the dopamine neurones move their response so that they always fire in response to the earliest stimulus that reliably predicts a future reward. This dopamine signal enables the learning of complex sequences where each movement in the sequence occurs in response to an external stimulus and results in another stimulus that has been paired with the next movement in the sequence. The absence of a predicted reward or stimulus results in a brief lowering of the tonic levels of activity of the dopamine neurones. This is interpreted as an error signal showing that the stimulus just seen is

no longer an accurate predictor of reward and therefore the action that triggered that stimulus is depotentiated.

This model has been the subject of criticism, particularly from Redgrave *et al.* (1999a) who point out that the dopamine signal occurs with too short a latency following the presentation of a stimulus. This means that the dopamine signal occurs before the animal has made the visual saccade to the stimulus that is needed to see it and consequently decide whether or not it constitutes a reward. Redgrave *et al.* (1999b) propose an alternative model of basal ganglia function. In this model the basal ganglia plays the role of a central action selection mechanism. At any given times there may be a large choice of actions to be performed. Many of these possible actions may be in competition with each other, as they would require the use of shared motor resources. Thus the brain must have a system for deciding between competing actions. Redgrave *et al.* (1999b) show that of all the potential architectures for fulfilling this role a central action selection mechanism is the most efficient both in terms of ease of implementation and versatility. They propose that the basal ganglia are the architecture in the vertebrate brain that is best suited to this role. The basal ganglia are thought to consist of a number of parallel cortico-basal ganglia-thalamo-cortical loops (Alexander & Crutcher, 1990). Redgrave *et al.* (1999b) extend this hypothesis such that functional systems capable of specifying actions operate as parallel '*channels*'. These channels are preserved throughout the basal ganglia. Upon entry to the striatum each channel carries a signal of the salience of that channel. It is in the striatum that competition between the channels occurs. When a 'winner' is selected that channel is opened *via* the direct pathway. Neurones

projecting to the EP/SNr inhibit only those neurones that constitute the winning channel. Therefore the action specified by the winning channels is disinhibited whilst all other channels remain inhibited. In order that clean switching should occur, and that only the selected channel is opened Redgrave *et al.* (1999b) propose that the STN provides a diffuse excitation to the EP/SNr. At the termination of a particular movement a diffuse pulse of activity from the STN could also act to reset activity in the EP/SNr.

The role of dopamine in this system is to modulate switching. Increases in dopaminergic transmission in the striatum facilitate switching whilst decreases might retard it. Thus the symptoms of PD can be reinterpreted as a failure to select the appropriate actions. It is interesting in the light of the model proposed by Schultz (1997) that Redgrave *et al.* (1999b) also suggest that the early dopamine response may play a role in learning by placing the basal ganglia into a 'state of readiness' to modify selections on the basis of subsequent experience. Thus the Schultz (1997) and Redgrave *et al.* (1999b) models may not have to be mutually exclusive. A more realistic model of basal ganglia function may emerge from a fusion of these two models.

3 Computer Models of the Basal Ganglia

We have seen how theoretical models of basal ganglia function can aid our interpretation of experimental data. Both the Schultz (1997) and the Redgrave *et al.* (1999b) models have been implemented in computer models (Suri & Schultz, 1999; Humphries & Gurney, 2000; Montes-Gonzalez *et al.*, 2000). Computer models are particularly useful in attempts to elucidate the functioning of complex systems like the basal ganglia (Gillies & Arbuthnott, 2000). These two models use a top-down approach, trying to fit the basal ganglia architecture to the execution of a particular function. Where there is a wealth of experimental data, compiling this data into a meaningful theory of function can be difficult. An alternate approach to the top-down method of modelling is the bottom-up approach. Here, experimental data is collected together into a model that can be analysed for features that might help us to discern function. Both of these approaches are of the most use when they produce testable predictions about the behaviour of the system.

The complexity of both the intrinsic and extrinsic circuitry of the STN makes it difficult to discern its normal function. This system then may be one in which our understanding could be furthered by the use of computer models. Gillies and Willshaw (1995; 1996; 1998b) have used a multilevel approach, building two models of the STN; a network model, and a single cell model.

3.1 A Network Model of the Subthalamic Nucleus

Before it is possible to address the influence of the STN on the structures to which it projects, it is necessary to examine the information processing performed within the nucleus itself. By doing this we can discover how the nucleus will react to its various inputs.

The rat STN can be thought of as a single population of neurones, of which as many as 50% may possess intranuclear axon collaterals. The network model consisted of simplified model neurones called 'units'. These units were intended to capture three major computational properties of the STN projection neurone; these being:

1. A bounded firing rate up to a maximum of 500Hz.
2. A firing threshold.
3. The simple integration of afferent inputs (see Gillies and Willshaw (1998b) for further elaboration).

From the data of Nakanishi *et al.* (1987) the membrane potential-frequency relationship of STN neurones was calculated. Each unit was assumed to receive input from cortex and from the collaterals of neighbouring cells. The connectivity between neighbouring cells was calculated using a geometric model of the arrangement of the neurones within the STN. From this, it was possible to calculate the percentage of units in the STN that have an overlap of their dendritic field with a particular collateral (figure 3.1). The STN is estimated to contain 13,560 ± 1,410 neurones

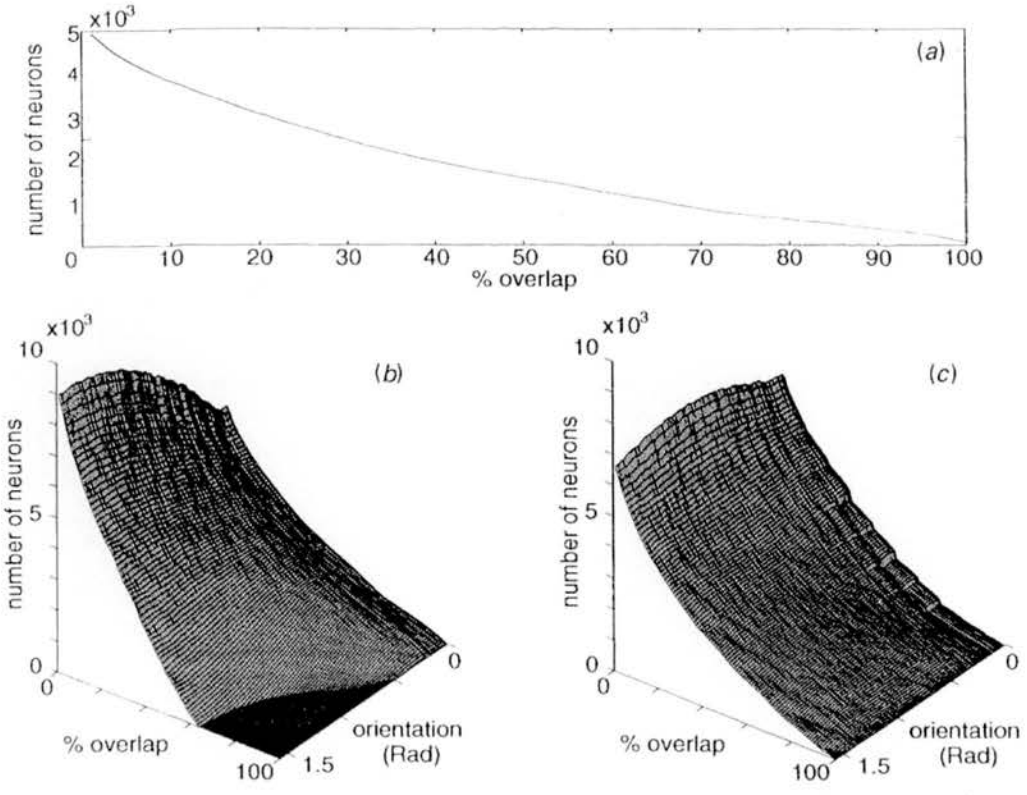

Figure 3.1 Results gained from the geometric modelling of the rat subthalamic nucleus. **A** shows the number of units whose dendritic field has at least a certain percentage overlap with any single collateral field. **B** and **C** show the effect of orientation and length of the axon collateral on the possible interconnectivity. Collateral lengths **B** = 200 μm; **C** = 100 μm. Taken from Gillies and Willshaw (1996).

(Oorschot, 1996), giving a neurone density of 138,000 cells.mm^{-3}. This gave an average of 4939 units having at least a 1% overlap with a given collateral field and 1557 units overlapping with over 50% of the field. In order to account for the number of assumptions made in the above calculations, the number of cells contacting each other within the network was constrained. This was done by assuming that one cell could only begin to affect another when there was a 50% overlap of its collateral field with the dendritic field of the second cell. Thus, any given collateral is capable of making significant contact with the dendritic field of roughly 1000 units meaning that a unit with three collaterals could theoretically make significant contact with up to a quarter of the nucleus. Of these cells contacted, half will have collaterals themselves each contacting up to another possible independent quarter of the nucleus. This gives a massive degree of interconnections including many recurrent connections. Even if it is assumed that only 10% of the significantly overlapping collaterals form synapses the degree of interconnectivity is huge.

The weight of each of these connections was calculated using a function of the distance between units and therefore the strength of the recurrent connections between them.

For simplicity, the first network model that was constructed only contained two units. This network was constructed in order to analyse with bifurcation theory (see Gillies and Willshaw (Gillies & Willshaw, 1998b) and Gillies (Gillies, 1995)) to find the set of asymptotic behaviours (figure 3.2). These behaviours are around

equilibrium points to which the system will tend to return following disturbance by any external influences. Depending on the conditions used, this two-unit network could either have one or two stable states. Figure 3.2A and C show examples of systems with only a single stable state, figure 3.2B shows an example of a system with two stable states. When the network was extended to the n-unit case the system proved more likely to reside above the critical point at which two stable states become possible. A single stable state would only be possible if the weight of the connections between units was very small.

These two network models above assumed full interconnectivity between the units in the STN. A 500-unit network was then constructed with a more realistic level of interconnectivity. This system was capable of three different asymptotic behaviours. A prebifurcation system had only a single equilibrium point, to which it always returned following the removal of any external input. This was the case if the connections between units were very weak. When the strength of the interconnections was increased, there also emerged two types of postbifurcation behaviour. A two-state system had two stable states between which the units activities could be moved by external inputs. These states corresponded to a low activity (resting) state and a high activity (500Hz) state. Finally, a single state, postbifurcation system was possible in which all units existed continuously in the high activity state. This was discarded as unrealistic, the parameters used being outside of biologically realistic constraints.

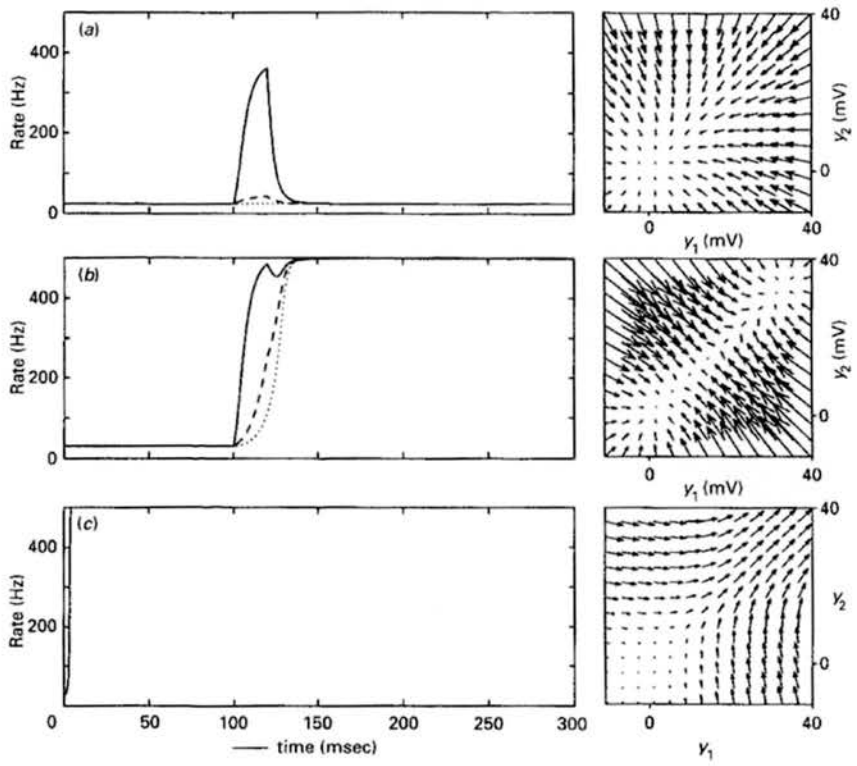

Figure 3.2 The three possible behaviours of units in the network model of the rat subthalamic nucleus. The first pair of graphs show data from a network in which there is only a single stable state at the resting firing rate of the units. Units receiving excitatory inputs respond with a brief pulse of excitation before returning to rest. The next pair of graphs show data from a network in which the units have two stable states, one at rest and one near their maximum firing rate. Neurones receiving an excitatory input are moved from their resting state to the high activity state. The lower pair of graphs show data from a network which again has only a single stable state. This time the stable state is at the maximum firing rate of the units. Thus the units immediately move to this state and are unaffected by excitatory inputs.

In addressing the prebifurcation system, we need to ask what the function of very weak interconnections, in a system containing a large number of such connections, would be. A network containing weak lateral connections was compared to a network that had no lateral connections. It was found that weak lateral connections led to a doubling of the resting firing rate and an increased response to external inputs. The response to such an input was also spread more widely around the network.

Due to the observation that neurones in the STN are highly interconnected, it was predicted that the second system would be more likely to occur. Even when the weights of the interconnections are relatively low this system generated postbifurcation behaviour. This produced the possibility of a state known as *hysteresis*, a persistent hyperactive state in which each unit receives sufficient input from other units in the network to maintain it at a high level of activity. Such a state has never been observed in neurones of the STN and would seem to be undesirable, as it would be liable to cause excitotoxic damage within the nucleus itself, and at the nuclei to which the STN neurones project. The persistent hyperactive state is stubborn and can only be attenuated by a diffuse inhibitory input over the entire network.

This postbifurcation system predicts a response widespread across the entire network following an external input. Fujimoto and Kita (1993) have observed such a response, although this behaviour was much more complex than the behaviour of the model. The model also predicts that non-synchronous correlation in activity should

be more likely in the high activity state than the low activity state. This fits the observations of Ryan *et al.* (1992) that there is little correlation between the firing of STN neurones when they are at rest.

As we know that the STN manages to avoid being trapped in a state of persistent hyperactivity, it was necessary to ask what features the model is missing that would enable this to be the case. One possibility was to add a delay on the lateral connections, this made it more difficult for the system to reach the persistent hyperactive state. Gillies suggested that, on becoming persistently hyperactive, the recurrent connections between the STN and the GP could provide a massive wave of inhibitory feedback to the neurones of the STN forcing them back to their resting state. It is also possible that the simplification of the STN neurones used to produce the network model may have missed a membrane property of the neurones that could stop them from becoming persistently hyperactive. For this reason, Gillies produced a more complex model of a single STN neurone.

3.2 A Model of a Single Subthalamic Nucleus Neurone

In order to capture accurately the computational behaviour of a particular neurone it is necessary to consider the ion channel dynamics and composition that underlie the behaviour. The classical approach to modelling the membrane properties of neurones, which is still used today, is to assume that an electrically excitable membrane involving many populations of different channel types can be described

by a simple electrical circuit (Hille, 1992). The properties of each population of channels are described by its membrane conductances. This is the method that Gillies (1996) used for his model of the single STN projection neurone. In doing this, he encountered two main problems. Firstly, there were no data available on the kinetics of individual ion channels in the STN. Secondly, there are little data as to the actual channel composition of a STN neurone. However, it was possible to use known properties of certain types of ion channel from other populations of neurones to consider the channel composition that would be necessary to produce the observed behaviour of STN neurones.

The soma of the neurone was idealised to be perfectly spherical with an average diameter of 18.8μm yielding a surface area of 110μm. The neurone had two primary dendritic trees that were reduced to equivalent electrical cylinders. The capacitance of the cell was $1\mu F.cm^{-2}$, its membrane time constant 6ms, the passive membrane resistance $6000\Omega cm^2$, and the cytoplasmic resistance $123\Omega cm$. For a complete description and derivation of the properties of the model cell see Gillies (1995; 1996).

It was assumed that STN neurones contain the voltage-gated sodium and potassium channels (NaCh and KCh respectively) that are necessary for the generation of action potentials. From the data of Nakanishi *et al.* (1987) low voltage activated (LVA) calcium T-channels (Ca(T)Ch), an amalgamation of the high voltage activated (HVA) L- and N- type calcium channels, and calcium activated potassium channels (K(Ca)Ch) were also added. All of these channels had kinetics of the Hodgkin-Huxley form (see Hille (1992)). It was necessary to modify the kinetics of both the

NaCh and the KCh as no known kinetics for these channels were able to reproduce the high frequency firing rates observed in STN neurones.

The model neurone had a resting potential of -52mV, which is very close to the threshold for firing action potentials. Hyperpolarising injections of current demonstrated the characteristic fast time constant and also an inward drift towards the resting potential due to mild activation and subsequent inactivation of Ca(T)Ch. Post current injection spikes, similar to those seen experimentally were observed after the removal of significantly hyperpolarising currents due to the de-inactivation of Ca(T)Ch during the hyperpolarisation. The model cell also demonstrated the initial clustering of spikes observed by Nakanishi *et al.* (1987). This was shown to be due to the inactivation of Ca(T)Ch.

Many authors have observed a post-response inhibition of neurones of the STN both *in vitro* and *in vivo*. It was clear from the observations that this inhibition was not due to inhibitory input from other nuclei. Fujimoto and Kita (Fujimoto & Kita, 1993) propose that the inhibition may be due to cortical disfacilitation similar to that observed in striatal neurones. Gillies (1995; 1996) points out, however, that because of the significant intranuclear connections of the STN and the widespread response to cortical stimulation, this post-response inhibition could be caused by an intrinsic property of the neurones' cell membranes. The model cell predicts that there will be such and intrinsic, calcium dependent, post-response hyperpolarisation of 100 - 500 ms, which is not observed in a calcium free medium.

3.3 A Hypothesis of the Function of the Subthalamic Nucleus Based on the Predictions of the Two Models

The network model of the STN demonstrated a clear likelihood that the STN could enter a persistent hyperactive state. In this state, all of the neurones of the STN would be firing at, or near to, their maximum firing rate of around 500 Hz. It is obvious that, if this state were to persist for any length of time, it would result in the death of these neurones. However, the model also revealed that the attractor to this state is small and thus, any mechanism that could slow the firing of all of the neurones could be enough to pull the nucleus back to its resting state. The single cell model showed that Ca(T)Ch inactivation may provide such a mechanism which, when combined with GABAergic feedback inhibition from the GP could stop hysteresis once it had started. Thus, the two models combined predict that the STN is likely to respond to excitatory input from the cortex or thalamus with a massive wave of excitation during which all of the STN neurones will be firing at their maximum rate. This wave of excitation will be brief as it would lead to both inactivation of Ca(T)Ch, slowing the firing rate, and a pulse of feedback inhibition from the GP. Gillies (1995) termed this the 'subthalamic nucleus pulse'.

Such uniform and widespread excitation has been observed to follow cortical stimulation *in vivo*. However, it is unclear from these experiments whether the spread of activity occurs in the cortex or the STN (or in between the two). The model predicts that the internal connections in the nucleus are sufficient to account for this spread of activity. Fujimoto and Kita (1993) also observed a significant reduction in firing rate following this widespread excitation; a phenomenon also exhibited by the neurones in the models.

The generation of this pulse will be under the control of both cortical and thalamic inputs, and the striatal inputs (*via* the GP). Such a pulse would produce a massive uniform excitation of the target structures of the STN, principally the EP and SNr. Kitai and Kita (1987) have shown that different conduction velocities along the branches of the axons of STN neurones means that the pulse would reach both the EP and the SNr at the same time. It is possible, due to the arrangement of terminals in the EP and SNr, that such a pulse of excitation from the STN could override all other inputs. The EP and SNr are the output structures of the basal ganglia, sending inhibitory projections to the thalamus and brain stem. This has lead Gillies to propose that the STN pulse acts as a brake, terminating processing in the EP and SNr and providing a wave of inhibition to their targets.

When thought of in terms of the disorders of the basal ganglia it is possible to see that PD, which by the model of Albin *et al.* (1989) should result in a reduced inhibitory input to the STN from the GP, will render the STN pulse more likely to occur. When pulses do occur in this situation, they may also have a longer duration.

Pulses that occur at inappropriate times and that have too long a duration may underlie the hypokinetic nature of many of the symptoms of PD. Such a theory is supported by evidence that surgical techniques that reduce or remove the influence of the STN alleviate Parkinsonian symptoms. The opposite of this situation may occur in Huntington's Disease and ballism. Here, damage to the STN may result in the loss of these pulses. This loss of braking may lead to the inappropriate movements seen in this hyperkinetic disorder.

4 How do Neurones in the STN Fire so Fast?

4.1 Introduction

We have seen that a striking feature of the STN is the high frequency at which its component neurones are capable of firing. This can be as high as 500Hz both in vitro (Nakanishi *et al.*, 1987) and in vivo (Fujimoto & Kita, 1993). Gillies and Willshaw (1995; 1996) found that the kinetics used for modelling the voltage-gated sodium channels (NaCh) and potassium channels (KCh) of neurones, which were derived from hippocampal pyramidal neurones, were insufficient to account for such a high firing rate. Therefore it was concluded that these neurones might contain hitherto undescribed members of the NaCh or KCh families. Experiments were therefore performed in order to try to characterise some of the kinetics that underlie this high frequency firing. These aimed (1) to investigate the recovery kinetics of the spike inactivation and (2) to ask what is the contribution of NaCh inactivation to the frequency of firing particularly focusing on the role of the β-subunit composition of these channels.

When a sufficiently large depolarising pulse of current is delivered to a STN neurone to cause it to fire at rates up to its maximum rate, the action potentials reduce in size over the course of the pulse. Often the neurones will stop firing before the end of the pulse. Figure 4.1 shows a representative trace from an STN neurone. Upon depolarisation this neurone fires at a peak rate of around 300 Hz but the spikes

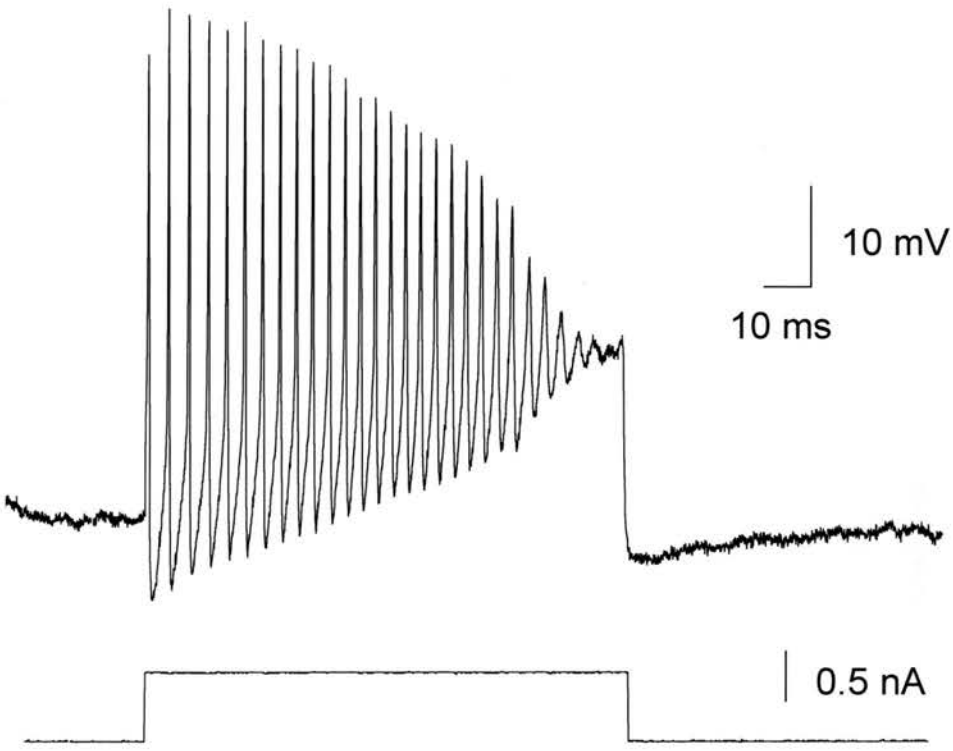

Figure 4.1 Depolarisation block of a subthalamic nucleus neurone. The neurone was depolarised from a holding current of -0.1 nA to 0.6 nA for 100 ms. From the start of this current pulse there was a rapid increase in the firing rate of the neurone to a peak at around 300 Hz. Over the course of the current pulse the neurone becomes subject to depolarisation block. The action potentials get smaller until they fail just before the end of the current pulse.

rapidly get smaller until the neurone stops firing altogether. This phenomenon ('block') can be largely attributed to a build-up of inactivation of the voltage-gated ion channels that underlie action potential generation. In particular the NaCh are likely to play a role in this (Jung *et al.*, 1997). However the involvement of KCh, calcium channels and calcium activated potassium channels can not be ruled out totally. NaCh are responsible for the rapid depolarisation that forms the rising phase of the spike. Inactivation of these channels therefore would eliminate spikes completely. KCh are responsible for the repolarisation that forms the falling phase of the spike. Inactivation of these channels would reduce the rate of repolarisation and disrupt subsequent action potential generation. The role of calcium channels and calcium activated potassium channels in action potential generation is less well defined. Calcium channels can generate slow action potentials in the absence of the sodium dependent fast action potential. Opening of calcium channels may lead to a gradual depolarisation of the cell, which could accelerate the formation of block. Calcium activated potassium channels are responsible for the slow afterhyperpolarisation (AHP) that follows a train of action potentials in the STN (Bevan & Wilson, 1999), and elsewhere. Activation of these channels could hyperpolarise the cells and prevent spiking from occurring. However, inactivation of NaCh appears to play the major role in the development of depolarisation block.

It was decided that it might be possible to use this phenomenon to gain an estimate of the time it takes the NaCh to recover from this inactivation. In the classical voltage-clamp experiments the rate of recovery from NaCh inactivation is measured using a protocol that involves two holding potentials. The neurones are initially held at a

lower potential at which inactivation does not occur. Test depolarisations are made to a higher holding potential at which inactivation does occur. The cells are held at this test potential for long enough for complete inactivation of NaCh to occur. Two such test pulses are used separated by a gap of time *t*. The maximum current *I* that flows in the second pulse is expressed as a proportion of the maximum current I_{max} that flowed in the first pulse. Plots of I/I_{max} against *t* reveal the time-course of recovery from inactivation (figure 4.2A). These plots are usually fitted to either a single or a double exponential curve from which the time constant τ_h can be calculated (figure 4.2B). It was decided that an adaptation of this protocol might be useful for investigating the recovery from depolarisation block. Two depolarising current pulses of sufficient size to induce this block could be delivered separated by a recovery period. The length of this gap between the two pulses could be varied. Comparing measurements of the amount of time it takes the cell to block during the pulses before and after the gap would allow the recovery from block to be estimated. A plot showing the time-course of recovery could then be constructed. This plot would allow the estimation of the rate of de-inactivation of NaCh represented by the time-constant τ_h. This time constant is voltage dependent and so estimation of recovery at a wide range of membrane potentials would be necessary for complete characterisation of the inactivation kinetics of NaCh. However, for the purposes of these experiments, a single estimate of τ_h is sufficient for comparison with previous data.

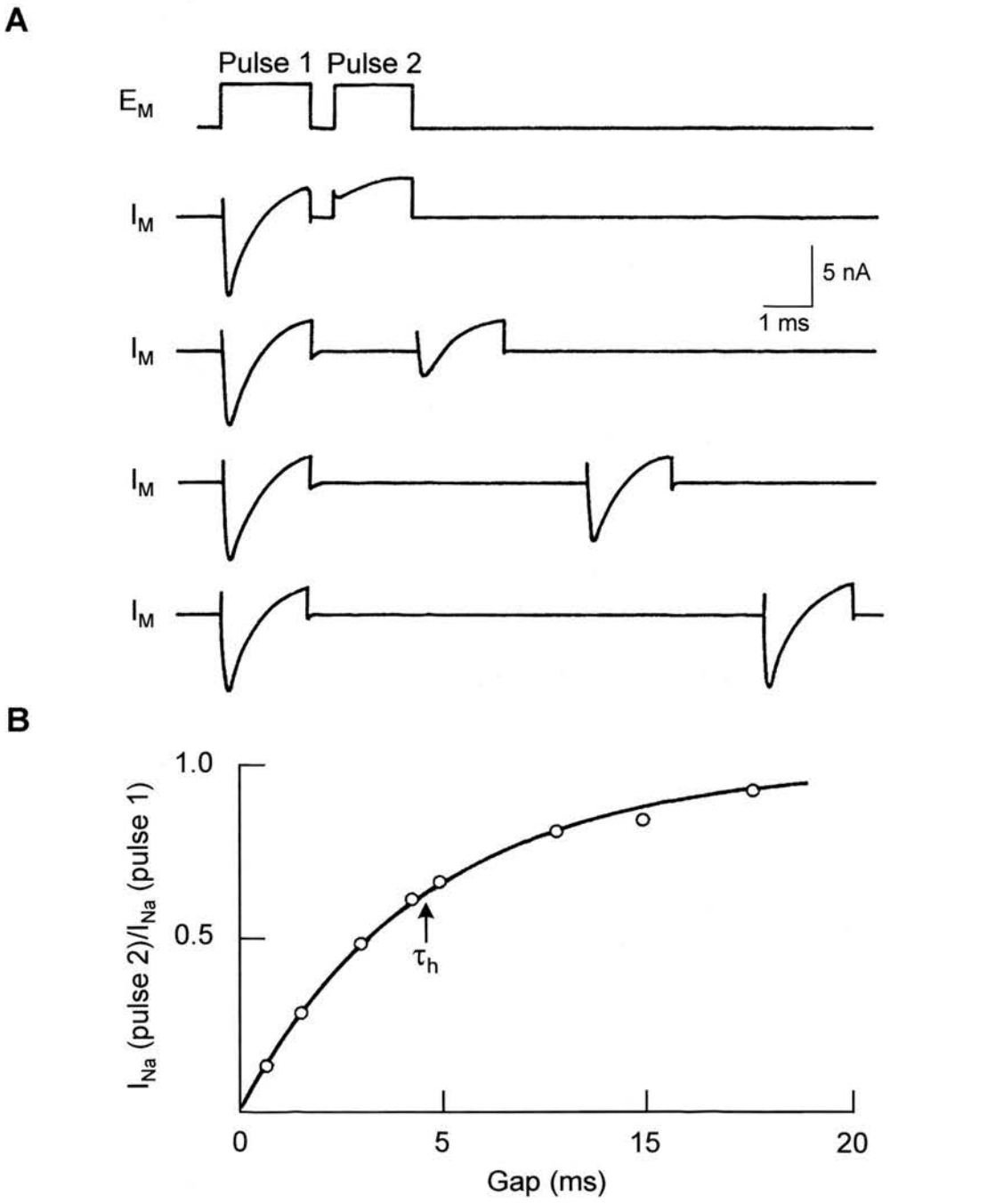

Figure 4.2 The two-pulse protocol for the investigation of the inactivation kinetics of voltage gated sodium channels. **A** Two pulses are delivered to a frog node of Ranvier, stepping the membrane potential from -75 mV to -15 mV. The gap between these pulses is increased with each successive sweep. **B** The peak current to flow during each pulse (I_{Na}) is measured and the ratio I_{Na} (pulse 2)/ I_{Na} (pulse 1) calculated. This ratio is plotted against the length of the gap between the pulses to give a curve from which the time constant τ_h can be calculated. Adapted from Hille (1992) p.45.

Voltage gated sodium channels are thought to consist of a single 260 kDa transmembrane α subunit. This is associated with two β subunits, a 36 kDa β1 subunit and a 33 kDa β2 subunit (figure 4.3). The α subunit has four transmembrane domains, which together form a pore. When expressed in *Xenopus* oocytes the α subunit is capable of forming a functional NaCh (see references in Catterall (1992)). The β subunits however do not form functional NaCh when expressed in the absence of the α subunit. This subunit has a substantial extracellular domain with only a single membrane-spanning α-helical segment. Expressed alone, α subunits show abnormally slowed inactivation. However, co-expression with the β1 subunit accelerates inactivation. Interestingly this coexpression also increases the size of the peak sodium current. When the α subunit was expressed alone step depolarisations from -100 mV to -10 mV revealed a τ_h at -10 mV of 6.27 ± 1.24 ms. But when the α subunit was coexpressed with the β1 subunit the value of τ_h derived using the same protocol had decreased to 1.15 ± 0.14 ms (Isom *et al.*, 1992). This evidence suggests that the function of the β subunits may involve the modulation of the rate of NaCh inactivation.

If neurones in the STN were found to have altered NaCh inactivation it may be due to changes in the expression of either the β1 or β2 subunit. Therefore it was decided to investigate the β-subunit composition of NaCh in the STN using immunohistological staining with antibodies raised against these proteins.

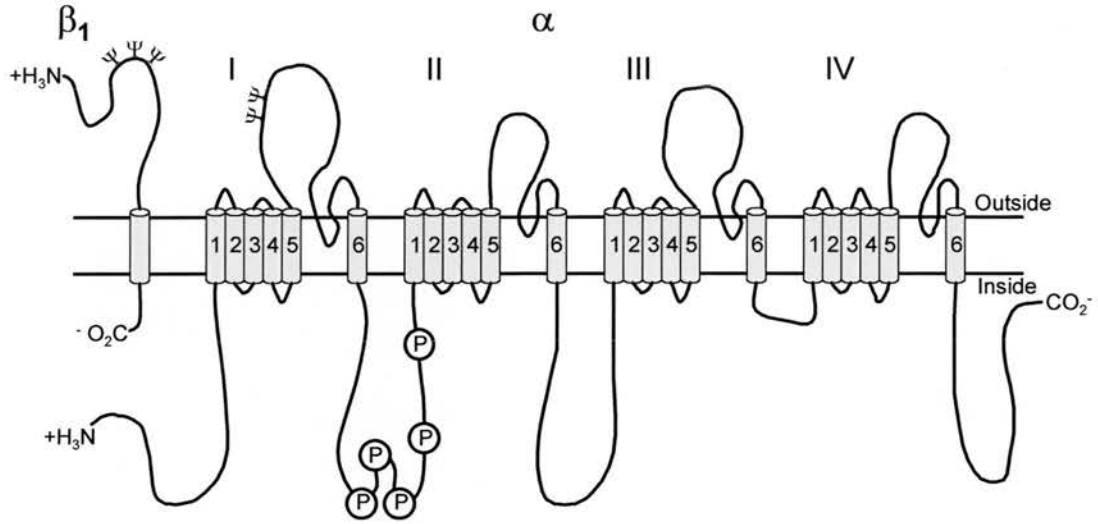

Figure 4.3 The structure of the rat brain voltage gated sodium channel. The α subunit consists of four membrane spanning domains (I to IV) each of which contains six transmembrane α-helices (represented by cylinders). The β_1 subunit consists of only a single transmembrane α-helix with a short intracellular section and a longer extracellular loop. Ψ represents a glycosylation site. P in a circle represents a phosphorylation site. Adapted from Catterall (1992) p.S24.

It was necessary to show that the records made in the present experiments were obtained from STN neurones that had the same basic characteristics as those STN neurones that have been described previously (Hammond & Yelnik, 1983; Kita *et al.*, 1983b; Afsharpour, 1985; Kita & Kitai, 1987; Nakanishi *et al.*, 1987; Beurrier *et al.*, 1999; Bevan & Wilson, 1999; Beurrier *et al.*, 2000). In order to do this, protocols for calculating the relationship between injected current and either membrane potential (I-V curves) or firing frequency (I-f curves) were adapted from Nakanishi, *et al.* (1987). Some cells were also filled with biocytin to confirm their location and compare their morphology with previously described STN neurones.

4.2 Methods

4.2.1 Electrophysiology

Artificial cerebrospinal fluid (aCSF) was made according to recipe 1 (see appendix A). This was made in two components; a normal component ($aCSF1^N$) and a sodium and calcium free, sucrose-containing component ($aCSF1^S$). Male Sprague-Dawley rats (150 – 300 g) were anaesthetised with avertin (1 ml/100 g; See appendix A, recipe 3). They were then decapitated, their brains rapidly removed and placed into a beaker containing ice-cold $aCSF1^S$ which had previously been saturated with carbogen (95% Oxygen, 5% Carbon Dioxide). Blocks of the brains were cut which contained the subthalamic nucleus and these were glued onto a Teflon chuck. This was then secured in place in a well containing ice-cold $aCSF^S$. 400 μm slices of brain were cut using a vibroslice (figure 4.4) and placed in a holding chamber (Krimer &

Goldman-Rakic, 1997). One or two slices were moved to the recording chamber (figure 4.5) where they were placed on a small rectangle of lens tissue (18×42mm) that was mounted on a wire mesh, angled at roughly 3° to the horizontal. The slices were continually perfused with aCSF1^{N} at 35° C, which entered the chamber through a well into which one end of the lens tissue was submerged. Thus the aCSF was drawn over the lens tissue (and brain slices), down the gradient, and into a second well where it was removed with a suction pump. Microelectrodes were pulled from glass capillaries (O.D.=1.5mm; I.D.=0.86mm; Clark Electromedical Instruments) using a Flaming-Brown micropipette puller (Sutter Instrument Co., USA; Model P-80 PC). These were filled with 1.5mM KCl, and mounted in an electrode holder (Axon Instruments Inc. (Axon)). The electrode holder was connected to an Axoclamp 2B amplifier (Axon). Experimental protocols and online analysis of data were controlled using a microcomputer (Research Machines, Pentium II PC) running Clampex 7 (Axon). This was interfaced to the amplifier using a Digidata 1200A (Axon) DAC/ADC. Data was also saved on the computer for offline analysis using Origin 5 (Microcal Software, Inc. USA).

The electrode puller was programmed to give electrodes with a resistance of between 90 and 150 MΩ. The STN was targeted visually as a small disk of grey matter on the surface of the internal capsule (figure 4.4B). STN cells were identified by their characteristics of regular firing of action potentials when at rest (between 4 and 40 Hz), rectification of membrane potential during hyperpolarising current injection, and rebound firing of action potentials following injection of hyperpolarising current. Once a cell was obtained a small continuous injection of hyperpolarising current was

Figure 4.4 A photomicrograph showing a parasagittal section of the rat brain showing the extent of the slices used in the electrophysiological preparations. The subthalamic nucleus can be seen as a small oval area in the centre of the lower portion of the photograph.

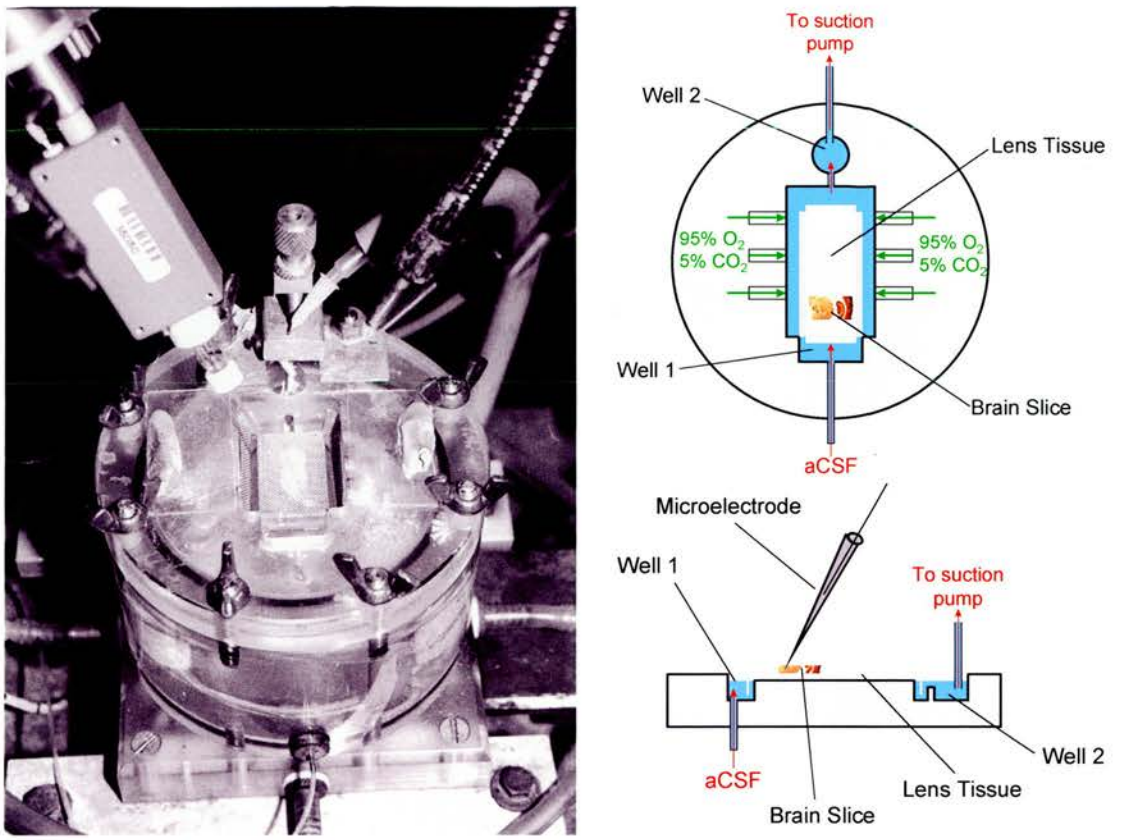

Figure 4.5 The Interface Recording Chamber. The diagrams on the right represent a plan and cross-section view of the recording chamber shown in the photograph on the left. The brain slice was placed on a small rectangle of lens tissue that was mounted on a wire mesh. This wire mesh had been fixed into the recording chamber at an angle of roughly 3° to the horizontal. The leading edge of the lens tissue was dipped into well 1. Artificial cerebrospinal fluid (aCSF) entered the chamber through well 1 where it was drawn over the lens tissue and the brain slice by capillary action. Waste aCSF overflowed left the chamber through an overflow into well 2 where it was sucked out by a suction pump. The chamber was continuously perfused with 95% O_2, 5% CO_2 which was heated by bubbling it through a water bath at 35° C. The same water bath was used to maintain the temperature of the recording chamber at 35° C.

applied. The amount of current used was adjusted to be just enough to arrest the spontaneous firing of action potentials. Using a similar protocol to that used by Nakanishi *et al.* (Nakanishi *et al.*, 1987), stepped 150 ms pulses of current were applied starting at -1 nA and increasing in steps of 0.2 nA up to +0.4 nA (figure 4.6A). Measurements of the cell's membrane potential were taken as close to the end of the current pulse as possible. Graphs of injected current (x) against membrane potential (y) were then constructed and the steepest section of the resulting I-V curve was fitted with a straight line of the form:

$$y = mx + c$$

where m is the gradient of the line and is therefore an estimate of the membrane input resistance, and c is the membrane potential when there was no injected current. Because the cells fired at rest and this was stopped with a small constant injection of hyperpolarising current, c does not represent the true resting potential of the cell. An estimate of the resting potential was therefore calculated by solving the equation for the situation when $x = -1 \times$ *injected constant current*.

To investigate the relationship between injected depolarising current and action potential firing frequency cells were injected with either incremental steps of depolarising current (figure 4.6B) or a ramped depolarising current (figure 4.6 C). Instantaneous firing frequency (f) was calculated from the interspike intervals (ISI). ISI was defined as the time in ms between two successive action potential peaks giving:

$$f = 1000 * (1 / ISI)$$

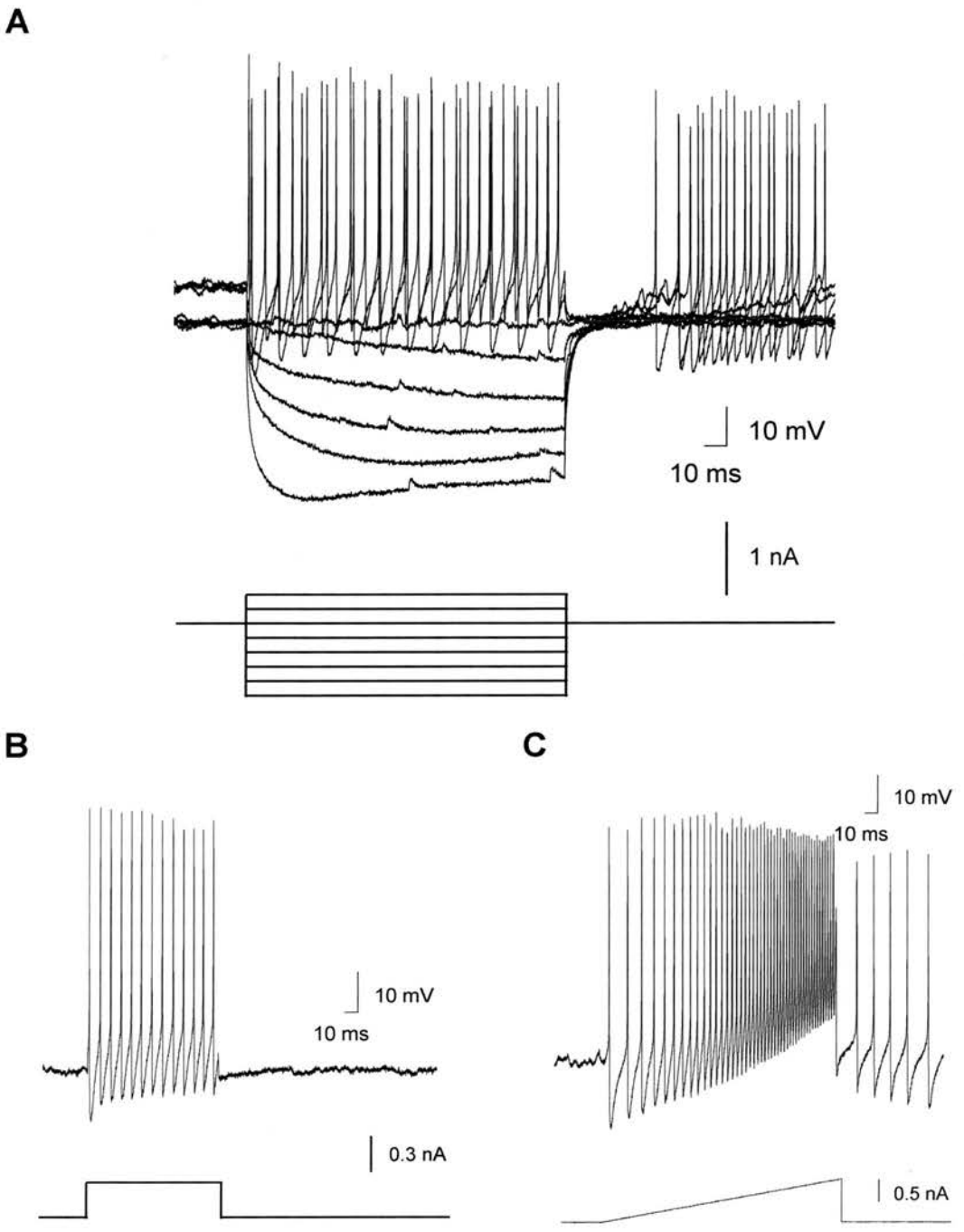

Figure 4.6 Three experimental protocols used in the characterisation of subthalamic nucleus neurones. **A.** The cell is given a series of 150 ms current pulses starting from -1 nA and increasing by 0.2 nA each sweep up to +0.4 nA. **B.** A train of action potentials fired in response to a 100 ms current step of 0.3 nA. This is one of a series of depolarising current steps. The last interspike interval from each train of action potentials was used in the construction of the relationship between injected current and firing frequency. **C.** Response to a ramp current pulse going from 0 to 1 nA over 150 ms.

I-f curves were then constructed using the last ISI of each train in the stepped pulse protocol or every ISI in the ramp protocol.

Having characterised the neurones in this manner a two-pulse protocol was used to assess the rate of recovery of the cells from depolarising block. This consisted of two large (>1 nA) pulses of depolarising current separated by a gap of varying time. The time taken for the cell to block (time-to-block; TTB) was defined as the time from the peak of the first action potential in the train to the peak of the last action potential to reach 15 mV above the membrane potential during block (figure 4.7). A ratio was calculated for the time-to-block after the gap (TTB_{after}) divided by the time-to-block before the gap (TTB_{before}). This was plotted against the length of the gap. This data was then fitted to a curve, which could be represented either by a single exponential equation of the form:

$$TTB_{after}/TTB_{before} = 1 - exp(-t/\tau_h) \quad - \quad Exponential\ 1$$

where t is the gap, τ_h is the time constant (Ragsdale *et al.*, 1991), or by a double exponential equation of the form:

$$TTB_{after}/TTB_{before} = 1 - (c1 \times exp(-t/\tau_f) + c2 \times exp(-t/\tau_s)) \quad - \quad Exponential\ 2$$

where t is the gap, τ_f is the fast time constant, and τ_s the slow time constant (Ragsdale *et al.*, 1991; Virginio & Cherubini, 1995). At the end of the experiments some cells were filled with biocytin (Nε-Biotinyl-L-lysine) hydrochloride (Sigma-Aldrich Company Ltd., Poole, UK). If this was done then the solution with which the electrode had been filled at the start of the experiment had been substituted with 1.5 M KCl containing 5% biocytin. Cells were filled using repetitive -1 nA current pulses at 2.5 Hz (200 ms on; 200 ms off) for 20 minutes.

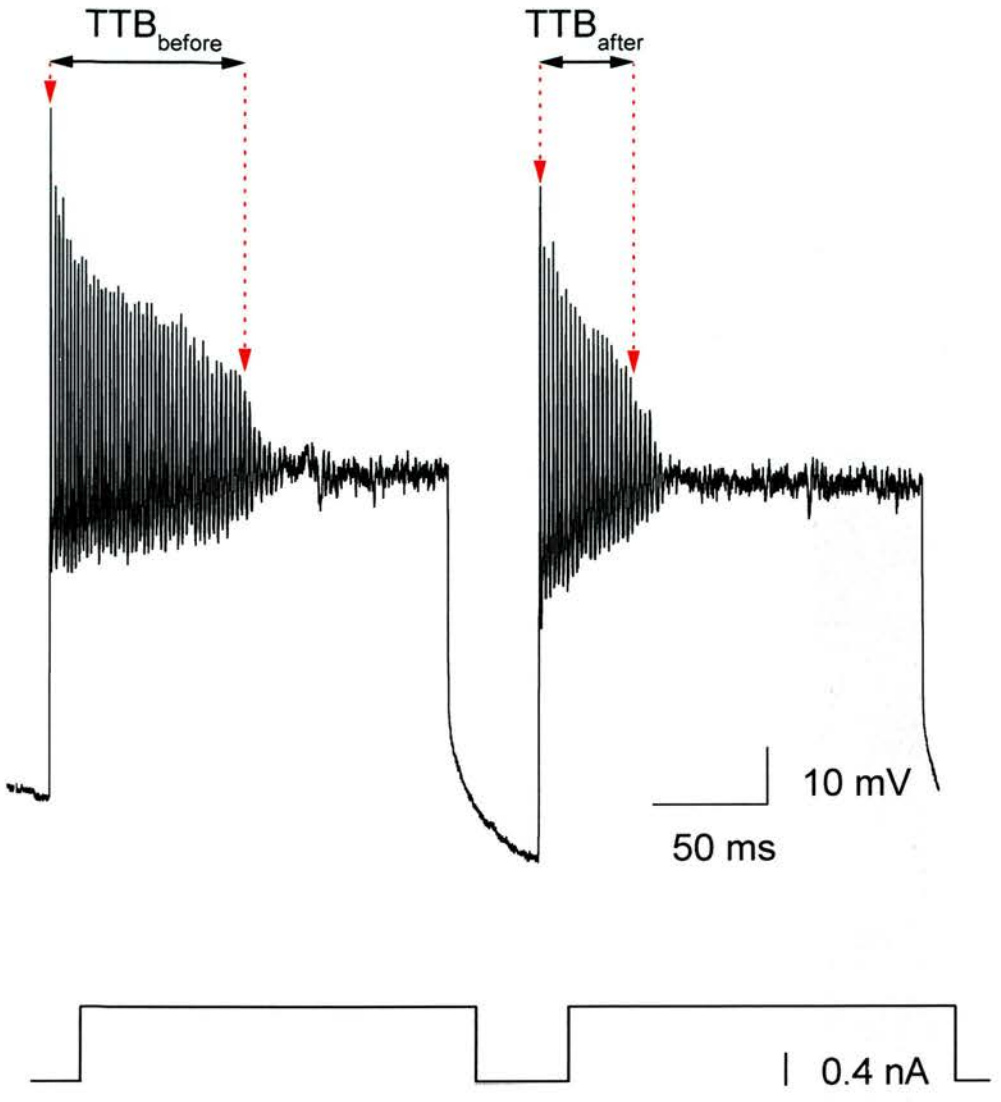

Figure 4.7 Measurement of the amount of recovery from depolarisation block that occurs during a gap between two depolarising current pulses. Two 150 ms current pulses of at least 1 nA were delivered separated by a gap of variable width. Time to block (TTB) was measured as the time from the peak of the first spike in the train to the peak of the last spike to be at least 15 mV above the membrane potential during depolarisation block. TTB was measured before (TTB_{before}) and after (TTB_{after}) the gap.

4.2.2 Immunohistochemistry for Sodium Channel β subunits.

Adrian Corbett conducted the following experiments.

50μm sections of rat brain were stained using antibodies raised against the NaCh β_1 and β_2 subunits. These antibodies were acquired by injecting hens with the purified subunits and harvesting the antibodies from their eggs as described by Jarnot & Corbett (1995).

Young male Sprague-Dawley rats (200 - 250 g) were deeply anaesthetised with pentobarbital and perfused intracardially with 25 ml of sodium phosphate buffered saline (PBS), then 70 ml of 4% paraformaldehyde in 0.01M PBS, pH 7.3. Brains were removed, post-fixed in PBS-paraformaldehyde, and stored at least overnight in 15% sucrose-PBS at 4°C. 50μm free-floating coronal sections were cut on a freezing microtome and collected into PBS. Sections were blocked for one hour in PBS-0.1% Triton X-100 with normal goat serum added (PBST-NGS), then incubated overnight at room temperature with primary antibody, or antibody pre-absorbed with peptide. After incubation, sections were washed with PBS-Triton and then incubated with biotinylated goat anti-rabbit IgG (1:10 dilution in PBST-NGS; Vector Laboratories, Burlingame, CA, USA) for two hours with an avidin-biotinylated horseradish peroxidase conjugate (ABC reagent; Vector). After a final wash, antibody binding was visualised by reacting sections with 3',3-diaminobenzidine tetrahydrochloride (20mg/ml Tris, pH 7.6 + 33 μl 30% H_2O_2).

In each experiment, control sections were included that were incubated with antibody pre-absorbed overnight with different concentrations of peptides derived from β1 or β2 NaCh subunits.

4.2.2 Immunohistochemistry for Biocytin.

In a proportion of the experiments STN neurones, from which intracellular records were taken, were filled with biocytin. At the end of these experiments the brain slices were fixed overnight with 2% paraformaldehyde and 1.25% glutaraldehyde in 0.1M phosphate buffer (pH 7.4). The following morning the slices were transferred to a 50:50 solution of fixative and 20% aqueous sucrose and left in this solution for between 3 and 24 hours.

These 400 μm sections were then re-cut on a freezing microtome into sections of 50 μm thickness and collected in 0.05 M PBS (pH 7.4). The sections then received four 10 minute washes in PBS before being left for 30 minutes in a solution of 1% hydrogen peroxide and 30% methanol in PBS. Following this the slices were given a further seven 10 minute washes to completely rinse off the hydrogen peroxide. The sections were then incubated in PBS containing 0.3% Triton X-100 (PBS-TX) for 5 hours at room temperature and placed into Elite ABComplex (Vector Laboratories Ltd., Peterborough, UK), using a 1:50 dilution in PBS-TX, for 60 hours at 4°C. Following this the slices receive a further two ten minute washes in PBS (no Triton X-100) and were incubated in 3,3′-diaminobenzodine (DAB; Vector Laboratories Ltd., Peterborough, UK) for 10 minutes at room temperature. After another four 10

minute washes in PBS the slices were mounted on gelatine coated slides and left to dry for one week in an oven at 45°C. The slices were then dehydrated in a graded series of increasing concentrations of ethanol. This involved being left for 2 minutes in each of the following: 70%, 90%, and three sets of 100% ethanol before being placed in two separate sets of xylene for two minutes each set. Coverslips were then placed on the slides using DPX mountant (Merck Ltd., Lutterworth, UK).

4.3 Results

Intracellular recordings from 8 cells were selected for full analysis. Selection was made on the grounds of the electrophysiological properties of the cells, the criteria used being the same as those used by Nakanishi, *et al* (1987). Specifically these were that the membrane potential should be more negative than -40 mV and action potentials should have an amplitude great enough to cross 0 mV. The membrane potential element of these criteria was adjusted slightly to fit the protocols used in the current experiments. Cells were selected for inclusion if the membrane potential at which they stopped firing (i.e. during the continuous hyperpolarising current injection) was more negative than -40 mV. This was because all cells fired at rest making accurate online measurement of a resting membrane potential difficult. This method of selection meant that, when the final estimate of resting membrane potential was calculated, it was found to be less negative than -40 mV for some cells.

4.3.1 Characterisation

I-V curves were plotted using a series of negative through to positive current steps with a duration of 150 ms. The positive pulses caused all cells to fire action potentials and so this section of the curve gave unreliable measurements of the membrane potential and was not used for the calculation of resistance. Figure 4.8A shows a typical response of an STN neurone to a pulse of hyperpolarising current, this shows the characteristic rectification and rebound depolarisation which results in the firing of action potentials. Figure 4.8B shows a typical response of an STN neurone to a pulse of depolarising current, this includes the firing of action potentials and a long-lasting afterhyperpolarisation (total extent not shown). Figure 4.8C shows overlaid the typical responses of an STN neurone to a sequence of current pulses starting at -1.0 nA and increasing by +0.2 nA with each step to a maximum of +0.4 nA. The membrane potential at the end of each current pulse was measured and plotted against the injected current. Figure 4.8D shows an example of an I-V curve plotted in this way. These curves were generally sigmoidal in shape and so the input resistance was calculated from these plots by calculating the gradient of a line fitted to the steepest section of the curve. In this way the mean (± S.E.M.) input resistance of the STN neurones used in this study was found to be 70.61 ± 15.04 MΩ (range: 26.00 MΩ to 145.50 MΩ). The resting membrane potential of the STN neurones was also calculated using the lines fitted to the steepest section of the *I-V* curve. The mean resting potential of the STN neurones used in this study was found to be -45.64 ± 4.08 mV (range: -56.95 mV to -31.32 mV).

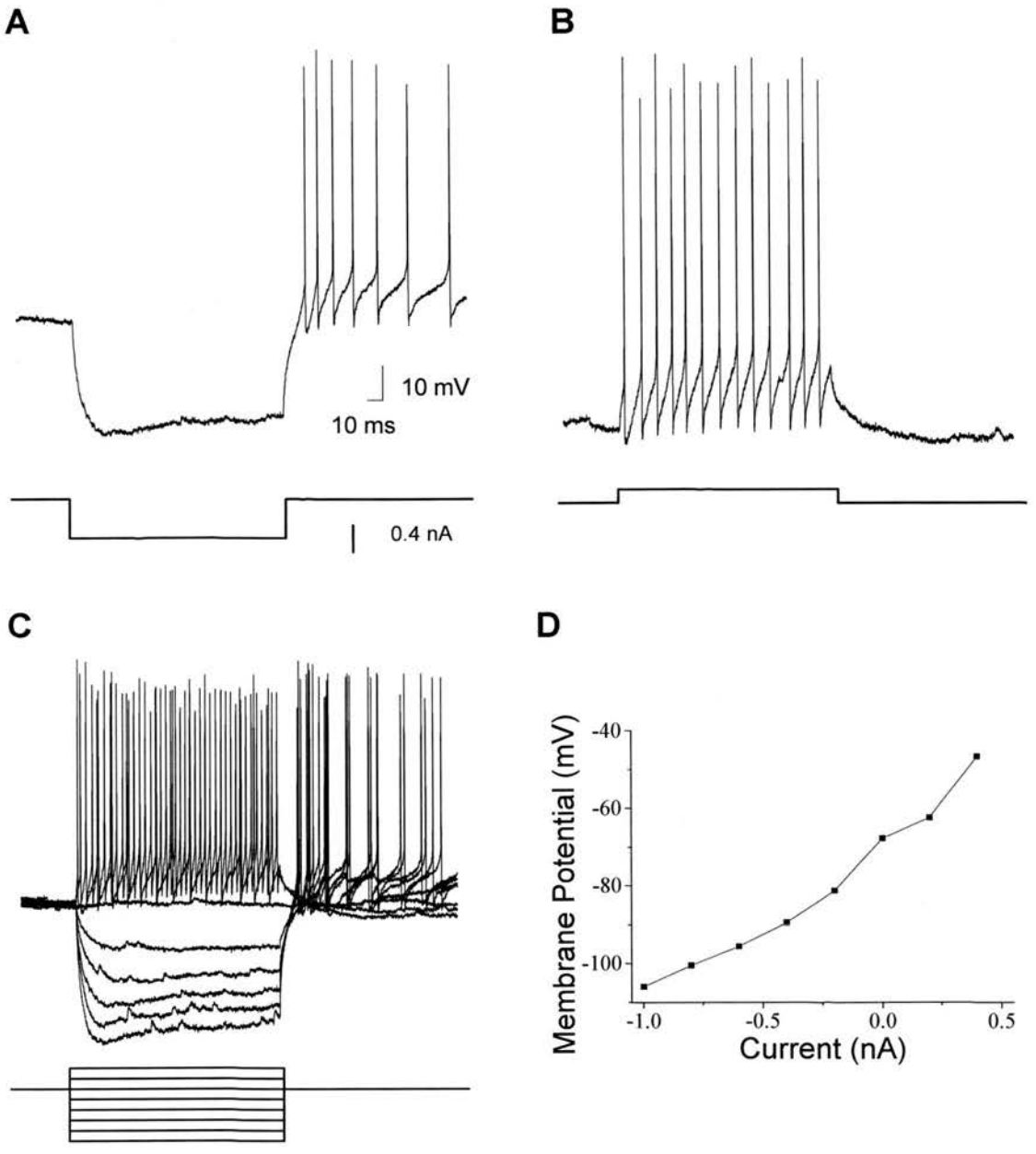

Figure 4.8 Recordings from a subthalamic nucleus neurone. **A.** Response to a 150 ms hyperpolarising current pulse of -0.6 nA. The neurone shows many of the characteristics of a subthalamic nucleus neurone including inward rectification and action potentials fired on a rebound depolarisation. **B.** Response to a 150 ms depolarising current pulse of 0.2 nA. The neurone fires action potentials and becomes slightly hyperpolarised when the current is removed. **C.** Overlaid traces showing the responses to the entire series of current pulses from -1.0 nA to 0.4nA. The traces shown in **A** and **B** formed a part of this series. **D.** The relationship between injected current and membrane potential derived from the recordings shown in **C**. The input resistance of this cell was calculated to be 67.5 MΩ.

A

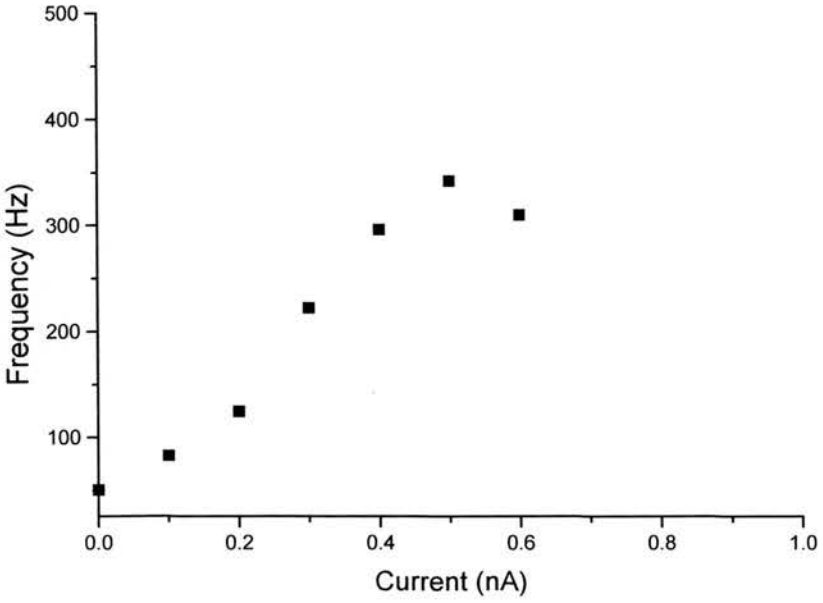

B

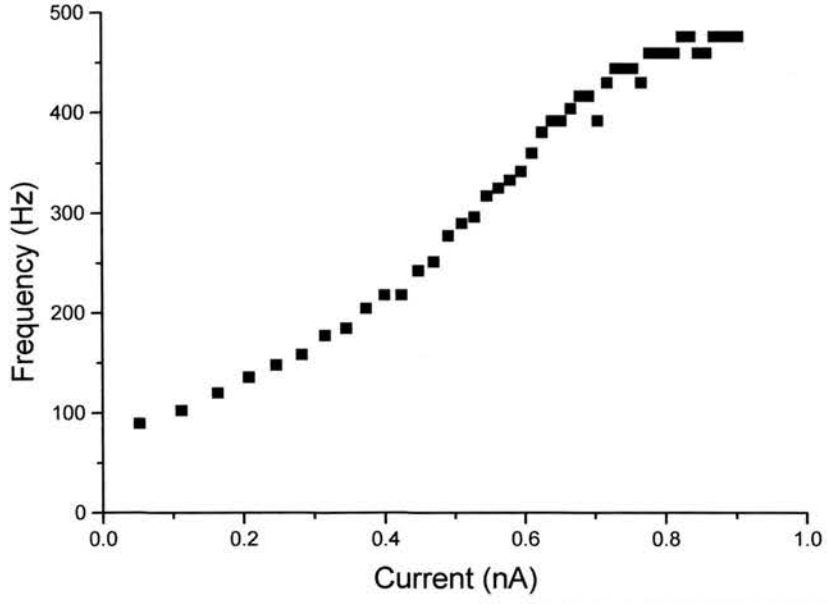

Figure 4.9 Graphs showing the relationship between injected current and firing frequency of a rat subthalamic nucleus neurone. **A** Data attained using a series of depolarising current steps from a holing current of -0.04 nA with a duration of 100 ms. Frequency represents the instantaneous firing frequency at the end of the pulse. **B** data attained using a 200 ms ramp depolarisation from -0.04 nA to 0.92 nA. Frequency represents the instantaneous firing frequencies throughout the duration of the ramp.

Cells generated action potentials when positive current was injected and so either a similar series of positive current steps or a ramped depolarising current pulse was used to characterise the current-firing frequency relationship. Figure 4.9 shows examples of I-f curves obtained from the same cell using either stepped depolarisations (figure 4.9A) or a ramp depolarisation (figure 4.9B). The average maximum firing rate obtained during these depolarising current pulses was 365.14 ±38.03 Hz for the stepped pulses and 414.25 ± 29.72 Hz for the ramped pulses. Fitting a straight line to the steepest part of the curves gave a gradient of 769.28 ± 98.04 Hz/nA and 617.81 ± 70.13 Hz/nA for the stepped and ramp current pulses respectively.

4.3.2 Recovery from Depolarisation Block

Figure 4.10 shows a series of traces from a single STN neurone. These represent the responses of the cell using the gap protocol over the whole range of gaps used. The mean (± S.E.M.) TTB before the gap was 68.07 ± 6.88 ms (range 42.75 ms to 90.81 ms). The TTB following the gap varied according to the length of gap used. Figure 4.11 shows these TTBs after the various different lengths of gap normalised to the TTB before the gap, and plotted against the length of the gap. The period of recovery from depolarisation block was defined as the length of time for which TTB_{after}/TTB_{before} was less than 1. The single exponential curve fitted to this data (figure 4.10A) gave a value for τ_h of 58.19 ± 2.06 (χ^2 = 0.00054). When the double exponential equation was fitted (figure 4.10B), χ^2 was found to be smaller (χ^2 = 0.00025) indicating that this curve produced a better fit to the data. For the double

Figure 4.10

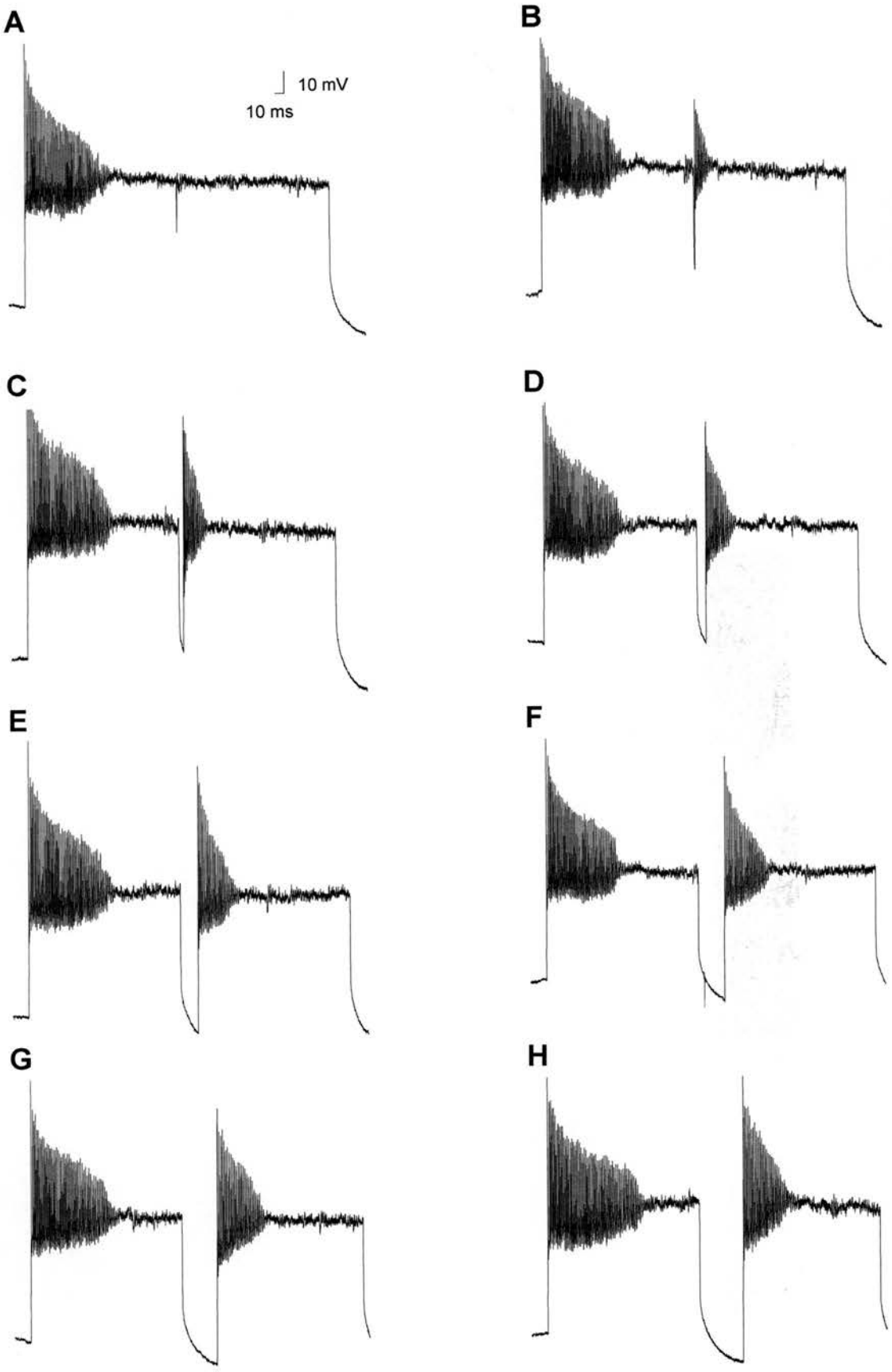
A
10 mV
10 ms
B
C
D
E
F
G
H

A

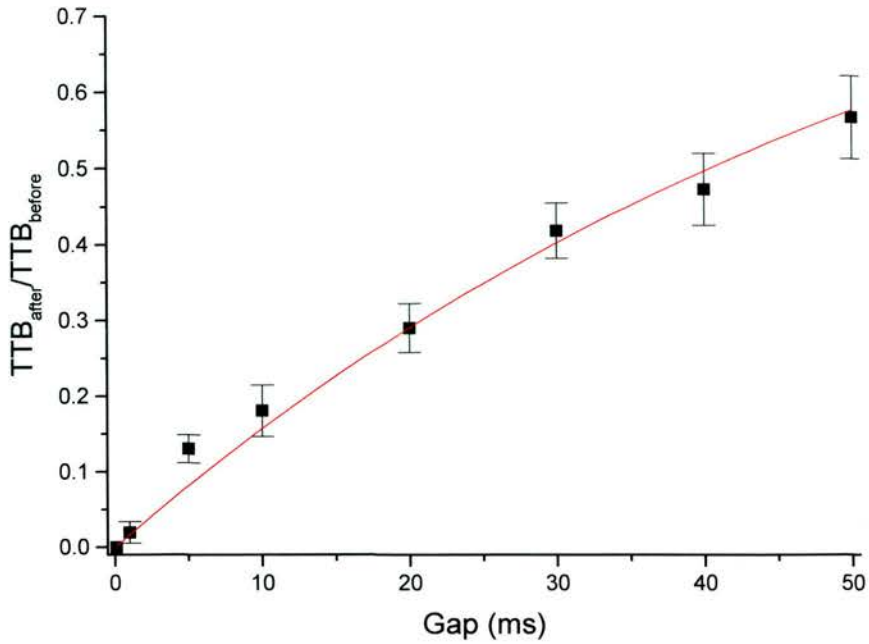

B

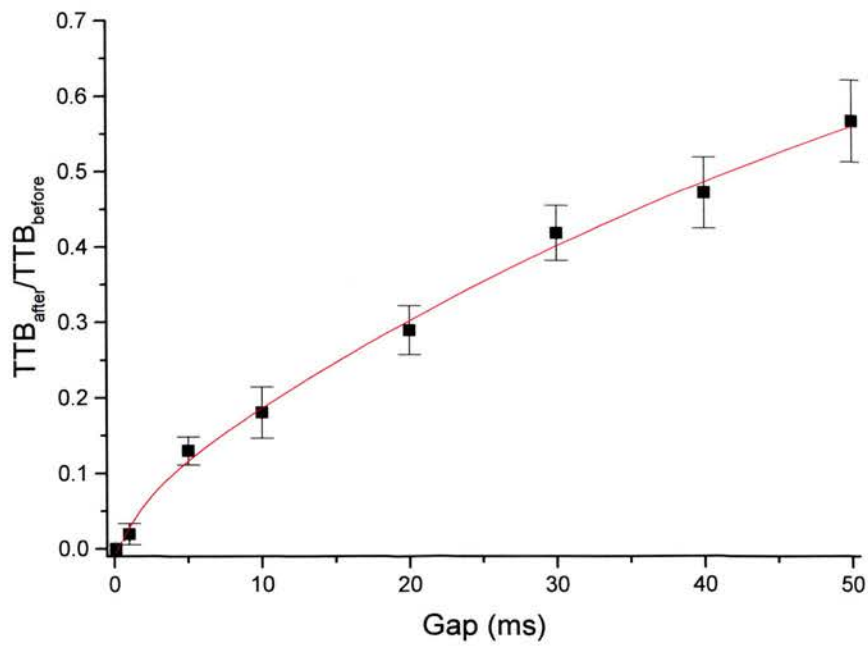

Figure 4.11 Graphs showing the rate of recovery from depolarisation block for subthalamic nucleus neurones (n = 7). Experiments were performed as in figure 4.10. The time taken to block after the gap (TTB_{after}) was divided by the time to block before the gap (TTB_{before}). The means (± S.E.M.) of this ratio are shown plotted against the length of the gap. **A** and **B** show the same data fitted with curves represented either by a single exponential equation (**A**) or a double exponential equation (**B**).

exponential equation c1 = 0.06 ± 0.02, c2 = 0.95 ± 0.02, τ_f = 2.04 ± 2.41, and τ_s = 65.23 ± 3.57.

Figure 4.12 shows the immunostaining for NaCh β subunits. The STN was found to be expressing the β_1 subunit at levels comparable with other brain areas (figure 4.12A & B), whilst the β_2 subunit was not present in the STN neurones (figure 4.12C & D). Figure 4.13 shows examples of STN neurones filled with biocytin. All neurones filled in this way were confirmed to be within the STN.

4.4 Discussion

4.4.1 Summary of Results

Intracellular records were obtained from neurones in the STN. These cells were characterised in terms of their input resistance and current-frequency relationship. Some cells were filled with biocytin to enable their anatomical location and morphology to be examined. Recovery from spike inactivation after a large depolarising current pulse was investigated.

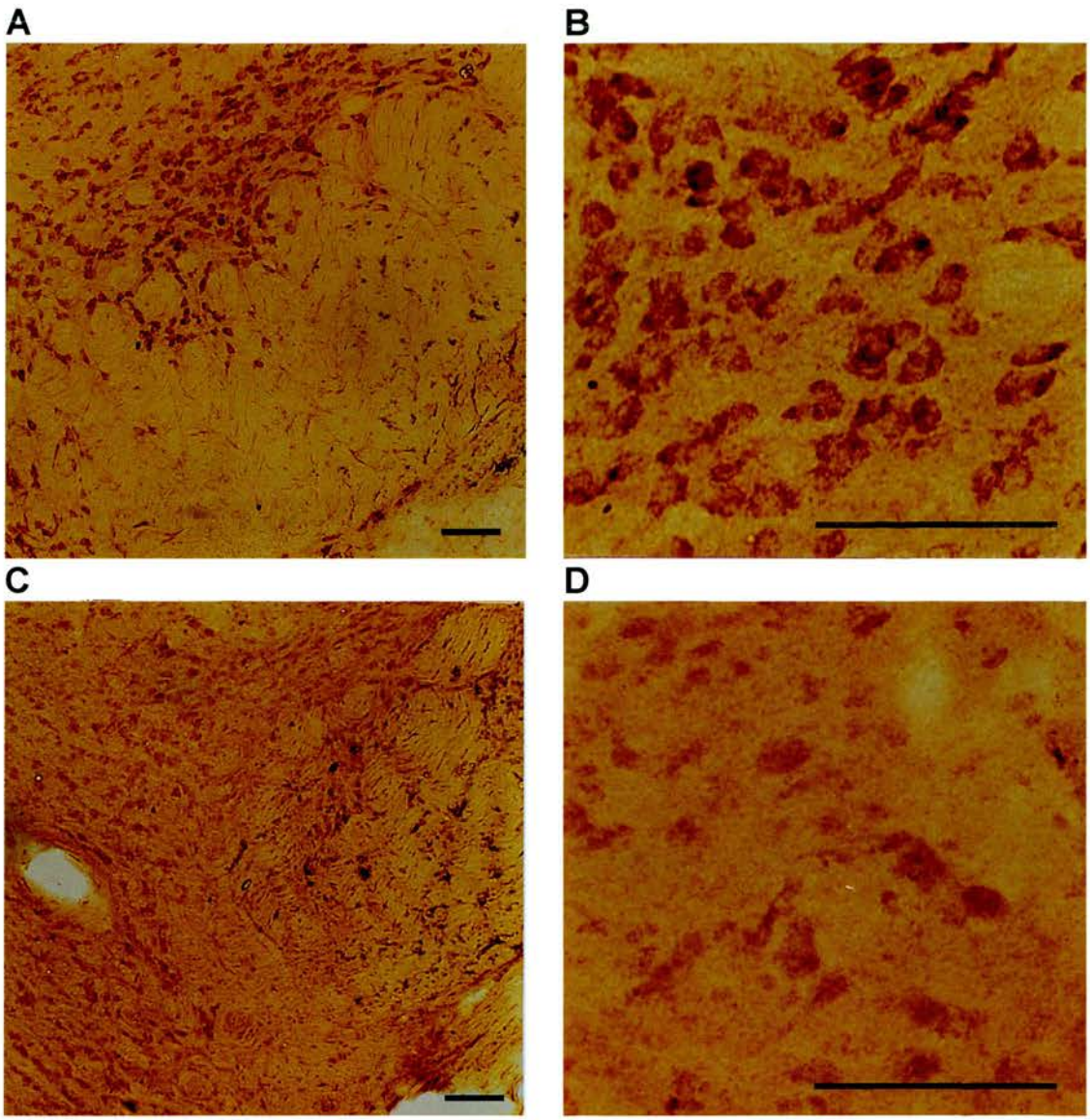

Figure 4.12 Photomicrographs of coronal rat brain slices showing immunolabelling against the voltage gated sodium channel β subunits. **A** & **B** show staining using antibodies raised against the β_1 subunit. **C** & **D** show staining using antibodies raised against the β_2 subunit. **A** & **C** Low power showing the subthalamic nucleus at the lower end of the cerebral peduncle. **B** & **D** High power showing subthalamic nucleus neurones. Scale bars = 100 μm.

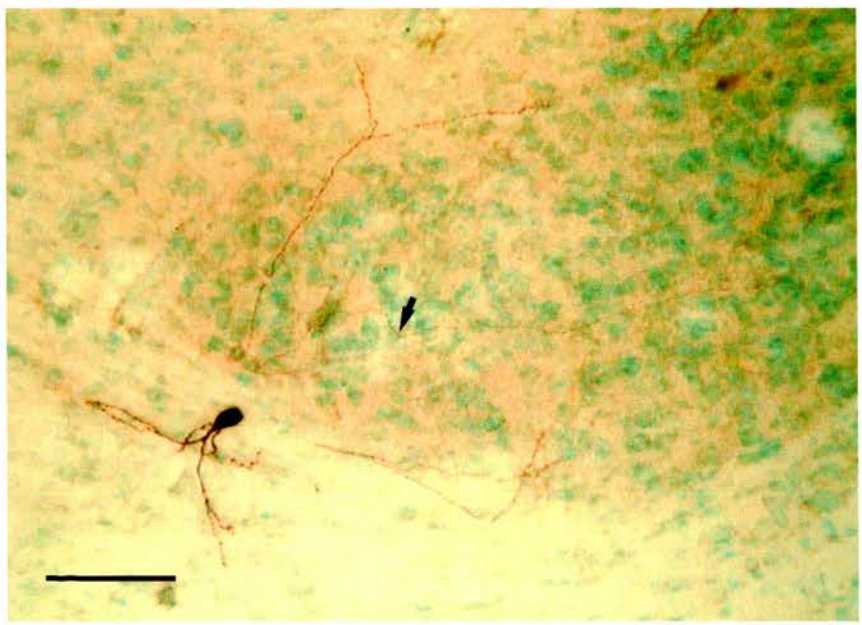

Figure 4.13 A photomicrograph showing a parasagittal section of the rat brain at the level of the subthalamic nucleus. Intracellular recordings were obtained from a subthalamic nucleus neurone using glass microelectrodes filled with 1.5 M KCl and 5% biocytin hydrochloride. At the end of the experiment the neurone was filled with biocytin using -1 nA current pulses at 2.5 Hz (200 ms on; 200 ms off). The section is counter-stained with methyl green to reveal the extent of the subthalamic nucleus. The axon of the neurone branches at the point marked with an arrowhead. One branch travels towards the globus pallidus (to the right of the picture), the other towards the substantia nigra (to the left).

4.4.2 Are the Neurones Used in This Study Subthalamic Nucleus Neurones?

The resting membrane potential of STN neurones is difficult to measure. This is because the neurones rest at a membrane potential that is above the threshold for firing action potentials. This means that, rather than resting, the neurones have a continuously changing membrane potential. Bevan and Wilson (1999) and Beurrier, *et al* (2000) have shown that this is due to a fast afterhyperpolarisation that follows the action potentials followed by a ramp depolarisation due to the presence of a persistent sodium channel. For this reason the resting membrane potential was estimated from the linear fit to the steepest part of the neurones *I-V* curve. The resulting estimate of mean resting potential of -45.64 mV was similar that seen in to previously described STN neurones (Nakanishi *et al.*, 1987; Bevan & Wilson, 1999; Wigmore & Lacey, 2000). The mean input resistance of the STN neurones used in this study (70.61 MΩ) was smaller than the estimate of Nakanishi, *et al* (1987) of 146 ± 48 MΩ, although it was higher than values obtained from *in vivo* recordings (Kita *et al.*, 1983a). This indicates that the electrodes used in the present study did not form as good a seal as in this previous study. Other *in vitro* studies using patch electrodes found much higher values for the input resistance, this is because patch electrodes allow the formation of a much better seal onto the cell than those attained with sharp electrodes. Thus the resting membrane potentials and the input resistances for the cells used in this study are sufficiently within the range of previously reported values to indicate that these neurones are not significantly different in these respects from other STN neurones.

A defining feature of STN neurones is their I-f relationship. This has two key characteristics. Firstly it is sigmoidal in shape, secondly the maximum firing rate is very high at around 500 Hz (Nakanishi *et al.*, 1987). The neurones used in this study all displayed these features (see figure 4.9) although the range of depolarising current pulses used was not great enough to fully show the sigmoidal shape of the I-f curve for some neurones. The maximum firing rate of 500 Hz was not achieved in the I-f curves attained using either the step or the ramp protocols. This is because the measurement of maximum firing frequency was always taken from the last ISI in the spike train. Over the course of the spike train a small amount of spike-frequency adaptation occurred. This is in common with both the data of Nakanishi, *et al.* (1987) and that of Bevan and Wilson (1999). Nakanishi, *et al.* (1987) took measurements from both the first and last ISI in the spike train using a stepped current pulse protocol. However, this was not possible in the current experiments as, in common with Bevan and Wilson (1999), the cells were observed to exhibit a rapid speed-up of their firing frequency during the first few ISIs.

Finally, those cells that were filled with biocytin were all found to be located in, or close to[2] the STN. These filled neurones were also similar in morphology to STN neurones that have been described previously. For one neurone, in which the axon was filled (figure 4.9), it was even possible to see the splitting of the axon into two branches, one projecting towards the GP and the other towards the SN (Kita *et al.*, 1983b; Kitai & Kita, 1986; Kita & Kitai, 1987). Put together these data provide

strong evidence that the neurones used in this study were located in the STN and were similar electrophysiologically to STN neurones recorded from *in vitro* by previous authors.

4.4.3 What is Depolarisation Block?

When a large depolarising current was injected into the neurones of the STN they were seen to be subject to depolarisation block. This block did not form immediately, the neurones were able to generate action potentials for a short time. These action potentials gradually got smaller and eventually failed.

Jung, *et al* (1997), investigating spike trains in hippocampal pyramidal neurones, showed that during each spike of the train a certain amount of NaCh inactivation occurs. Over the course of a train of action potentials NaCh inactivation can build up if the time between the spikes is not enough for complete recovery from this inactivation to occur. The result of this was a reduction in the inward current passed in each successive action potential causing a reduction in the action potential size over the course of the spike train. A similar phenomenon has also been seen in rat visual cortical neurones. When the cortex is cooled the neurones become hyperexcitable. As cooling continues the action potentials begin to reduce in size over the course of a spike train and eventually they stop altogether. This has been attributed to a build up of NaCh inactivation during the course of a spike train due to

---

[2] groups of STN cells can be seen in the internal capsule and cerebral peduncle

the slowing of NaCh inactivation and depolarisation of the membrane potential (Volgushev *et al.*, 2000). These data suggest that the depolarisation block seen in the experiments reported here was due to a gradual build up of NaCh inactivation.

It is possible that other voltage sensitive channels could contribute to the formation of the depolarisation block seen in the present experiments. Data from experiments using pharmacological agents to block specific channel types can help us to understand how inactivation of different channel types might affect action potential generation.

Evidence that NaCh are necessary for spike generation comes from experiments using tetrodotoxin (TTX). This is a puffer fish toxin that selectively blocks I_{Na} (Narahashi *et al.*, 1964). Application of TTX to brain slices containing the STN completely blocks the generation and transmission of fast action potentials in the STN neurones (Nakanishi *et al.*, 1987; Bevan & Wilson, 1999). This blockade of the generation and transmission of fast action potentials by TTX is a phenomenon common to all other excitable tissues (Hille, 1992).

Inactivation of KCh could also be involved in the development of depolarisation block by disrupting the repolarisation phase of the action potential. Tetraethylammonium chloride (TEA) is a selective blocker of I_K (Hille, 1992). Application of this drug to STN neurones increases their input resistance and lengthens the duration of the fast action potentials (Nakanishi *et al.*, 1987). This lengthening of action potentials is due to the inability of the neurones to properly

repolarise in the absence of I_K leading to an extension of the repolarisation phase of the action potential. TEA does not however eliminate the formation of fast action potentials altogether, once the repolarisation is complete the neurone is capable of firing further action potentials. Thus, in the present experiments inactivation of KCh is likely not to be involved in the development of depolarisation block.

During action potentials calcium channels are opened and calcium can enter the cell. STN neurones express the high-voltage activated (HVA) calcium channels (Bevan & Wilson, 1999). These channels can lead to the generation of a slow action potential in the absence of fast spiking. However, they probably do not contribute much to the fast action potentials seen in STN neurones rather, their activation during the course of fast action potentials is responsible for the slow component of the single-spike AHP (Bevan & Wilson, 1999). It is possible that, over the course of a train of spikes, activation or inactivation of this current may build up. Cadmium can be used to block HVA calcium currents. Application of cadmium to rat brain slices containing the STN does not cause the failure of action potential generation (Bevan & Wilson, 1999). This suggests that inactivation of calcium channels alone is not the mechanism responsible for the formation of depolarisation block. Activation of HVA calcium currents my play a role though as they may cause further depolarisation of the cell.

Another channel type that may play a role in action potential generation is the calcium activated potassium channel SK_{Ca}. Opening of HVA calcium channels increases calcium entry and could lead to the opening of these calcium activated

potassium channels. Blockade of this channel with apamin fails to block action potential generation in the STN but the normal rhythmic firing seen at rest is disrupted (Bevan & Wilson, 1999). Therefore inactivation of SK_{Ca} would not interrupt firing. However, activation of SK_{Ca} by the calcium influx that accompanies each action potential can cause a loss in size of action potentials accompanied by a slowing of the firing rate (Hille, 1992). This effect called *spike frequency adaptation* and is due to the development of a slow AHP (*afterhyperpolarisation*) over the course of the spike train. This slow AHP can be strong enough to prevent the cell from firing by stopping it from reaching its firing threshold again. STN neurones do show a small amount of spike frequency adaptation. This indicates that SK_{Ca} may be playing a role in the development of depolarisation block seen in the present experiments. However blockade of calcium entry through HVA calcium channels with cadmium or directly blocking SK_{Ca} channels with apamin both fail to remove spike frequency adaptation in STN neurones (Bevan & Wilson, 1999). Therefore SK_{Ca} may not have a very big influence on the development of depolarisation block.

Thus, only the blockade of I_{Na} with TTX leads to the inhibition of action potential generation. These data provide strong evidence that it is inactivation of NaCh that plays the major role in the development of depolarisation block in STN neurones.

4.4.4 The Relationship Between Recovery From Spike Inactivation and Fast Firing

Given the evidence discussed above we conclude that the reduction in size and eventual failure of action potentials seen in the present experiments can be assumed to be due, in the most part, to the inactivation of NaCh. This being the case, measuring the rate of recovery of spiking from this block would give an estimate of the rate of deinactivation of NaCh. To this end the present experiments were designed. Here, an estimate of the amount of recovery that occurred in the gap between two depolarising current injections was made. This was calculated by measuring the time that it took from the start of a depolarising current injection to the point at which the neurone stopped firing (measured by the time of the last spike). This time taken to block was measured before and after a gap in the depolarising current injection. The recovery that had occurred during the gap was estimated by the ratio of the TTB after the gap against the TTB before. Plotting this ratio against the length of the gap produced a curve that could be fitted by the equation *exponential 1*. This fit, although good ($\chi^2 = 0.00054$), did not fully match all of the data points so the data was fitted with the equation *exponential 2*. This curve produced a much better fit to the data ($\chi^2 = 0.00025$) and so the fit to the curve *exponential 1* was disregarded. As the depolarisation block can be largely attributed to NaCh inactivation, this equation can be used to give an estimate of the τ_h of that inactivation. The double exponential gives two estimates relating to τ_h; a fast component τ_f, and a slow component τ_s. The value found for τ_f in these experiments was 2.04 ms, τ_s was 65.22 ms. The constants c1 (0.06) and c2 (0.95) in the equation

of the line *exponential 2* showed that the fast component τ_f contributed only a small amount to the overall shape of the fitted curve. Therefore τ_s was used as the main estimate of τ_h.

The parameter τ_h is one that is a function of the membrane potential. This makes a direct comparison with published data difficult. Gillies (1996) used kinetics taken from a model hippocampal CA1 neurone (Pongráz *et al.*, 1992) for his model of an STN cell. The inactivation characteristics of these NaCh were of the Hodgkin-Huxley form:

$$\tau_h = 1/(\alpha_h-\beta_h)$$

where:

$$\alpha_h = 0.128\exp((17-V)/18)$$

$$\beta_h = 4/(\exp((40-V)/5)+1)$$

The plot for this τ_h is shown in figure 4.14. The maximum value of τ_h in this plot is not greater than 6 ms. Despite these relatively small values for τ_h Gillies (1995) found that the model STN cell was not able to attain the high firing rates seen in real STN cells. Hille (1992) reports the values of τ_h measured from the node of Ranvier of a myelinated frog nerve fibre at 22°C. The value of τ_h in these experiments was also never greater than 6 ms. Ragsdale, Scheuer, and Catterall (1991) measured value of τ_h at -85 mV and -128 mV for type IIA NaCh expressed in the mammalian cell-line derived from CHO cells. At -85 mV τ_h was 5.5 ms, at -128 mV it had decreased to 1.0 ms.

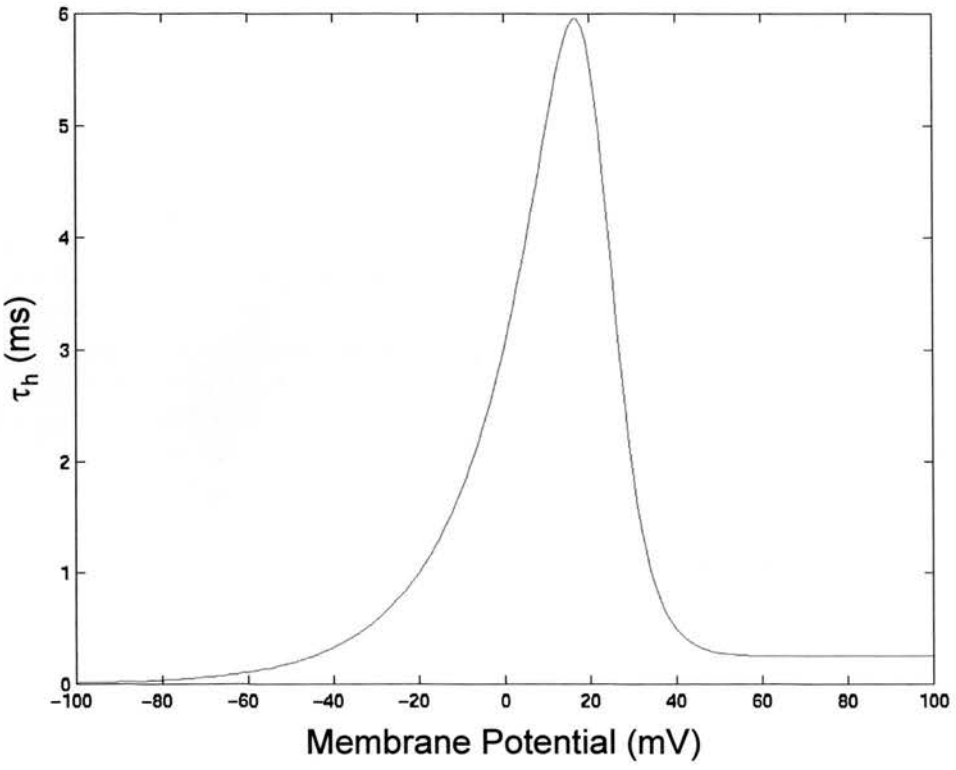

Figure 4.14 A graph showing the voltage dependence of the voltage gated sodium channel inactivation time constant τ_h. The graph was drawn using the kinetics described by Pongráz *et al.* (1992) for a model of a hippocampal CA1 neurone. Gillies (1996) also used these kinetics in his model of a subthalamic nucleus neurone.

Plots of τ_h form a bell-shaped curve like the one shown in figure 4.14. The value measured in the present experiments was taken at a potential slightly hyperpolarised from the resting membrane potential of the cell. The data from other authors suggests that the τ_h is near maximal at the resting potential of the cell. Comparison with this data shows that, even if the τ_h found in the present experiments is not the maximum value for these cells, it is still around seven times larger than any normal value for τ_h reported by these authors. This comparison leads us to the conclusion that inactivation of NaCh in STN neurones is a distinctly slower process than it has been observed to be elsewhere in the brain.

Slowly inactivating or persistent NaCh are known to be present in the STN (Bevan & Wilson, 1999; Beurrier *et al.*, 2000). The TTX-sensitive current associated with this channel type is known as I_{NaP} (Crill, 1996). This current is activated between -60 mV and -25 mV, it is maximally activated at -45 mV to -30 mV (Bevan & Wilson, 1999). At these membrane potentials there is little evidence of inactivation of this current. I_{NaP} was found to be very small (<250 pA) and is hypothesised to drive the depolarising phase of a subthreshold oscillation that is responsible for the spontaneous firing seen in STN neurones. I_{NaP} does inactivate at higher membrane potentials. In the layer V neurones of mouse neocortical slices an I_{NaP} was observed that closely resembles that seen in the STN. This current showed no signs of inactivation in the range from -60 mV to -25 mV. However at +20 mV inactivation occurred with a τ_h of 2060 ms (Fleidervish & Gutnick, 1996). It is possible that the slowed inactivation seen in the present experiments is due to the superimposition of this slow inactivating sodium current over the normal fast inactivating current. This

could explain why the inactivation curve best fitted a double exponential. It may be that τ_f represents the fast inactivating NaCh and τ_s the slow inactivating channels. However, the persistent current seen in STN neurones is only a very small current. Such a small current will have little role in the generation of action potentials. The present experiments measured only the ability of the neurones to generate action potentials. Also, this current is maximally activated between -45 mV and -30 mV in which range inactivation has not been observed. The neurones used in the present experiments had a membrane potential of between -35 mV and -20mV when they became blocked. This is well within the range where I_{NaP} does not inactivate. Therefore it is reasonable to assume that this current plays little or no role in the present observations. It seems likely then that the main population of NaCh in the STN neurones has slower inactivation than the NaCh in neurones elsewhere.

Following the discovery of abnormally slow inactivation in the STN neurones we hypothesised that these neurones may have an abnormal β subunit composition. NaCh β subunits are known to modulate the rate of inactivation of I_{Na} (Isom *et al.*, 1992; Isom *et al.*, 1995). In order to investigate this possibility rat brain slices were stained with antibodies against either the β_1 subunit or the β_2 subunit. β_1 subunits were present in STN neurones but β_2 subunits were not, suggesting that this may be at least in part responsible for the slowed inactivation.

How can slowed NaCh inactivation account for the ability of STN neurones to achieve such high firing frequencies? Neurones that lack inactivation of NaCh, for example through the action of toxins, exhibit massively prolonged action potentials (Hille (1992), chapter 7). However, there is evidence that if a depolarised neurone is repolarised before NaCh inactivation has occurred then the NaCh can close through the reverse process of activation (Oxford, 1981). This method of closing is termed deactivation (Patlak, 1991). When closed through deactivation NaCh are able to reopen almost immediately upon depolarisation with their normal activation kinetics (Patlak, 1991; Hille, 1992). The slowing of NaCh inactivation may allow the NaCh to be closed by deactivation. This process would rely on there being large and fast enough potassium currents present in the STN neurones that are powerful enough to bring the membrane potential back down to resting levels without inactivation of NaCh. If this were the case it provides a possible explanation of how the neurones in the STN are able to fire at rates of up to, and above, 500Hz and also of the progressive development of 'block' as the level of slow NaCh inactivation builds up during repetitive firing (Jung *et al.*, 1997).

4.4.5 The Role of Potassium Channels in Fast Firing

The hypothesis described above is dependent on there being an unusual KCh present in the STN that is capable of repolarising the neurones after an action potential whilst NaCh are still open. Kv3.1 is a voltage gated KCh that displays similar properties to the delayed rectifier type of KCh. When expressed in *Xenopus* oocytes Kv3.1 mRNA produces a delayed rectifier-like K^+ current that displays fairly rapid activation with

little or no inactivation (Luneau *et al.*, 1991). It is expressed most strongly in cerebellar cortex, but also in the cortex and hippocampus. Amongst the other brain areas seen to express Kv3.1 there are a number of basal ganglia nuclei (Perney *et al.*, 1992; Weiser *et al.*, 1995; Gan & Kaczmarek, 1998). Kv3.1 is seen in the GP, EP, SNr, and STN. One thing that many areas of the brain that show expression of Kv3.1 have in common is that they contain neurones which show narrow action potentials and are able to achieve high firing frequencies (Perney *et al.*, 1992; Gan & Kaczmarek, 1998; Whim & Kaczmarek, 1998). Wang, *et al.* (1998) present evidence that implicates the KCh Kv3.1 in the high firing rates seen in mouse auditory neurones. These neurones are able to attain firing rates of up to 400 Hz. However, when low concentrations of TEA are added to brain slices containing these neurones, the high frequency firing is lost. This occurs without changing the cells ability to fire at lower frequencies. Modelling of these neurones revealed that model mouse auditory neurones could also only fire at high frequencies if Kv3.1 was included in the model. Kv3.1 is strongly expressed in the STN (Perney *et al.*, 1992; Weiser *et al.*, 1994; Weiser *et al.*, 1995) and may therefore provide the strong and fast potassium current that would be necessary to return the membrane to its resting potential without inactivation of the NaCh occurring. Wigmore and Lacey (2000) have recently characterised a persistent outwardly rectifying current in the STN that closely resembles Kv3.1. This channel type, alongside the normal delayed rectifier KCh may provide the necessary potassium current in order for this proposed mechanism of fast firing to occur.

4.4.6 Implications

The data presented here provides evidence that inactivation of NaCh in the STN may have slower kinetics than was previously thought. The hypothesised mechanism of fast firing that we have developed as a result of this discovery generates many testable predictions:

Experiments designed to measure NaCh inactivation kinetics using a more classical protocol should provide further evidence for the slow nature of these kinetics. These experiments should be performed using voltage clamp techniques to investigate the current that flows when cells are moved between hyperpolarised and depolarised membrane potentials. These current measurements should be performed both when NaCh are fully deinactivated and at various delays following a long depolarising step that would induce full inactivation. In this way the recovery of the sodium current could be charted.

If the inactivation of NaCh was indeed confirmed to be slowed then the nature of the repolarising phase of the action potential needs investigation. The hypothesis predicts that repolarisation can occur in the absence of NaCh inactivation. There exist various toxins and proteolytic enzymes that can either slow or stop NaCh inactivation. For example pronase, a mixture of endopeptidases, applied inside squid giant axons can destroy the inactivation gating process. Application of drugs inside neurones, though possible, is technically more complex than application through the extracellular medium. α-Scorpion venom includes a cocktail of toxins that, when applied outside

the neurone, lead to a marked slowing of inactivation. *Leiurus quinquestriatus* venom, when applied to a node of Ranvier of a frog myelinated nerve fibre increases action potential duration from ~2 ms to ~15 ms (Schmitt & Schmidt, 1972). The hypothesis formulated from the present results generates the prediction that these toxins would have no effect on the length of the action potentials in STN neurones as NaCh inactivation is already slow. Because of this, these toxins would also have little effect on the maximum firing rate of STN neurones. Further to this the toxins should slow the rate of the formation of depolarisation block as this is predicted to be dependent on the rate of NaCh inactivation. These experiments would also test the prediction that the STN expresses KCh that generate a large and fast enough I_K to repolarise the cell membrane whilst NaCh are still activated.

The role of Kv3.1 in the high frequency firing of STN neurones could be further investigated using selective antagonists of this channel. At present there are no drugs known to target Kv3.1 without blocking other potassium channels. Wang, *et al.* (1998) found that application of 1 mM TEA to mouse brain slices restricted the maximum firing frequency that neurones of the medial nucleus of the trapezoid body (MNTB) could attain. This concentration of TEA broadened action potentials and induced a progressive decrease in their amplitude during a depolarising current pulse. The Kv3.1 channel is extremely sensitive to TEA and may be blocked selectively by application of TEA at these low concentrations (Critz *et al.*, 1993; Kanemasa *et al.*, 1995). If Kv3.1 is responsible for the rapid repolarisation of STN neurones following an action potential then application of 1 mM TEA to brain slices containing STN neurones would limit the maximum firing frequency that the neurones can attain.

From the data of Bevan and Wilson (1999) we concluded that SK_{Ca} channels played little or no role in the development of depolarisation block in the present experiments. Apamin is a selective blocker of the SK_{Ca} channel. Therefore this conclusion could be verified by performing the present experiments again with 100 nM apamin added to the aCSF.

Finally, further modelling could be used to test the hypothesis presented here. Gillies (1996) model of a single STN neurone was unable to replicate the high firing frequencies attained by STN neurones. Only with alterations to the kinetics of both the NaCh and KCh was he able to simulate these firing frequencies. It would be interesting to construct a model STN neurone in which inactivation of NaCh could be slowed or removed. This could then be investigated together with the presence of Kv3.1 channels to see if, in the model at least, this mechanism of high-frequency firing is possible.

5 An Electrophysiological Investigation Into the Interconnections Between STN Neurones

5.1 Introduction

Geometric computer modelling has revealed that the intranuclear axon collaterals seen on up to 50% of rat STN neurones could lead to a massive degree of interconnectivity between these cells. Subsequent network computer models showed that even if each of these collaterals contacted only a small number of cells, they would still have a significant effect on the behaviour of the nucleus as a whole. In agreement with this, stimulation of sensorimotor cortex gives a virtually identical response from neurones throughout the STN (Fujimoto & Kita, 1993) suggesting that the cortical stimulation is spreading either at some point *en route* to the STN or in the nucleus itself. However, no evidence can be found for any correlation in firing between pairs of STN neurones at rest (Ryan *et al.*, 1992; Magill *et al.*, 2000). Interestingly, the network computer model predicts this. In this model neurones in the STN fire action potentials independently of each other at rest. Then when the neurones are stimulated, their increased firing rates begin to affect the behaviour of other neurones within the nucleus through the intranuclear collaterals. Thus at higher firing rates there is a degree of non-synchronous correlation between the activity of the neurones within the nucleus. It is through the neurones affecting the firing of each other in this manner that the model develops a persistent hyperactive state. Therefore the model generated the hypothesis that depolarising the whole nucleus

would have a different effect on the neurones within the nucleus if they have functional interconnections between them, than it would if they are isolated from each other. In order to test for this an *in vitro* experiment was devised using slices of rat brain, which were cut in such a way as to isolate the neurones of the STN from all of their external inputs. Using this preparation it would be possible to determine the effects of a glutamatergic antagonist on the behaviour of the neurones. The effects of the drug on neurones in their resting state could also be compared with the effects when the neurones are depolarised.

5.2 Methods

5.2.1 Extracellular Electrophysiology

Artificial cerebrospinal fluid was made according to recipe 2 from appendix A. This was made in two components; a normal component ($aCSF2^N$) and a sodium-free, sucrose-containing component ($aCSF2^S$). The container of $aCSF2^N$ was placed in a water bath at 35°C and the $aCSF2^S$ was placed in an ice bucket to chill. Both aCSF mixtures were then bubbled with carbogen and left to equilibrate for at least 20 minutes before use.

Male Sprague-Dawley rats (150 – 300 g) were anaesthetised with avertin (1 ml/100 g) and decapitated. Their brains were rapidly removed and placed into ice cold $aCSF2^S$. The brains were then trimmed to form a block, which contained the STN. This block was glued on to a Teflon chuck and replaced into the ice-cold $aCSF2^S$.

400 μm thick parasagittal sections were then cut using a vibroslice. These sections were trimmed rostral to the STN so that the internal capsule was cut as close to the STN as possible (figure 4.4). Then the sections were moved into an interface recording chamber where they were perfused with $aCSF2^N$ at 37°C for at least an hour prior to recording (see chapter 4 for a more detailed description of the recording chamber). Extracellular recordings were attained using glass micropipettes pulled with a Flaming-Brown micropipette puller (model p80; Sutter Instrument Co., CA, USA) to have a final resistance of 50 - 80 MΩ when filled with 1M NaCl.

In order to obtain control data, extracellular recordings were taken from cells prior to any treatment. Cells were then perfused with aCSF2, which contained one of the following three different drug/chemical treatments:

1) **CNQX** - 10 μM of the glutamatergic antagonist 6-cyano-7-nitroquinoxaline-2,3-dione (CNQX; Tocris Cookson Ltd., Bristol, UK).

2) **High K** - 10 mM potassium gluconate (Sigma-Aldrich, Poole, UK).

3) **K+CNQX** - Both 10 mM potassium gluconate and 10 μM CNQX.

5.2.2 Statistical Methods

Trains of 1000 spikes were used to calculate the mean (± S.D.) interspike interval (ISI). The coefficient of variation (CV) was also calculated according to the formula:

$$CV = S.D.\ of\ the\ mean\ ISI\ /\ mean\ ISI$$

These values were then compared to look for effects of the three treatments on the cells firing rate (measured by ISI) and pattern (measured by CV). Statistical comparisons of the control mean ISIs with the mean ISIs under experimental conditions were performed using paired *t*-tests (Origin 5, Microcal Software, Inc. USA). The Wilcoxon signed-ranks test (Greene and D'Oliveira (1982); Minitab 13.1 (Minitab Inc., USA)) was used to compare the control CVs with the CVs in the experimental conditions.

The trains of 1000 spikes were used in the construction of normalised autocorrelograms. From each spike the time to all neighbouring spikes was calculated up to a distance of 10 ISI (using the mean ISI). These times were then placed in bins with a width of 0.1 ISI and the count frequency in each bin was normalised by the total number of spikes used so as to give a probability of a spike occurring within each bin. This data was then plotted as histograms, which, due to the normalisation, could be overlaid, and a mean autocorrelogram produced for each experimental condition.

5.3 Results

Extracellular recordings from 31 neurones were selected for use in this study. Selection criteria were that the neurones were located within the STN (identified visually in the slices) and that they fired at rest. Figure 5.1 shows representative traces from neurones in each of the three experimental conditions. A few neurones

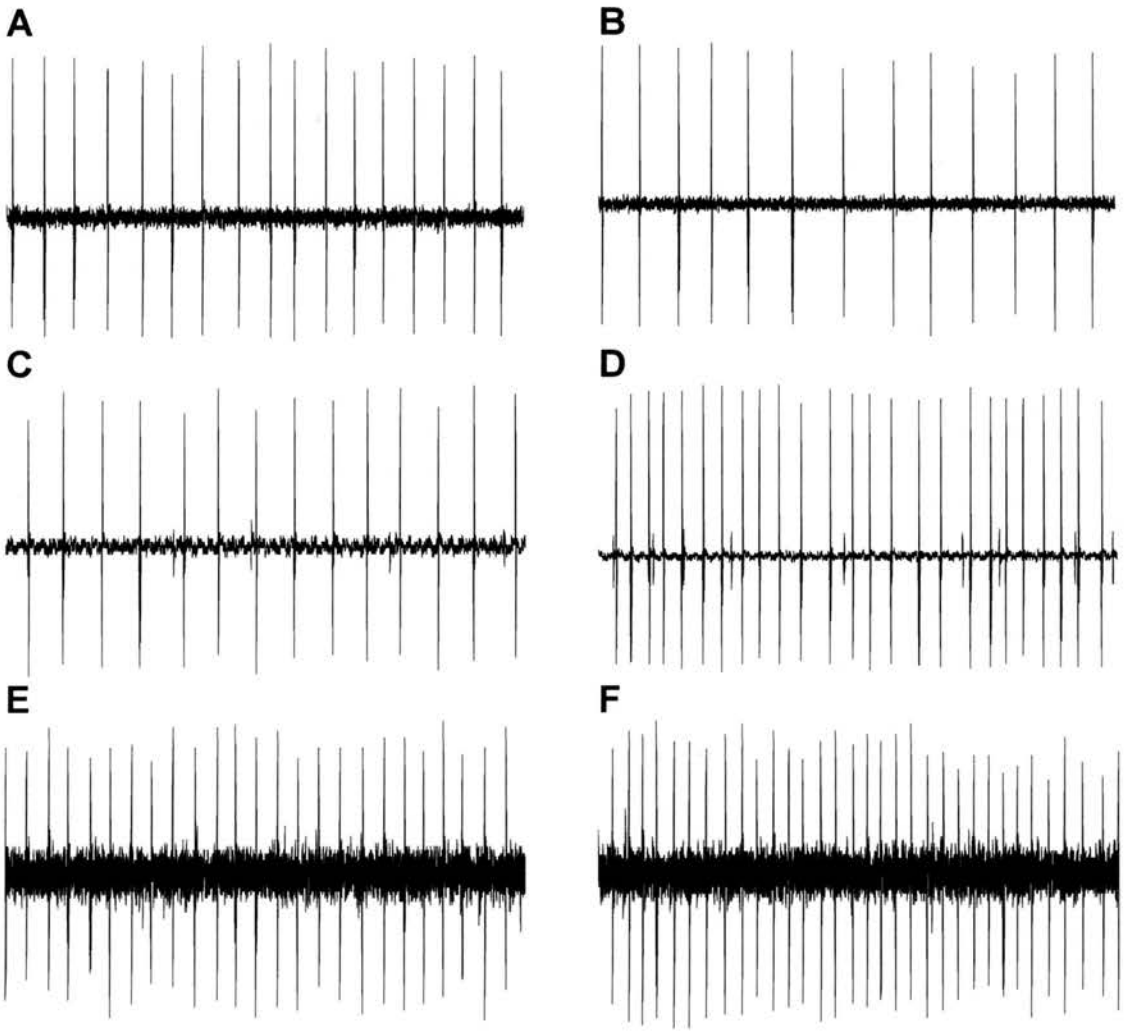

Figure 5.1 1000 ms extracellular records from neurones in the subthalamic nucleus. Each pair of traces represents the same neurone under control and experimental conditions. **A-B** Records from a neurone before and during the application of 10 μM CNQX. **C-D** Records from a neurone before and during the application of 10 mM potassium gluconate. **E-F** Records from a neurone before and during the application of both 10 μM CNQX and 10 mM potassium gluconate. In **C** and **D** the record contains action potentials from two neurones. In this case only the data from the neurone with the largest spikes (closest to the electrode) was used in the analysis.

that exhibited bursting behaviour were omitted from the main study and kept for separate analysis as they formed a very small subpopulation of STN cells. The 31 neurones used had a mean (± S.D.) resting firing rate of 19.03 ± 10.15 Hz with a range from 3.45 Hz to 47.94 Hz. These cells generally exhibited a very regular firing pattern with an average CV of 0.15 ± 0.13 (range: 0.05 to 0.56). There was no correlation between the firing rate of the neurones and their CV (figure 5.2). However, whilst the values of CV were distributed fairly evenly throughout the whole range, the firing rates were clustered towards the higher end of the range with only two outliers at the bottom end of the range. These two cells not only had the slowest firing rate they also had the highest CV.

Overall 10 μM CNQX, when added to the aCSF, had no effect on the firing rates or CV of the cells (n = 11). The mean (± S.E.M.) ISI when CNQX was present was 71.35 ± 14.21 ms (range: 18.01 ms to 193.97 ms) compared with a mean of 78.65 ± 22.90 ms (range: 20.86 ms to 289.69 ms) for the same neurones under control conditions. The average CV in this condition was 0.15 ± 0.05 (range: 0.05 to 0.56) before the application of CNQX and 0.13 ± 0.07 (range: 0.07 to 0.56) when CNQX was present.

Changing the aCSF from control to an aCSF mixture containing 10 mM potassium gluconate (High K) increased the firing rate of all the neurones that were treated in this way (n = 10). The mean ISI in this condition was changed from a mean (± S.E.M) of 63.46 ± 7.94 ms (range: 23.61 ms to 114.14 ms) to 40.87 ± 9.65 ms (range: 10.84 ms to 99.98 ms). The CV of these neurones was also generally

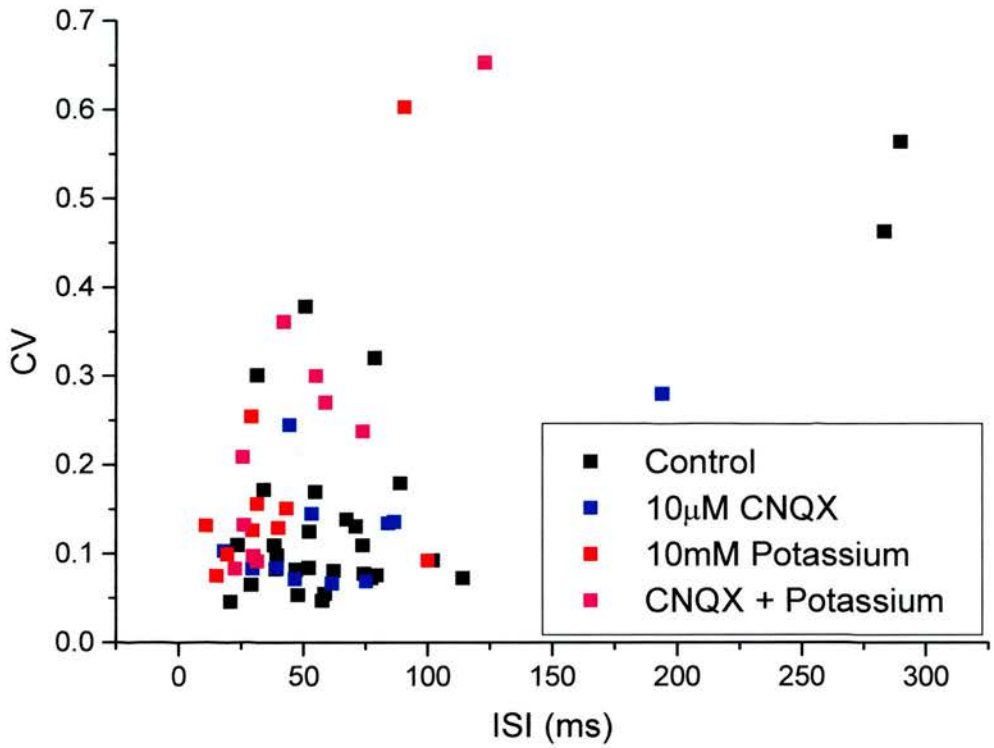

Figure 5.2 A graph showing coefficient of variation (CV) plotted against interspike interval (ISI) for subthalamic nucleus neurones (n = 31). Black squares represent the control data from all 31 neurones. Blue squares represent data attained during the application of 10 μM CNQX (n = 11). Red squares represent data attained during the application of 10 mM potassium gluconate (n = 10). Purple squares represent data attained during the application of both 10 μM CNQX and 10 mM potassium gluconate. There was no correlation between CV and ISI in any of these conditions.

increased by the high K. The average CV in the presence of high K was changed from 0.10 ± 0.01 (range: 0.05 to 0.18) to 0.18 ± 0.15 (range: 0.08 to 0.26).

When 10μM CNQX was added to the aCSF along with High K the firing rate of all neurones treated in this way was increased (n = 10). The mean (± S.E.M.) ISI in this condition was changed from 85.74 ± 23.43 ms (range: 31.50 to 283.29 ms) to 48.82 ± 9.85 ms (range: 22.62 ms to 123.09 ms). The CV in this condition was generally either increased or unchanged from control levels. The average CV changed from 0.20 ± 0.05 (range: 0.08 to 0.46) to 0.24 ± 0.17 (range: 0.08 to 0.65). In none of the experimental conditions was any correlation seen between firing rate and CV (figure 5.2).

In order to compare the behaviour of STN neurones in each of the experimental conditions two trains of 1000 spikes were used from each cell, one in its resting state and one during infusion of the High K or CNQX. The mean ISI and CV of the second train were expressed as a percentage of the mean ISI and CV of the first train. When CNQX alone was present the mean ISI was an average of 103.09 ± 8.78% (mean ± S.E.M.) of control levels. The corresponding CV was an average of 111.17 ± 14.10% of control. For the cells treated with high K the mean ISI was decreased to an average of 61.61 ± 8.36% of control, whilst the CV increased to an average of 190.93 ± 28.80 of control. High K and CNQX together led to a decrease in the mean ISI to an average of 63.44 ± 5.24% of control levels and the CV was an average of

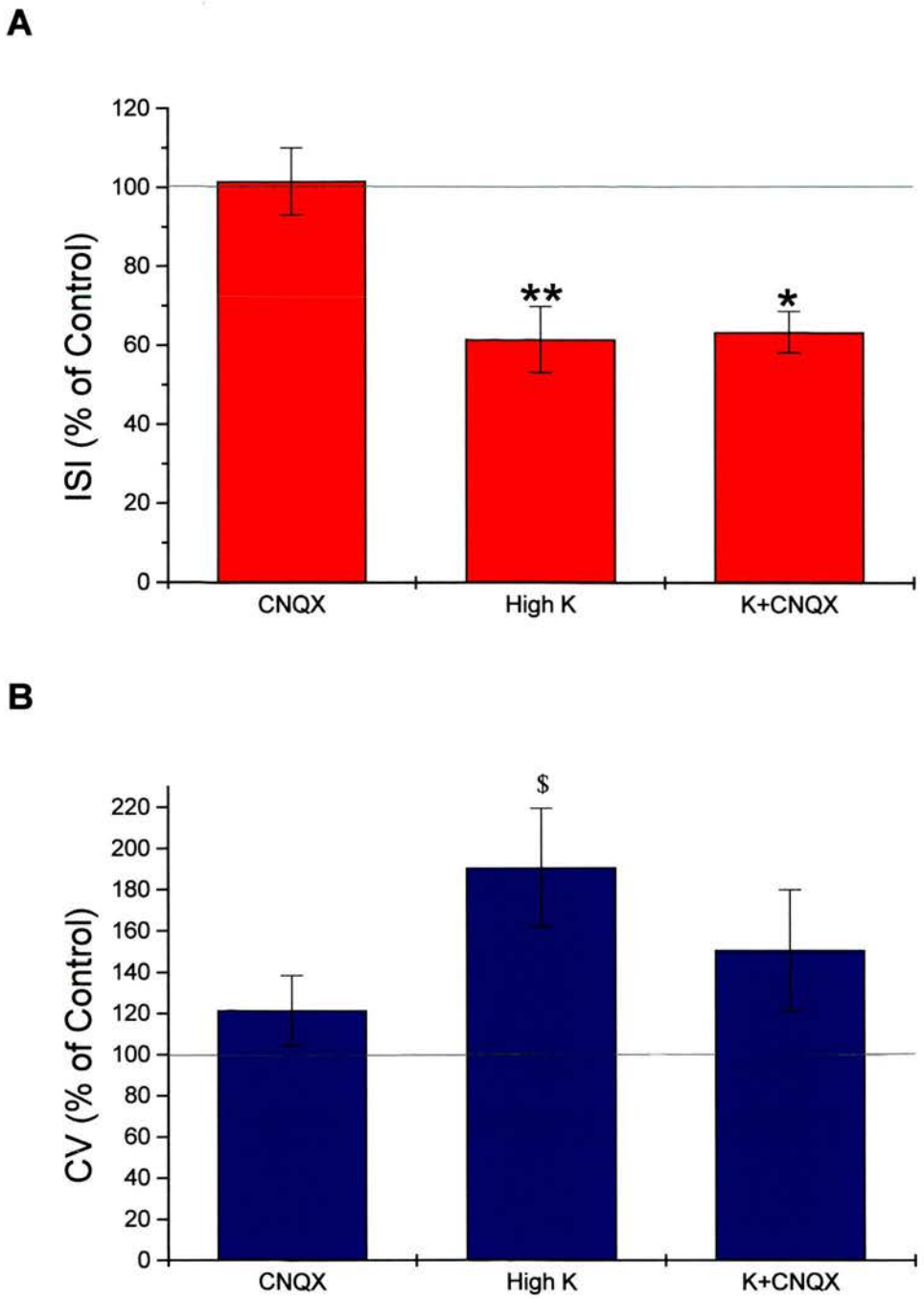

Figure 5.3 Graphs showing the mean (± S.E.M.) percentage change from control levels of **A** interspike intervals (ISI) or **B** coefficient of variation (CV) following the application of 10 μM CNQX, 10 mM potassium gluconate (High K), or both (K+CNQX). * $P < 0.05$; paired *t*-test. ** $P < 0.01$; paired *t*-test. $ $P < 0.05$; Wilcoxon signed-ranks test.

150.76 ± 29.28% of control. Figure 5.3 shows the changes in ISI (figure 5.3A) and CV (figure 5.3B) expressed as the percentage of control levels.

Figure 5.4 shows examples of autocorrelograms constructed from trains of 1000 spikes from cells under control conditions and the three experimental conditions (CNQX (figure 5.4A & B); High K (figure 5.4C & D); K+CNQX (figure 5.4E & F)). Figure 5.5 shows the mean autocorrelograms for each of the three experimental conditions. Examining these autocorrelograms it is possible to see that 10μM CNQX alone had very little effect on the shape of the mean autocorrelogram (figure 5.5A & B). Increasing the potassium concentration leads to the levelling off of the autocorrelogram much more quickly relative to each spike than under control conditions (figure 5.5C & D). This shows that the correlation that each spike has with spikes up to 10 spikes away from it is decreased when potassium levels are raised. This change in the mean autocorrelogram is not so marked when 10 μM CNQX is present along with the raised potassium levels (figure 5.5E & F). These changes that were seen in the autocorrelograms match the changes seen in the CV showing that in these experiments CV provides a good measure of the regularity of the spiking patterns of STN neurones.

CNQX was found to have not significantly affected either the mean ISI ($t = 0.70$; $P = 0.50$) or the CV ($W = 38$; $P = 0.69$). The reduction in mean ISI seen when high K alone was present was found to be statistically significant ($t = 4.36$; $P = 0.001$). A statistically significant reduction in mean ISI was also found when both CNQX and high K were present ($t = 2.55$; $P = 0.03$). The CV found when high K alone was

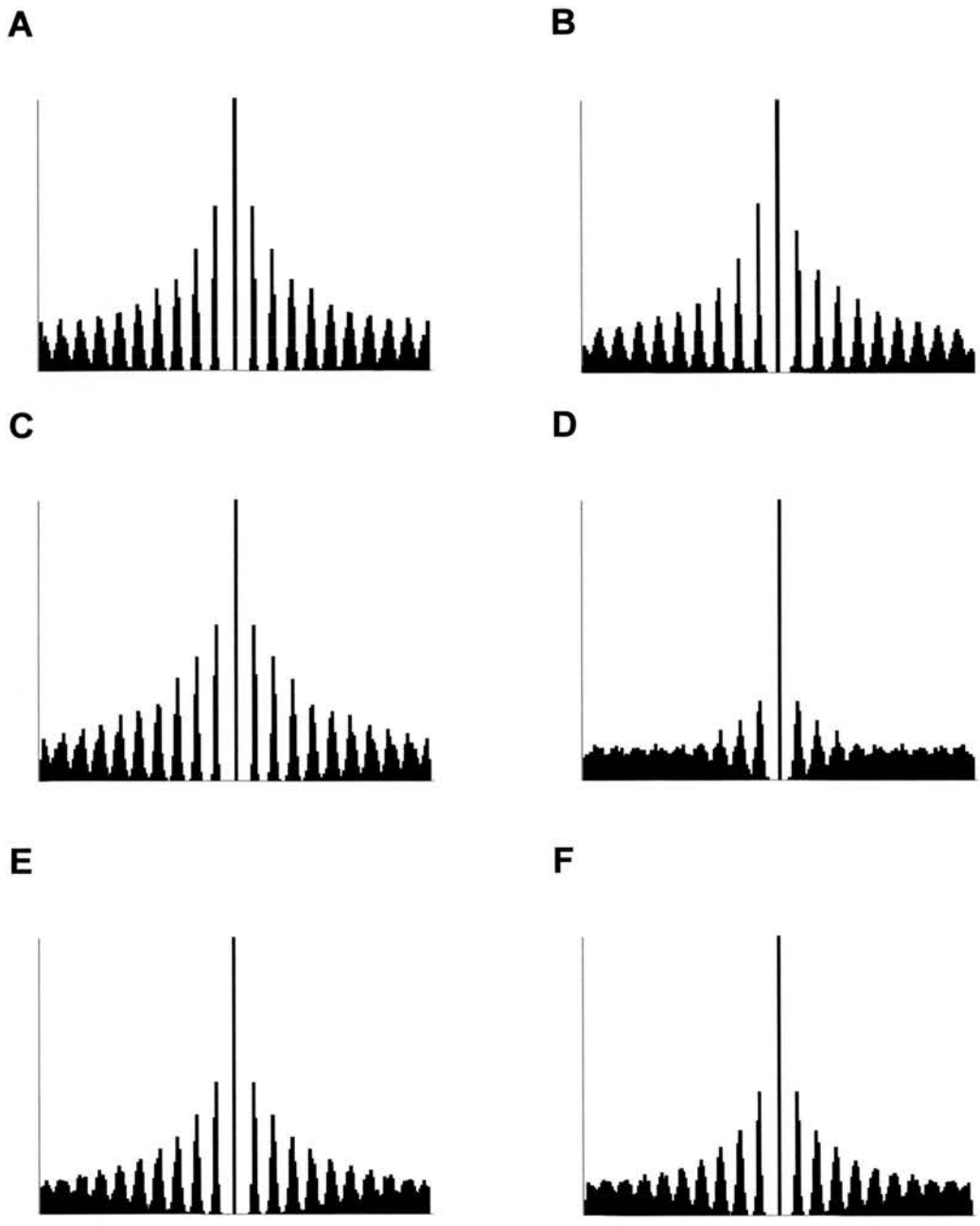

Figure 5.4 Example autocorrelograms from each experimental condition. Each pair represents autocorrelograms from a single subthalamic nucleus neurone under control (**A, C, E**) or experimental (**B, D, F**) conditions . **A** and **B** are autocorrelograms from a subthalamic nucleus neurone before and during the application of 10 μM CNQX. **C** and **D** are from a neurone before and during the application of 10 mM potassium gluconate. **E** and **F** are from a neurone before and during the application of both 10 μM CNQX and 10 mM potassium gluconate.

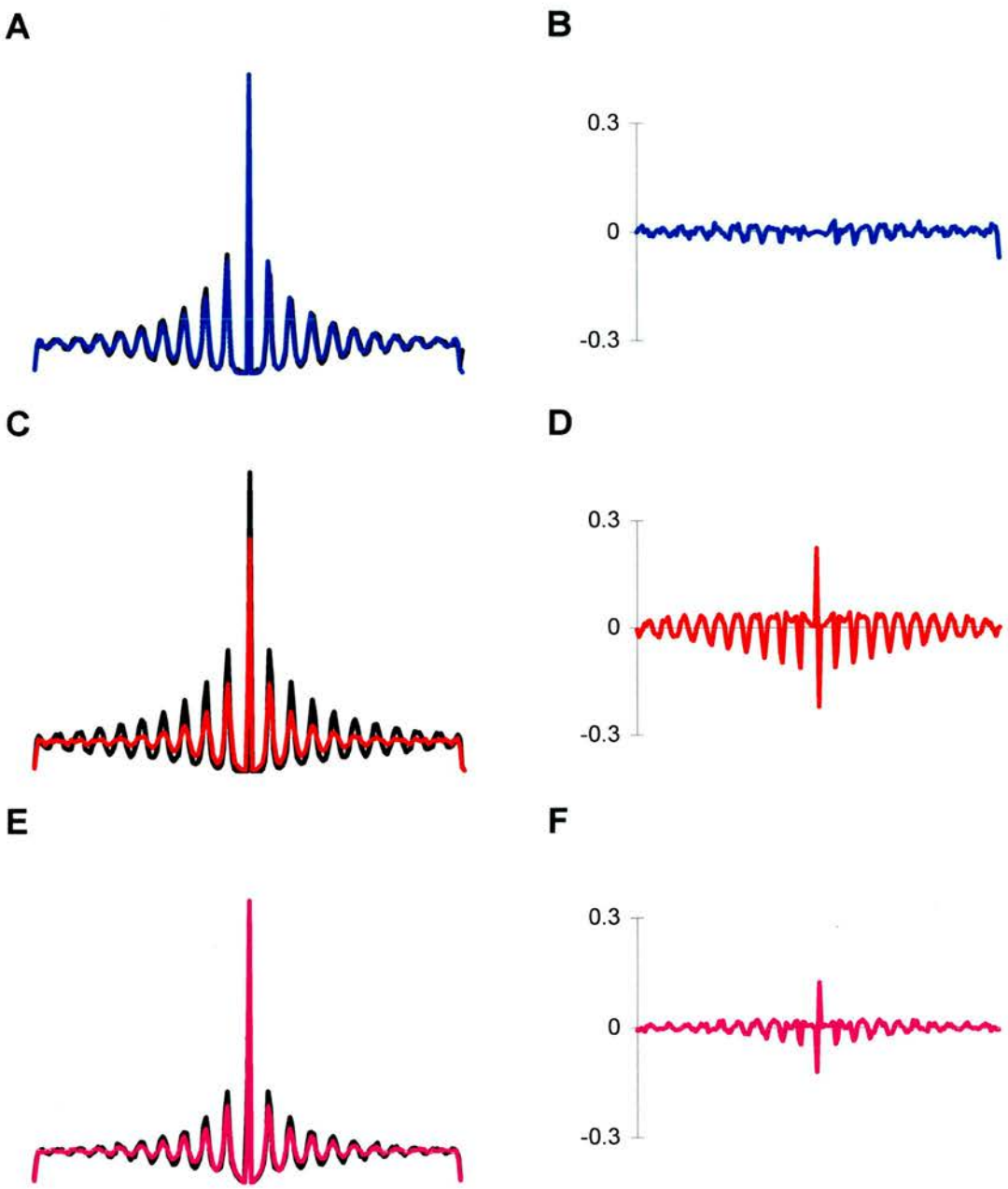

Figure 5.5 Mean and subtracted autocorrelograms. Autocorrelograms from each neurone in each experimental condition were normalised so that their width was 10 times the mean interspike interval (ISI). The bin width used was 0.1 ISI. The resulting traces could be overlaid and a mean trace produced. **A** Data taken before (black line) or during (blue line) the application of 10 μM CNQX. **B** Subtracted trace showing the changes attributable to the CNQX. **C** Data from before (black) or during (red) the application of 10 mM potassium gluconate. **D** Subtracted trace showing the changes attributable to the potassium gluconate **E** Data taken before (black) or during (purple) the application of 10 μM CNQX and 10 mM potassium gluconate. **F** Subtracted trace showing the changes attributable to the CNQX and potassium gluconate together.

present was found to be statistically significantly ($W = 50$; $P = 0.025$) increased over control levels. However, the CV found when CNQX was present along with the High K was not statistically significantly greater than control levels ($W = 36$; $P = 0.415$).

5.4 Discussion

5.4.1 Summary of Results

Extracellular recordings were obtained from STN neurones. The firing rate and pattern were assessed at rest. Neurones were found to fire very regularly at between 3.5 and 48.0 Hz. Increasing the potassium concentration in the aCSF nearly doubled the firing rate of these neurones. This increase in firing rate was accompanied by a disruption of the regular firing pattern. The glutamatergic antagonist CNQX had no discernible effect on either the firing rate or pattern of the neurones when they were at rest. When the neurones were depolarised with potassium and CNQX was also present there was no longer a significant change in the pattern of firing. However, there were no significant differences between the group given depolarisation alone and the group that was depolarised with CNQX present.

5.4.2 The Location of the Neurones Used

The extracellular recordings from neurones used in this study were obtained under visual guidance. The location of the STN in parasagittal brain slices had been previously confirmed using intracellular recording. Neurones from which

intracellular records had been obtained were filled with biocytin, the sections re-cut and the biocytin visualised (Chapter 4). The location of these neurones could then be confirmed as being within the STN as defined by the atlas of Paxinos and Watson (1986). This data was used in the present study to guide visual confirmation of the location of the STN in the rat brain slices.

In addition to the visual localisation of the STN in the rat brain slices, the STN neurones were identified by their characteristic regular and rapid firing at rest. Many previous authors have reported STN neurones within brain slices to have a resting firing rate within this range (Nakanishi *et al.*, 1987; Beurrier *et al.*, 1999; Bevan & Wilson, 1999; Beurrier *et al.*, 2000; Wigmore & Lacey, 2000). In rat brain slices the regularity of the resting firing rate is also a defining feature of STN neurones. The coefficient of variation found in the present study is also comparable to previously reported values (Bevan & Wilson, 1999). In combination these data suggest that the neurones recorded from in the present study were located in the STN.

5.4.3 The Effects of Depolarisation on Subthalamic Nucleus Neurones

Neurones in the STN responded to perfusion with aCSF to which 10 mM potassium gluconate had been added with a marked increase in their firing rate. This showed that the increased potassium levels were depolarising the neurones as had been intended. The increase in firing rate to nearly double the resting level was unaffected

by application of CNQX. This showed that it was unaffected by glutamatergic synaptic transmission and so was driven by the depolarisation.

Alongside the increase in firing rate, the coefficient of variation of STN neurones was increased by the depolarisation. The disruption of the regular firing pattern was attenuated by the addition of CNQX to the aCSF. This shows that glutamatergic synaptic transmission was, in part, responsible for the disruption of the firing pattern.

The lack of any discernible effects of CNQX on STN neurones when they are at rest confirms the observations of previous authors that the resting firing rate of STN neurones is independent of any input to the neurones. Bevan and Wilson (1999) have shown that the resting firing of STN neurones is driven by a stable oscillation in the membrane potential of the neurones. Action potentials were found to be followed by a powerful and long-lasting afterhyperpolarisation. After this there was a slow ramp depolarisation which ended with another spike. This oscillation was dependent on the occurrence of action potentials and was entirely blocked by TTX. The afterhyperpolarisation was shown to be dependent on HVA calcium channels and the SK_{Ca} calcium-activated potassium channels. The slow depolarisation phase was shown to be due to a small persistent, TTX sensitive, sodium current that is similar in nature to I_{NaP} (Beurrier *et al.*, 2000). Thus neurones in the STN are capable of generating action potentials in the absence of synaptic inputs, and this is how the resting firing rate of STN neurones in rat brain slices is generated.

The attenuation by CNQX of the disruption of the regular firing pattern of STN neurones by depolarisation shows that, under these conditions, action potential generation is no longer independent of synaptic input. CNQX is a competitive glutamatergic antagonist that is specific for the AMPA and kainate classes of ionotropic glutamate receptor. It inhibits 50% of binding of AMPA to cortical membranes at a concentration of 0.50 ± 0.10 μM (IC_{50}) and Kainate with an IC_{50} of 2.00 ± 0.10 μM. The IC_{50} of inhibition of CPP (3-(2-carboxypiperazine-4-yl)propyl-1-phosphoric acid) binding was 40 μM indicating a lack of action at the NMDA class of ionotropic glutamate receptors (Honoré *et al.*, 1988). These data indicate that the disruption of the normal regular firing pattern of STN neurones seen in the present experiments was partially mediated through AMPA and/or kainate receptors although at a concentration of 10μM the CNQX will have had a small action at NMDA receptors. Immunolabelling for AMPA receptors revealed multiple AMPA receptor subunits located at asymmetrical axodendritic synapses in the STN (Clarke & Bolam, 1998). These synapses had similar morphological characteristics to terminals in the STN derived from inputs from the cortex and thalamus suggesting that these are the sources of glutamatergic input to the STN. However, in the present study these inputs to the STN had been acutely cut. This suggests that the actions of CNQX cannot have been through these terminals (this proposition will be discussed further below). The STN sends glutamatergic projections to many basal ganglia structures where its axons also form asymmetrical synapses on dendrites which are immunopositive for AMPA receptors (Bevan *et al.*, 1994; Clarke & Bolam, 1998; Smith *et al.*, 1998; Chatha *et al.*, 2000). Similar synapses were also seen in the STN following injections of BDA into the GPi (EP) of squirrel monkeys (Shink *et al.*,

1996). These terminals contained round synaptic vesicles and formed asymmetrical axodendritic synapses. The authors conclude that the source of these terminals was the STN neurones themselves. The tracer had been retrogradely transported from the GPi to the STN and then transported anterogradely along the axons of STN neurones to the terminals. In the rat a proportion of STN axons have been shown to display up to three axon collaterals that innervate the STN itself (Kita *et al.*, 1983b). These terminals provide the most likely site of action for CNQX in the present experiments.

The geometric model of the STN produced by Gillies and Willshaw (1998b) showed that these intranuclear collaterals could lead to a massive degree of interconnections between neurones of the STN. Network modelling showed how these interconnections might affect the behaviour of the neurones within the nucleus. Correlation between the firing of pairs of STN neurones has not been observed (Ryan *et al.*, 1992; Magill *et al.*, 2000). However these recordings were taken from STN neurones when they were at rest. Analysis of the network model revealed that intranuclear interactions would produce some degree of non-synchronous correlation between the responses of pairs of neurones, but that this would occur primarily during periods when levels of activity are increased. This behaviour was a consequence of the sigmoidal nature of the I-f curve for these neurones. What form this non-synchronous correlation would take is uncertain as the model was not a spiking model. This means that it may not be expected to see any direct spike-to-spike correlation between pairs of cells but rather that the overall activity levels of groups of cells will change together. In agreement with the previous results the present study has shown no evidence for a glutamatergic influence on the behaviour

of STN neurones when they are at rest. But, in agreement with the modelling results, depolarisation of the neurones resulted in there being a noticeable effect of glutamatergic transmission on the firing patterns. The disruption of the normally regular firing pattern in the depolarised STN can then be explained if the neurones of the STN are either not firing in synchrony or if different lengths of axon collaterals produce variable delays in neurone-to-neurone transmission. In both these cases a neurone would be receiving asynchronous EPSPs from many other STN neurones. These inputs would interact with the normally rhythmical generation of action potentials and disrupt this rhythm. That this doesn't happen at rest could be due to the sigmoidal nature of the I-f relationship of STN neurones, as visualised by the model. When the neurones are at rest they are on the plateau at the lower end of this curve. In this case small changes in the membrane potential of a neurone such as those produced by EPSPs would have little effect on the firing rate of the neurone. When the neurone is depolarised it is moved to the steep linear section of the sigmoidal curve, now the same small changes in its membrane potential would have a much larger effect on its firing rate.

If this is the case then why does CNQX lead to only a partial attenuation of the disruption in firing pattern of STN cells? In addition to AMPA receptors, the neurones of the STN strongly express NMDA receptors (Standaert *et al.*, 1994). These are found on the postsynaptic membrane of asymmetrical synapses co-localised with the AMPA receptors (Clarke & Bolam, 1998). Activation of NMDA receptors requires the simultaneous presence of a ligand and postsynaptic depolarisation. This is due to the presence of a voltage sensitive Mg^{+} antagonism of

the receptors (Evans *et al.*, 1979). The depolarisation of the neurones will reduce the voltage sensitive Mg^{+} blockade of NMDA receptors making it more likely that they will be activated. Coupled with this is the fact that CNQX does not provide effective antagonism of NMDA receptors. Together this highlights the possibility that activation of NMDA receptors is playing a role in the disruption of regular firing of action potentials. Activation of NMDA receptors is associated with an influx of calcium ions and subsequent synaptic plasticity (Muller *et al.*, 1988).

The intranuclear collaterals are not the only possible source of the changes in firing patterns seen in this study. CNQX could have non-specific effects on the sodium and potassium channels of STN neurones. There is no evidence to support this explanation and the lack of effect of CNQX on the STN neurones when they were at rest suggests that this is not the case. However, the cut ends of the glutamatergic projections to the STN from the cortex and thalamus may still be able to release glutamate. Arbuthnott, *et al.* (1984) have shown that dopamine release can be stimulated in the striatum many hours after the preparation of brain slices in which the nigrostriatal pathway has been cut. Thus the corticosubthalamic axon terminals may release glutamate spontaneously in the resting slice. Raising the potassium concentration of the aCSF could increase such release (Su *et al.*, 1990). It is uncertain how glutamate release from these axon terminals would affect the behaviour of the STN neurones. If glutamate is released, this release will be random and so will not produce EPSPs in the same way that transmitter release following an action potential does. It is more likely that any glutamate released from these terminals would provide a constant depolarising influence on the postsynaptic STN

neurones amplifying the effects of the depolarisation due to the raised potassium concentration. When a combination of CNQX and high potassium aCSF was applied the firing rate of STN neurones was no different from neurones that had only had high potassium aCSF applied. This suggests that there was no extra depolarisation due to glutamate acting at AMPA or kainate receptors although it does not exclude an action through NMDA receptors. However, the concentration of potassium used in the high K condition (10 mM) was relatively small and may not result in much additional glutamate release. 10 mM potassium chloride resulted in only a minimal level of monoamine release in hippocampal slices (Su *et al.*, 1990). Thus, although glutamate release from the terminals of these cut axons cannot be ruled out entirely, it is likely that its contribution to the results of the present experiments was minimal. However, the only way to be completely sure that this is the case would be to redo the present experimental protocols using animals that had been chronically decorticated.

5.4.4 Neurones in the Subthalamic Nucleus Are Functionally Interconnected

The effects of CNQX on depolarised STN neurones indicate that these neurones are indeed functionally interconnected. The effects of this interconnectivity seen in the present experiments are entirely consistent with the predictions produced by Gillies and Willshaw (1998b) from their network model of the STN. This model was unable to reproduce one aspect of the experimental data. The model STN cells did not produce spikes, instead a parameter was calculated that represented their firing rate.

The effects of glutamatergic interconnections on the firing patterns of STN cells had therefore not been investigated in the model. This means that the discovery that depolarisation alters the firing pattern of STN neurones in a glutamate-dependent fashion was an addition to the data that had been gained from previous modelling experiments. In order to discover if a network model of the STN could behave in the manner that the STN neurones had done in the present experiments a new network model of the STN was constructed (Gillies *et al.*, 2000).

This model was constructed using the NEURON (Hines & Carnevale, 1997; Hines & Carnevale, 2000) simulation software. Networks were constructed from multicompartmental units representing STN neurones. These units included six channel types. NaCh, KCh, HVA and LVA calcium channels were modelled using the same kinetics as in the single cell model described in chapter 3. In addition to this I_{NaP} was added, represented by a sodium 'leak' current. This leak was intended to model the persistent sodium current (I_{NaP}) found in STN neurones, and thought to underlie the spontaneous firing of these neurones (Bevan & Wilson, 1999; Beurrier *et al.*, 2000). Indeed the addition of a sodium leak to the model STN units did lead to the spontaneous generation of action potentials. The conductance of the leak channels was then adjusted to give a physiologically realistic basal level of firing. At synapses, glutamatergic type channels were placed on the postsynaptic neurone such that presynaptic activity promoted the production of an *excitatory postsynaptic current* (EPSC). The single units were able to replicate the single-cell electrophysiology of STN neurones. When connected together to form a network these units were able to replicate the results of the present experiments. This

indicates that it is indeed possible to account for the behaviour of the STN neurones seen in the present experiments with mechanisms intrinsic to the nucleus. Thus this new model strengthens the evidence that neurones in the STN are functionally interconnected.

Interestingly, depending on the initial parameters used in the system, the model either replicated the present results exactly or performed in the opposite manner. Thus it was possible to get a situation where high K only increased the CV when CNQX was also present. The model very rarely produced results that were outside one of these two schemes. This means that there are certain parameters within the model that control whether the model replicates the experimental data or whether it performs in the opposite manner. Searching for these parameters revealed that the model was more likely to replicate the experimental data if the synapses that the intranuclear collaterals formed on other STN units were located on the soma or the proximal dendrites of these units. Further analysis of the model also showed that it was more likely to replicate the experimental results if the EPSPs, that occur following action potentials reaching these synapses, were small.

This new model then generated new predictions. Further experiments would be possible to reveal if these predictions are correct. It may also be possible, to use the model to estimate the level of interconnectivity that would have to be present within a network that replicates the present experiments. Using this prediction it would be possible to predict the likelihood of being able to find and record from two single STN cells that are connected together. Following this, dual cell records could be

obtained looking for pairs of STN neurones where stimulation of one neurone is able to drive activity in the other. Filling these two neurones with different tracers (e.g. biocytin and HRP) would enable possible reconstruction of any interconnections between them. It would take many such pairs to reveal whether the synapses are indeed mostly proximal to the soma, thus making this a difficult and lengthy series of experiments. This protocol would also enable the investigation of the size of the EPSPs generated by activation of the intranuclear collaterals.

The possibility that neurones in the STN are indeed interconnected has implications for the way in which the neurones of the STN may behave in response to excitatory inputs. The STN receives excitatory inputs from the cortex, thalamus and brainstem. As well as these inputs, the GABAergic inputs from the GP can potentially also lead to the excitation of STN neurones (Bevan *et al.*, 2000). Stimulation of a single area in the cortex leads to the excitation of neurones throughout the STN (Fujimoto & Kita, 1993). This may be due to the size of the dendritic fields of STN neurones, but the present study adds to the evidence that it could also be due to the presence of intranuclear collaterals in the STN. Thus an input to a small cluster of STN neurones could excite neurones in a much wider area of the STN. The results of Gillies and Willshaw's (1996; 1998b) modelling experiments and the present experiments suggest that the neurones in the STN may have two modes of operation. When they are at rest, neurones will respond individually to their excitatory inputs, as the effects of these individual neurones on other neurones within the nucleus will be minimal. However, if the neurones within the STN became depolarised, then an excitatory input to a single neurone (or a small cluster of neurones) has the potential to spread

throughout the nucleus. How such a dual mode of operation may fit into the functioning of the basal ganglia as a whole will be discussed further in chapter 7.

6 Is There a Link Between High Frequency Firing of Subthalamic Nucleus Neurones and Dopamine Cell Death in Parkinson's Disease?

6.1 Introduction

We have seen that neurones in the rat STN are capable of achieving and maintaining very high frequencies of action potential firing. Also, that when such raised levels of activity are occurring the influence of the intranuclear axon collaterals on the behaviour of the neurones in the nucleus is markedly increased. The network model of Gillies and Willshaw (Gillies & Willshaw, 1998b) predicted that this increased influence of the intranuclear collaterals on the STN neurones behaviour would lead to the generation of widespread pulses of activity within the STN. As predicted by the 'direct/indirect pathway hypothesis', neurones in the STN have been found to have increased levels of activity both in Parkinsonian patients and in animal models of the disease (Hassani *et al.*, 1996; Vila *et al.*, 2000; Magariños-Ascone *et al.*, 2000; Périer *et al.*, 2000). This hyperactivity, combined with changes in the patterns of neuronal firing, have been suggested to underlie many of the symptoms of the disease. Our data, combined with these findings, suggest that the STN in PD patients may be generating massive pulses of widespread activation that would flood the targets of the STN with glutamate. Such widespread hyperactivity of STN neurones could be damaging to neurones that are targets of the STN. Indeed it is possible that

STN hyperactivity may also be responsible for some of the ongoing dopamine cell death seen in PD patients as the disease progresses (Rodriguez *et al.*, 1998b).

The glutamatergic neurones in the STN are known to send projections directly to the dopaminergic neurones of the SNc. Under normal circumstances this projection can modulate the firing patterns of these dopamine cells (Chergui *et al.*, 1993; Chergui *et al.*, 1994; Kang & Futami, 1999). Indeed tetanic stimulation of STN neurones has been shown to induce NMDA receptor-dependent long-term potentiation (LTP) at the synapses with the dopamine cells (Overton *et al.*, 1999). It is possible, in situations where the firing rates of STN neurones is increased, or their pattern has changed to become more bursty, that the subsequent increased release of glutamate into the SNc by STN neurones could become toxic to the dopaminergic cells (Rodriguez *et al.*, 1998b). It has been known for a long time that glutamate can be toxic to neuronal cells (Lucas & Newhouse, 1957). When these neurotoxic effects of glutamate were associated with its excitatory effects on neurones (Olney *et al.*, 1971) the term *excitotoxicity* was coined for this mode of cell death (Coyle, 1983). There is an increasing body of evidence that the dopamine cell death seen in PD patients is, at least partly, due to excitotoxic mechanisms. Several studies have shown that NMDA receptor antagonists can be neuroprotective in both the MPTP and 6-OHDA models of PD (reviewed in Rodriguez *et al.* (1998b)). Agents that inhibit glutamate release have also been shown to have similar neuroprotective effects (Jones-Humble *et al.*, 1994; Boireau *et al.*, 1994; Benazzouz *et al.*, 1995; Barnéoud *et al.*, 1996). Also neuroprotective, are agents that disrupt the actions of NO (NO is believed to be involved in excitotoxic cell death). Further evidence comes from the brains of PD

patients themselves. Lewy bodies seen in the surviving dopaminergic cells show a marked increase in staining for 3-NT, which can be taken as evidence for increased NO and peroxynitrite formation (Good *et al.*, 1998). There is also evidence for mitrochondrial dysfunction and iron accumulation, both thought to be consequences of excitotoxicity.

Evidence for the involvement of the STN in this excitotoxic cell death comes from a number of sources. Most directly, lesions of the rat STN prior to a neurotoxic challenge with 6-OHDA can be neuroprotective (Piallat *et al.*, 1998), although not all authors agree on this (Baunez & Robbins, 1999a). In fact excitotoxic lesions of the STN made during the same operation as a partial 6-OHDA lesion of the nigrostriatal dopamine neurones can increase the dopamine cell death seen as a result of the 6-OHDA injection (Phillips *et al.*, 1998). Neuroprotection, in both the 6-OHDA and MPTP animal models of PD, can also be achieved by using NMDA receptor antagonists but not AMPA receptor antagonists. The action of the projection from the STN to the SNc is mediated through NMDA receptors (Chergui *et al.*, 1993; Chergui *et al.*, 1994) whereas other glutamatergic projections to the SNc (e.g. from the PPN) mostly use AMPA receptors (Di Loreto *et al.*, 1992). This evidence strongly suggests that a glutamatergic action from STN terminals is involved.

These data implicate the STN in the progressive destruction of nigral dopaminergic cells seen in Parkinsonian patients. That such progressive cell death can occur following an initial insult was recently illustrated by the first deaths of patients who had Parkinsonism caused by self-administration of MPTP (Langston *et al.*, 1999).

These patients still had signs of active degeneration in the SNc even though it was up to 16 years after the last time that they took the MPTP that had caused the initial dopamine cell death. As there is no chance that the MPTP or any of its metabolites could have survived this long, the only explanation for this observation is that the initial cell death caused by the MPTP has set up a cascade of events that can still be in progress many years later. There are many possible explanations for these observations. These include oxidative stress due to increased dopamine turnover or self-perpetuating inflammatory processes. However, excitotoxicity due to STN hyperactivity provides an attractive explanation as this could cause both oxidative stress and induce inflammatory processes.

A simple test of the excitotoxic hypothesis for dopamine cell death in PD would be to somehow induce the neurones of the STN to become chronically hyperactive *in vivo* and then to investigate the subsequent fate of dopaminergic neurones in the SNc. Many authors have made acute pharmacological manipulations of STN activity levels *in vivo* (Robledo & Feger, 1990; Feger & Robledo, 1991; Murer & Pazo, 1993; Chergui *et al.*, 1994; Hauber, 1998; Baunez & Robbins, 1999b; Kearney & Albin, 2000). However chronic changes in STN activity have only been achieved by lesions of either the STN itself or of other brain areas. Lesions of the GP have been shown to produce a relatively long lasting increase in the resting firing rate of STN neurones to approximately 20% above their normal level (Fujimoto & Kita, 1993; Hassani *et al.*, 1996). These lesions have also been shown to lead to an amplification of the response of STN neurones to cortical stimulation (Fujimoto & Kita, 1993). 6-OHDA lesions of the dopaminergic neurones projecting along the nigrostriatal

pathway lead to a much greater increase in STN resting firing rates to about 130% above normal levels. Therefore the 6-OHDA lesion would seem to be the most suitable choice of lesion for producing an increase in STN activity. However, the 6-OHDA lesion destroys the very cells whose fate we are interested in. It would be difficult to dissociate loss of nigral dopaminergic cells due to the 6-OHDA from loss due to STN hyperactivity. For this reason GP lesions present the best possible method of increasing STN activity levels whilst avoiding damaging dopamine cells in the course of making the lesion. A 20% increase in STN activity might not be enough to be excitotoxic to neurones in the structures to which the STN projects. An alternative possibility for increasing the firing rates of STN neurones would be through the chronic pharmacological manipulation of STN activity levels. Therefore the possibility of using this method also needed to be assessed. There are two possible protocols for achieving a chronic infusion of drugs into the rat brain. Firstly, regular injections of an agent that would increase STN activity could be made through a chronically implanted cannula. The limitations of this method are that each injection will cause damage around the tip of the cannula, which restricts the number of injections that can be made. There is also the possibility that repeated injections may cause the cannula to move. Minipumps provide another possibility for delivering a steady flow of pharmacological agents to the STN over a period of many days. The usefulness of this method is limited by the small size of the STN. It would be very difficult to restrict the diffusion of a drug just to the STN. Under many circumstances this may not cause a problem however, the most promising agent for stimulation of STN neurones is the $GABA_A$ antagonist bicuculline (Robledo & Feger, 1990; Feger & Robledo, 1991). If this were to diffuse away from the STN it

may get into the lateral ventricle which is very close by. This gives the possibility of widespread diffusion of a GABAergic antagonist throughout the brain, which could generate epileptic seizures. A small pilot study was undertaken to compare the feasibility using chronically implanted cannulae for regular infusions of bicuculline with GP lesions. Following this pilot, GP lesions were selected as by far the best and most reproducible of these two methods. GP lesions were then made in a number of rats and the numbers of dopaminergic neurones in the substantia nigra counted either three or six weeks later.

6.2 Methods

Experimental work presented in the following sections was conducted by A.K. Wright and K.E. McLaughlin.

6.2.1 Lesions of the Globus Pallidus or the Subthalamic Nucleus

Male Sprague-Dawley rats (250-300 g; Harlan, UK) were anaesthetised by placing them in a plastic chamber, which was circulated with a mixture of oxygen and fluothane gas. Once anaesthetised they were fixed in a stereotaxic frame. Their body temperature was controlled by a heated mat connected to a rectal probe. The skull was exposed and a small hole drilled through it. The dura was moved out of the way and a needle was lowered into place. The tip of the needle was positioned at the co-ordinates 2.8mm lateral to the midline, 1.1mm posterior to bregma, and 5.7mm

ventral to the cortical surface using the atlas of Paxinos and Watson (1986). 10μg of Ibotenic acid (Sigma-Aldrich Company Ltd., Poole, UK) made up with phosphate buffered saline to a total volume of 1μl was injected over 5 minutes. The needle was then left in place for a further 5 minutes in order to limit diffusion of the ibotenic acid back along the needle tract.

When the animals recovered from the anaesthetic they were given a non-steroidal anti-inflammatory drug (Zenecarp, C-Vet; 5 mg/kg) as an anti-nociceptive and ketamine (25 mg/ml) in order to control the seizures that inevitably occur during the first few hours following a excitotoxic GP lesion.

A subset of rats received lesions of the STN instead of the GP. These operations were conducted in exactly the same manner as the GP lesions except that glass micropipettes were used in place of a needle connected to a 5μl Hamilton syringe. 0.5μl of ibotenic acid (1mg/100ml in PBS) was injected, and the co-ordinates used were 2.2mm lateral to the midline, 3.8mm posterior to bregma, and 7.1mm ventral to the cortical surface.

Three or six weeks following the GP lesions and four weeks following the STN lesions the rats were injected with amphetamine (2mg/ml; 1ml/kg) and placed into spherical bowls (figure 6.1). The total numbers of full clockwise and anticlockwise turns that each rat made in a 60 minute period was then measured (Ungerstedt & Arbuthnott, 1970).

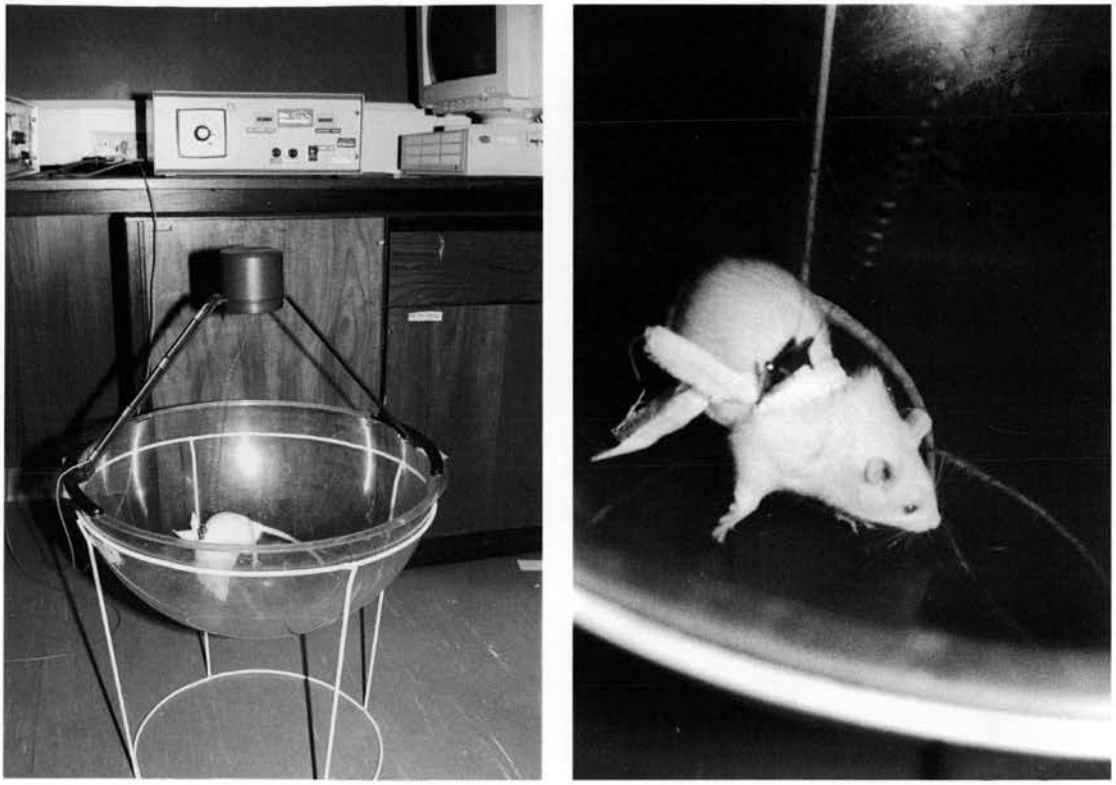

Figure 6.1 Illustration of the method for turning rats. Rats were injected with amphetamine (2 mg/kg) and placed into a spherical bowl. A loose-fitting bandage around the rats chest, just below the forelegs, was connected to a rotameter for the counting of complete clockwise or anticlockwise turns

Following this, the rats were deeply anaesthetised with pentobarbitone (1 ml/kg; Sagatal; Rhone Merieux, Harlow, UK) and perfused transcardially with fixative (4% paraformaldehyde, 0.05% glutaraldehyde in 0.1M phosphate buffer pH7.4). Their brains were removed and placed in a 50:50 solution of fixative overnight and 20% aqueous sucrose at 4°C.

6.2.2 Immunohistochemistry

50μm coronal sections of the fixed brains were cut on a freezing microtome and collected in 0.05M sodium phosphate buffered saline (pH 7.4) containing 0.3% Triton-X100 (PBS-TX). Sections were sorted as follows:

GP lesion 3 week rats

Sections containing the GP sorted into three groups:

Group 1 - stained with A60, an antibody against the neurone specific nuclear protein *NeuN.*

Group 2 - stained with an antibody against Glial Fibrillary Acidic Protein (GFAP).

Group 3 - stained with OX42 an antibody against the type 3 complement receptor.

Sections containing the SN sorted into two groups:

Group 4 - stained with an antibody against Tyrosine Hydroxylase (TH).

Group 5 - subdivided into two further groups:

Group 5a - stained with an antibody against GFAP.

Group 5b - stained with OX42.

GP lesion 6 week rats

Sections containing the GP were stained with A60.

Sections containing the SN were divided into two groups:

Group 1 - stained with an antibody against TH.

Group 2 - subdivided into two further groups:

Group 2a - stained with A60.

Group 2b - stained with OX42.

STN lesioned rats - sections were divided in the same manner as the 6 week GP lesioned group.

For all groups of sections, staining was performed on free-floating sections in multiwell plates.

A60 Immunohistochemistry

The antibody A60 was a present from W. Staines at the University of Ottawa. It is a neuronal specific antibody, recognising the nuclear protein NeuN (Mullen *et al.*, 1992; Wolf *et al.*, 1996). Sections were maintained on a rotational shaker (model

R100 rotatest shaker; Luckham Ltd., Sussex, UK) and maintained at room temperature (unless otherwise stated) at all times during the staining process.

The sections were given four 10 minute washes in PBS-TX. Then they were incubated in 20% donkey serum in PBS-TX for two hours. After this, the sections were left overnight on a shaker at 4°C to incubate in A60 monoclonal antibody (1:500 dilution with PBS-TX). The next morning the sections were given a further two 10 minute washes in PBS-TX before being incubated for one hour at room temperature in biotinylated horse anti-mouse-IgG (1:100 dilution in PBS-TX). This was followed by another two 10 minute washes, this time in sodium phosphate buffered saline without Triton-X100 (PBS). The antibody was then revealed using the Vectastain ABC Elite kit (Vector Laboratories Ltd., Peterborough, UK). This involved incubation for one hour in Elite ABComplex (1:50 dilution in PBS). This was followed by two 10 minute washes in PBS before the sections were placed in 3,3′-diaminobenzodine substrate (DAB; Vector Laboratories Ltd., Peterborough, UK) for 10 minutes. The sections were then given a further four 10 minute washes in PBS before being mounted on gelatine coated slides and left for a week at 45°C to dry.

GFAP Immunohistochemistry

GFAP is a protein that is expressed most strongly in activated astrocytes (McQueen *et al.*, 1990). Anti-GFAP antibody was obtained from Dako Ltd. (Cambridgeshire,

UK). At all stages sections were maintained on a rotational shaker at room temperature unless otherwise stated.

First the sections were given four 10 minute washes in PBS-TX. They were then incubated in 20% goat serum in PBS-TX for two hours before being left on a shaker overnight in rabbit anti-GFAP (1:2000 dilution in PBS-TX) at 4°C. The following morning they were given two 10 minute washes in PBS-TX before being placed in biotinylated goat anti-rabbit (1:200 dilution in PBS-TX) to incubate for one hour. Following this, the sections were given two 10 minute washes in PBS before the antibody was revealed using the ABC standard kit (Vector Laboratories Ltd., Peterborough, UK). This involved incubating the sections in standard ABComplex (1:100 dilution in PBS) for 1 hour, then giving them two 10 minute washes in PBS. Following this the sections were incubated in DAB substrate for 10 minutes and then given a further three 10 minute washes in PBS. The sections were then mounted on gelatine coated slides and left for a week at 45°C to dry.

OX-42 Immunohistochemistry

OX-42 is an antibody against the type 3 complement receptor and is a microglia specific marker (Robinson *et al.*, 1986). OX-42 was obtained from Serotec Ltd. (Oxford, UK). At all stages sections were maintained on a rotational shaker at room temperature unless otherwise stated.

The sections were given four 10 minute washes in PBS-TX. This was followed by placing the sections in 20% donkey serum in PBS-TX to incubate for two hours. They were then left overnight at 4°C in OX-42 (1:2000 dilution in PBS-TX). The next morning the sections were given two 10 minute washes before being placed into biotinylated horse anti-mouse (1:200 dilution in PBS-TX) to incubate for one hour. This was followed by two 10 minute washes before the antibody was revealed using the ABC Elite kit and DAB substrate (as for A60 Immunohistochemistry). The sections were then given a further three 10 minute washes before being mounted on gelatine coated slides and left to dry for one week at 45°C.

Tyrosine Hydroxylase Immunohistochemistry

TH is an enzyme in the dopamine synthesis pathway. Therefore the antibody against TH marks for neurones that are synthesising dopamine. This antibody was obtained from Eugenetec (Allendale, USA). At all stages sections were maintained on a rotational shaker at room temperature unless otherwise stated.

The sections were washed four times in PBS-TX and then placed in 20% goat serum in PBS-TX to incubate for two hours. Following this, the sections were left incubating in rabbit anti-TH (1:2000 dilution in PBS-TX) overnight at 4°C. In the morning the sections were washed twice with PBS-TX (10 minutes/wash) and left in biotinylated goat anti-rabbit (1:200 dilution in PBS-TX) to incubate for one hour. After two 10 minute washes in PBS, the antibody was revealed using the ABC Elite kit and DAB substrate (as for A60 immunohistochemistry). The sections were then

given a further three 10 minute washes in PBS before being mounted on gelatine coated slides and left to dry for one week at 45°C.

After they had been drying for a week all of the slides from all of the groups were dehydrated in a graded series of alcohols. This involved being left for 10 minutes in each of the following: 70%, 90%, and three sets of 100% ethanol before being placed in two separate sets of xylene for 15 minutes each set. Coverslips were then placed on the slides using DPX mountant (Merck Ltd., Lutterworth, UK).

6.2.3 Unbiased Stereological Counting of Tyrosine Hydroxylase Positive Cells

In order to make an accurate count of the total number of TH+ve neurones in the SN, systematic random sampling techniques were used.

From a random starting point, every second section of the area of the brain containing the SN had been selected for immunohistochemical staining using an antibody against TH (described above). This set of sections was then used for unbiased stereological counting of TH+ve cells using the optical fractionator method (West *et al.*, 1991) from the *stereo investigator* program (Microbrightfield Inc., VT, USA) on the Neurolucida (Microbrightfield) computer-controlled microscopy system. On each section a contour was drawn outlining the SN both on the ipsilateral and contralateral sides to the GP (or STN) lesion. Counting frames (150μm × 150μm) were placed at the intersections of a grid of frame size 700μm × 300μm that

had been randomly placed over the section (figure 6.2). Only counting frames for which at least a part of the frame fell within the contour of the SN were used for counting. A 3 μm guard zone was set at the top and bottom of the slice and then the focus of the microscope moved slowly down through the slice between the guard zones. Cells were marked only if they met the following criteria: a) The cell was TH+ve. b) The nucleus lay within the area delineated by a counting frame. c) The level of focus at which the uppermost point of the nucleus came into sharp focus lay in area in between the two guard zones. In this way the total number of TH+ve cells in a known fraction of the SN were counted. In order to estimate the total number of TH+ve cells in the whole SN, this number was multiplied up by the fraction of the volume of the SN that had been counted. The reliability of this estimate was assessed by calculation of the coefficient of error (CE) according to the formulae described in West and Gundersen (1990). The average CE was calculated according to the formula (Oorschot, 1996):

$$CE = \sqrt{(1/n \times \sum_i CE_i^2)}$$

In order to assess overall variability of the counts the observed coefficient of variation (OCV) was calculated according to the formula:

$$OCV = SD / mean$$

and the relative contributions to this variability of biological, between animal, variability (CV) and the counting error (as measured by CE) assessed according to the equation:

$$OCV^2 = CV^2 + CE^2$$

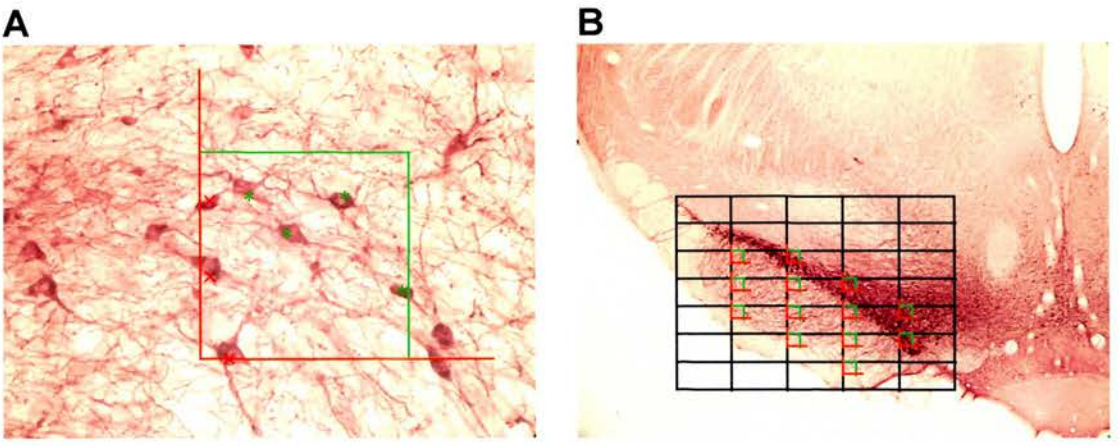

Figure 6.2 An illustration of the optical fractionator method for counting neurones. The photomicrographs show coronal sections of the rat brain stained with an antibody against tyrosine hydroxylase. **A** High power photomicrograph showing individual tyrosine hydroxylase immunopositive neurones. Superimposed over the photograph is a counting frame. Marked with a green asterisk are those neurones that lie within this counting frame or touching the green line and are therefore included in the count. Marked with a red cross are those neurones that lie partially within the counting frame but are not counted because they touch the red line. **B** A grid showing the distribution of counting frames has been superimposed over this low power view of a coronal section showing the substantia nigra.

As well as estimating the total number of TH+ve cells in the SN the outlines of the SN were used to gain an estimate of the total SN volume using the Cavalieri method (Coggeshall, 1992; Ingham *et al.*, 1998). The Cavalieri method uses the same systematic random sampling technique as described above and so can be performed on the same sections. The volume of the SN (V_{ref}) was estimated according to the formula:

$$V_{ref} = a \times t \times s$$

where a is the mean area of the SN contours, t is the section thickness (50μm), and s is the total number of sections defined as including the SN.

6.2.4 Statistical Methods

Immunohistochemical staining for A60, GFAP and OX42 were assessed qualitatively only. A60 staining was used to visualise the ibotenic acid lesions, which could be seen easily down the microscope as an area devoid of any stained nuclei. GFAP and OX42 staining were visually assessed for side-to-side differences.

Side-to-side differences in the numbers of TH+ve cells were assessed by expressing the number of cells on the side ipsilateral to the lesion as a percentage decrease from the contralateral side using the format:

Percentage decrease = 100 (1- (ipsilateral/contralateral))*

Absolute numbers of cells on the two sides were compared with a student's *t*-test. A comparison of the effects of time (3 weeks *vs.* 6 weeks) on these side-to-side differences was made using a general linear model ANOVA (Minitab). The α level

of 0.05 was used as the criterion value for *P* below which any observed differences between groups would be accepted as statistically significant.

6.3 Results

6.3.1 Confirmation of the Positioning of the Lesions

Immunohistochemical staining with A60 enabled confirmation of the size and position of the GP and STN lesions by inspection of the areas of brain in which there were no stained neurones on the ipsilateral side when compared to the contralateral side (figure 6.3A and B). The GP lesions were large and included the majority of the GP and usually a small part of the adjacent striatum. In one rat the GP lesion was off target and only the striatum was lesioned. However, this was fortunate as it provided a useful control against the effects of the minor striatal damage seen in the other rats.

The STN lesions were small and discrete causing damage only to neurones within the boundaries of the STN itself (figure 6.3C and D). As the lesions had been performed using micropipettes there were some rats in which the pipette had been lowered into the STN but had blocked *en route* with the result that no ibotenic acid had been injected and there was no visible damage in the STN. These rats were subsequently used as control animals.

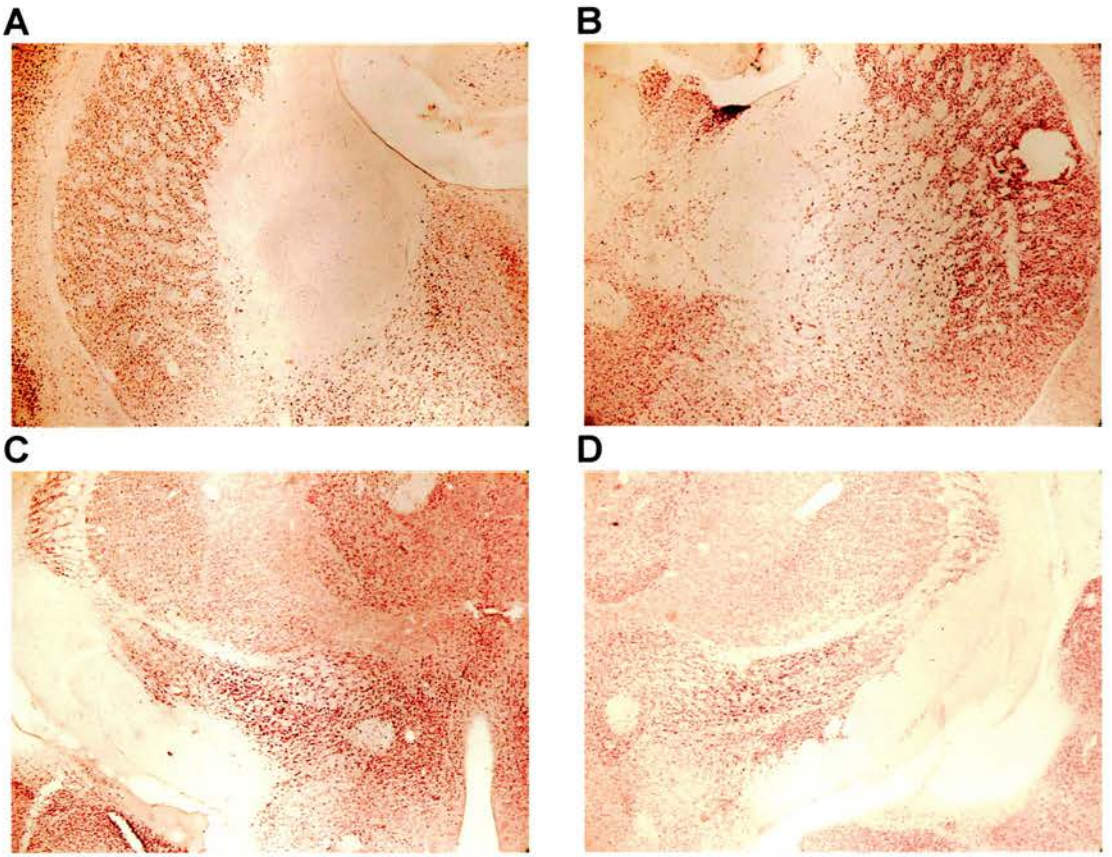

Figure 6.3 Ibotenic acid lesions of the globus pallidus and the subthalamic nucleus. **A** Shows a lesion of the globus pallidus revealed by immunostaining with the neurone specific antibody A60. **B** Shows the contralateral control from the same rat. **C** A lesion of the subthalamic nucleus also revealed using the A60 stain. **D** The contralateral control for **C**.

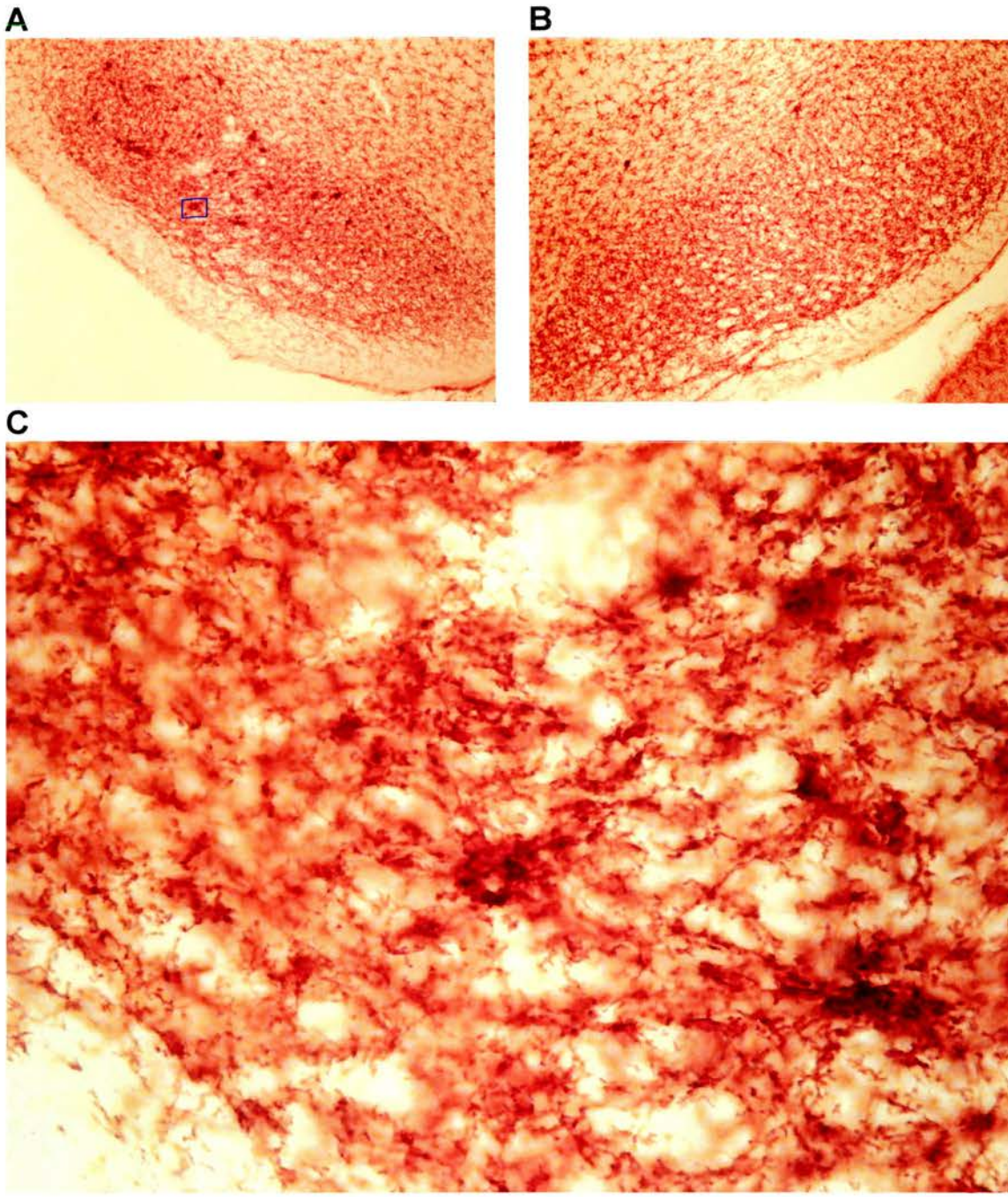

Figure 6.4 Coronal sections taken from rat brain three weeks following an ibotenic acid lesion of the globus pallidus stained with the OX-42 antibody. **A** Low power photomicrograph showing the substantia nigra ipsilateral to the globus pallidus lesion. **B** Photomicrograph showing the substantia nigra contralateral to the GP lesion. **C** High power photomicrograph of the ipsilateral substantia nigra showing the area enclosed in the box in **A**.

6.3.2 Microglial Activation

Microglial activation was assessed by the qualitative examination of the sections that had been stained with the anti-GFAP antibody or with OX42.

There was an increase in the staining for OX42 in the SN ipsilateral to the GP lesion at three weeks following the lesion (figure 6.4A and B). High magnification views of the area of increased OX42 staining revealed clusters of microglia apparently clustering around presumed dead or dying neuronal cell bodies (figure 6.4C). These changes were paralleled by a marked increase in the levels of GFAP staining in the SN ipsilateral to the GP (figure 6.5).

At six weeks following the GP lesions the side-to-side difference that had been seen in the OX42 stained sections, was no longer evident (figure 6.6). In agreement with this there were no longer any clusters of activated microglia in either the ipsilateral or the contralateral SN. There was also no obvious peculiarities in the OX42 staining in the brains of the STN lesioned rats at four weeks post-lesion.

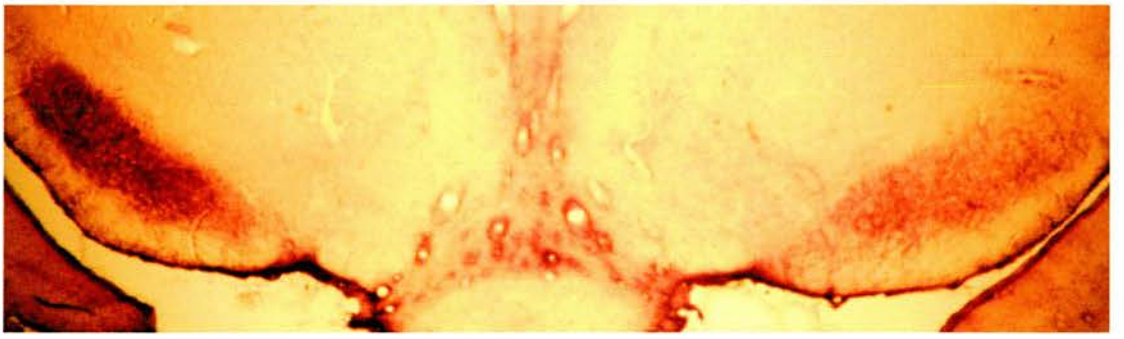

Figure 6.5 Photomicrograph of a coronal section of rat brain immunostained with an antibody against GFAP, three weeks after an ibotenic acid lesion of the globus pallidus. The ipsilateral substantia nigra (left) shows much stronger staining than the contralateral nigra (right).

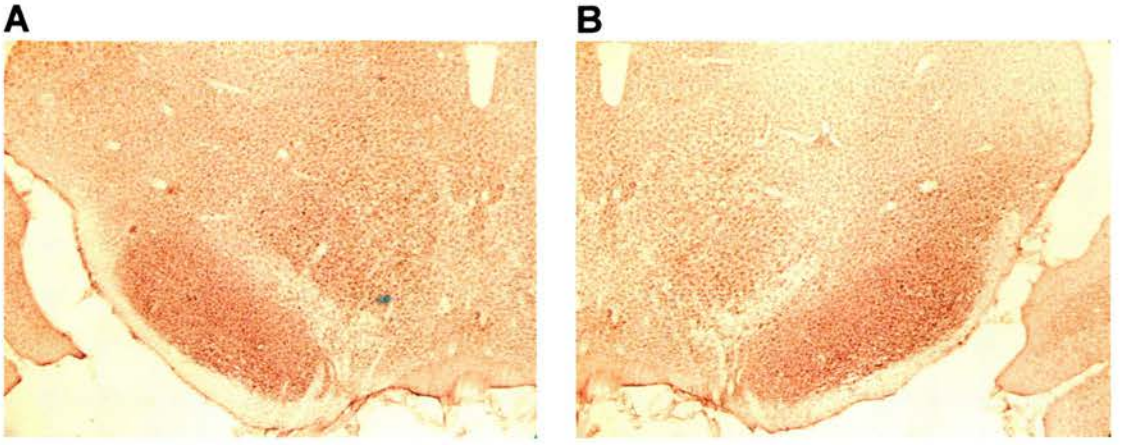

Figure 6.6 Photomicrographs showing coronal sections of the rat brain immunostained with OX-42 six weeks following an ibotenic acid lesion of the globus pallidus. The substantia nigra is shown **A** on the side ipsilateral to the lesion and **B** on the contralateral side. There is no qualitative difference between the two sides.

6.3.3 Tyrosine Hydroxylase Positive Cell Counts

All sections within the area predefined as the SN were used to make unbiased stereological estimates of the total numbers of TH+ve cells in the SN ipsilateral and contralateral to the GP lesion. The total numbers of cells on each side were then compared.

Three Weeks Post GP Lesion

There were a total of 10 animals in this group. One animal died before the end of the experiment, one animal had a misplaced lesion, and one animal was discounted because of damage to the brain during cutting on the freezing microtome. This left seven animals to be used in the data analysis.

There were an average of 122 sampling sites per side per animal (range 98 - 137), with an average of 303 cells counted (range 227 - 379). This gives an average of 2.5 cells per sampling site. The number of sampling sites and cells counted per animal were generally greater on the side contralateral to the lesion than they were on the ipsilateral side (ranges: ipsilateral 98 -135 and 227 - 328; contralateral 117 - 137 and 266 - 379 respectively).

The mean (± s.d.) estimated total number of TH+ve cells on either side in each animal was 7433 ± 842 on the side ipsilateral to the lesion and 8777 ± 626 on the contralateral side (figure 6.7A). This represents a 15.35 ± 7.03% decrease in the total

number of cells on the ipsilateral side when compared with the side contralateral to the lesion. A two-tailed paired *t*-test indicated that this ipsilateral-contralateral difference of 15.35% was statistically significant (t = -5.97, $P = 0.001$, n = 7).

The average CE for these cell counts was 0.067 on the ipsilateral side and 0.063 on the contralateral side. The OCV of the cells counts was 0.11 (ipsilateral) and 0.07 (contralateral). Taken together these give a value for the biological CV of 0.09 on the ipsilateral side and 0.03 on the contralateral side.

The volume of the SN used for counting was 1.20 ± 0.11 mm^3 on the ipsilateral side and 1.36 ± 0.09 mm^3 on the contralateral side (figure 6.7B). The ipsilateral volume was 11.94 ± 7.16% smaller than the contralateral volume. A two-tailed paired *t*-test indicated that this difference was statistically significant ($t = -4.42$, $P = 0.0045$, n = 7).

Six Weeks Post GP Lesion

There were a total of eight rats in this group. Three were lost post-operatively as a consequence of anaesthetic problems leaving five rats to be used for data analysis.

There were an average of 134 sampling sites per side per animal (range 115 - 147), with an average of 235 cells counted (range 185 - 282). This represents an average of 1.75 cells counted per sampling site. In these animals the side-to-side difference in

A

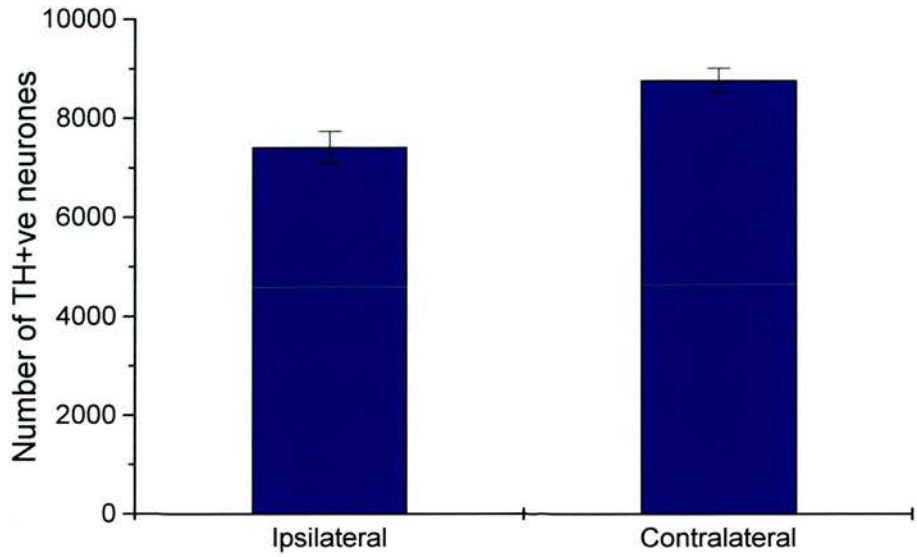

B

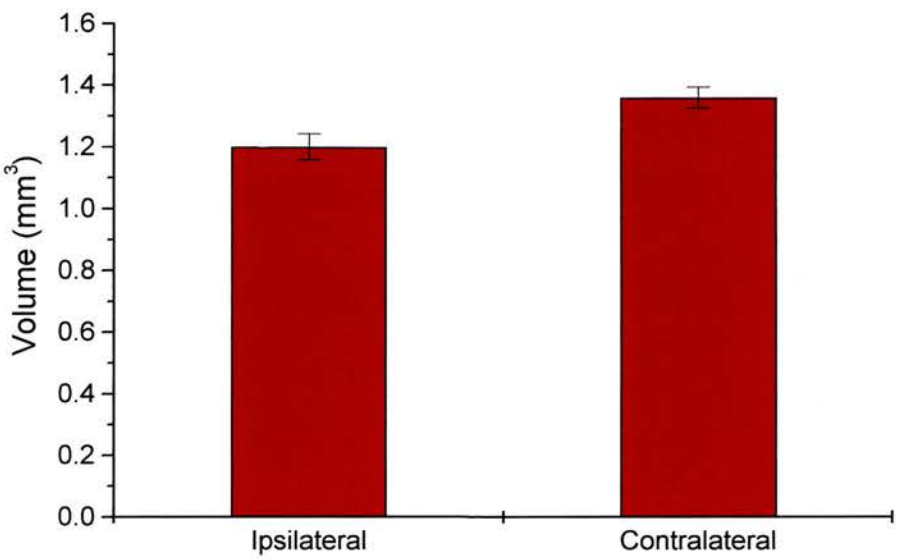

Figure 6.7 Graphs showing **A** the mean (± S.E.M.) total number of tyrosine hydroxylase immunopositive (TH+ve) neurones, and **B** the mean volume, of the substantia nigra at three weeks following an ibotenic acid lesion of the globus pallidus.

the number of sampling sites used or the total number of cells counted per animal was smaller than the equivalent differences in the three week group (mean number of sampling sites: ipsilateral = 130.8, contralateral = 137.8; mean total number of cells counted: ipsilateral = 221.0, contralateral = 249.6).

The mean (± SD) estimated total number of TH+ve cells in the substantia nigra was 5775 ± 787 on the side ipsilateral to the lesion and 6523 ± 666 on the contralateral side (figure 6.8A). This represents there being 11.59 ± 5.84% less cells on the ipsilateral side when compared with the side contralateral to the lesion. A paired *t*-test indicated that this 11.59% ipsilateral-contralateral difference was statistically significant (t = -4.29, $P = 0.01$, n = 5).

The average CEs of these cell counts was 0.07 on the ipsilateral side and 0.07 on the contralateral side. These are less than the criteria of 0.1 indicating that the estimated counts are reliable. The OCV for these counts was 0.14 (ipsilateral) and 0.10 (contralateral). Together these give a CV of 0.12 for the ipsilateral side and 0.07 for the contralateral side. As for the three week group, counting error was a smaller factor in the total error on the ipsilateral side than it was on the contralateral side despite the values of CE being very similar. This indicates that biological variability was much smaller on the contralateral side than it was on the ipsilateral side.

The volume of the SN used in the counts was 1.33 ± 0.14 mm^3 on the ipsilateral side and 1.53 ± 0.07 mm^3 contralaterally (figure 6.8B). The ipsilateral SN was 13.61 ±

A

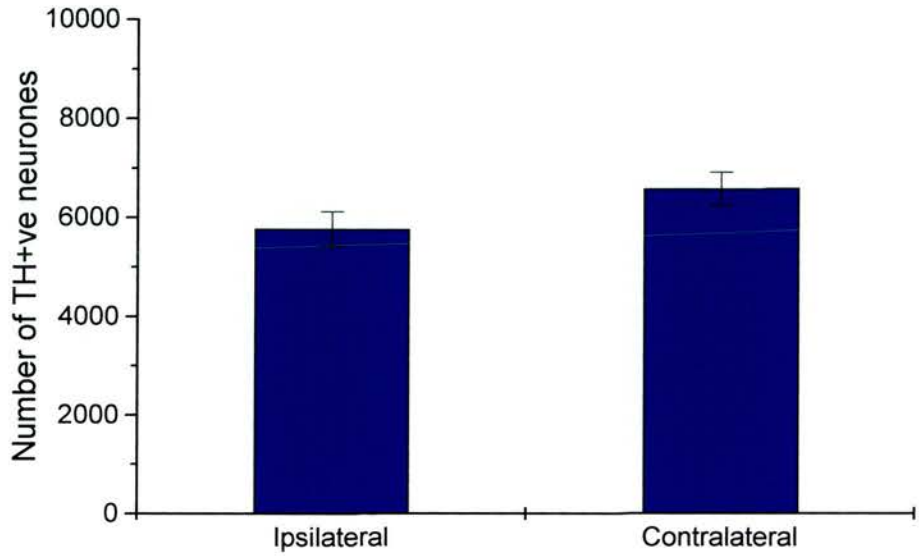

B

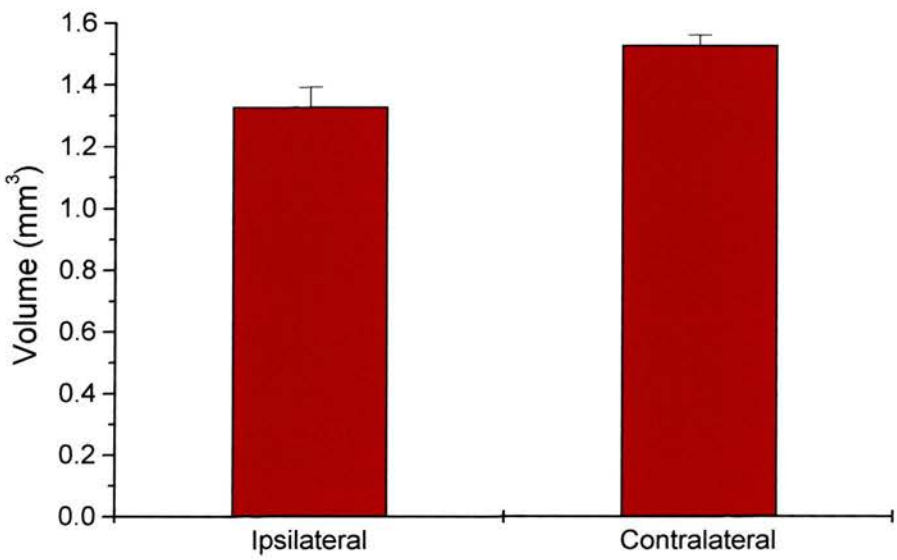

Figure 6.8 Graphs showing **A** the mean (± S.E.M.) total number of tyrosine hydroxylase immunopositive (TH+ve) neurones, and **B** the mean volume, of the substantia nigra at six weeks following an ibotenic acid lesion of the globus pallidus.

6.03% smaller than the contralateral SN. A two-tailed paired *t*-test showed this difference to be statistically significant ($t = -5.55$, $P = 0.0051$, n = 5).

Pairwise Comparisons

An ANOVA was used to compare the results from six weeks following the GP lesions with the three-week data. This indicated a statistically significant effect of the time post-lesion ($F = 38.15$; $P < 0.001$) and the side of brain ($F = 12.11$; $P < 0.01$) on the absolute numbers of TH+ve neurones in the SN. However, there was no interaction between time and side ($F = 0.71$; n.s.). Tukeys pairwise comparisons were used as a *post-hoc* test to reveal where these differences lie. This showed a statistically significant reduction in the number of cells on the ipsilateral side at six weeks post-lesion (5775.6 ± 786.9) when compared with the numbers of cells on both the ipsilateral (7433.1 ± 841.7) and contralateral (8777.1 ± 626.4) sides at three weeks post-lesion ($P < 0.01$ and 0.0001 respectively). There was also a statistically significant reduction in the number of cells on the contralateral side at six weeks post-lesion (6595.2 ± 739.8) when compared with the number of cells on the contralateral side at three weeks post-lesion ($P < 0.001$).

STN lesions

STN lesions were performed on six animals. A60 stained sections indicated that only in two of the animals had the lesion been successful. In the other four, although the

micropipette had been lowered to the correct place, there was no cell damage indicating that the micropipette had blocked and no ibotenic acid had been injected.

The two animals with successful STN lesions averaged 8193 TH+ve cells on the side ipsilateral to the lesion and 7971 on the contralateral side (figure 6.9A). The four animals with unsuccessful lesions averaged 10780 ± 1311 TH+ve cells on the ipsilateral side and 10185 ± 1462 on the contralateral side (figure 6.9B). This was 6.09% more cells ipsilaterally than there were on the contralateral side. With this size of group it is not possible to determine whether or not this small side-to-side difference represents an actual statistically significant difference.

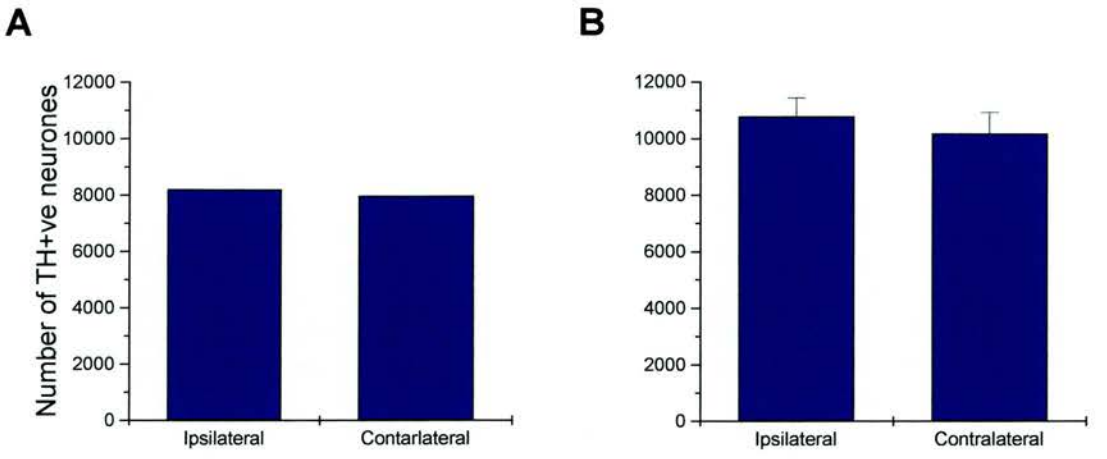

Figure 6.9 Numbers of tyrosine hydroxylase immunopositive (TH+ve) neurones in the rat substantia following successful (**A**) or unsuccessful (**B**) lesions of the subthalamic nucleus. **A** show average data from two rats, **B** shows mean (± S.E.M.) from four rats.

6.4 Discussion

6.4.1 Summary of Results

The data presented above show that three weeks after lesions of the GP there are markedly fewer TH+ve cells in the ipsilateral SN than there are in the contralateral SN. This difference in the numbers of TH+ve cells is accompanied by increases in immunohistochemical staining for OX42 and GFAP in the ipsilateral SN. These immunohistochemical changes are consistent with the activation of microglia and astrocytes that accompanies local tissue damage in the brain. The differences in TH+ve cell numbers seen at three weeks post GP lesion are also present at six weeks following the lesion, at this time point the difference is slightly smaller. At this time there is also evidence for bilateral changes the TH+ve cell numbers that might explain the reduction in the side-to-side difference.

6.4.2 The Validity of the Tyrosine Hydroxylase Cell Number Estimates

Tyrosine hydroxylase is an enzyme in the dopamine synthesis pathway. It catalyses the conversion of tyrosine to dihydroxyphenylalanine (DOPA). DOPA is subsequently converted to dopamine in a reaction catalysed by the enzyme DOPA decarboxylase. For this reason all dopaminergic neurones express TH and can be marked with antibodies against it. However, dopamine is also synthesised by noradrenergic neurones and by adrenergic neurones in which it is converted to

noradrenaline and adrenaline respectively. The biosynthetic pathway of this conversion uses the enzyme dopamine-β-hydroxylase to catalyse the conversion of dopamine to noradrenaline and phenylethanolamine *N*-methyl-transferase to catalyse the conversion of noradrenaline and adrenaline. Therefore all noradrenergic and adrenergic neurones express dopamine-β-hydroxylase. TH is strongly expressed in the soma of cells in the SNc and more sparsely in the SNr (Pickel *et al.*, 1975; Hédou *et al.*, 2000), but dopamine-β-hydroxylase is not found in the somata of cells in either of these areas (Pickel *et al.*, 1976). Reis, *et al.* (1978) found that lesions in the posterior midbrain, that destroy the ascending noradrenergic projections, markedly reduced dopamine-β-hydroxylase immunoreactivity in the SN without affecting TH-immunoreactivity. Taken together this evidence shows that all TH+ve neurones in the SN are dopaminergic neurones.

In order to make an unbiased estimate of the total number of TH+ve cells within each SN design-based stereological techniques were used. The basic principles behind these techniques are very simple. Firstly each object of interest (in this case TH+ve cells) is reduced to a single point in three-dimensional space in order to avoid double counting of large or irregularly shaped objects. For these experiments this was achieved by counting TH+ve nuclei rather than TH+ve cells. The nuclei were then reduced to single points by only counting them if the first point at which they came into sharp focus fell between the two guard zones. Secondly, efficiency of counting is increased if only a known fraction of the total number of objects present within the structure under investigation is counted. From the total number of objects within a known fraction, the total number of objects within the entire structure can be

calculated. To avoid bias it is important that at the start of the study every single object within the structure has an equal probability of being included within the count. To ensure that this is the case systematic random sampling techniques such as those used in these experiments have been developed (Gundersen & Jensen, 1987). In a heterogeneous structure, pure random sampling may bias results by concentrating the sampling sites within a region that has either a particularly sparse or dense distribution of the objects being counted. When systematic random sampling is used, the sampling sites are spread evenly throughout the structure by placing them on a grid. However, the positioning of the grid over the structure is random, this means that every object within the structure still has a statistically equal chance of being included in the count. In practice the systematic random sampling occurs twice; at the level of choosing the sections to be included in the count and at the level of positioning the counting grid over the structure of interest on each section.

The main drawback with counting in this manner is that it produces only a single value that is the estimated total number of cells. There is no equivalent of the standard error of the mean to tell you how accurate the estimated value is relative to the real value. It is for this reason that the function CE (see section 6.2.3) has been developed. This is a pseudo-statistical method for estimating the reliability of counting. In these experiments it was decided, in line with previous authors (Gundersen & Jensen, 1987; West & Gundersen, 1990; Oorschot, 1996), that CEs of less than 0.1 would be accepted as indicating that the estimates of the total numbers of neurones in the SN were reliable. The CE is reduced by increased sampling,

ideally every cell would be counted giving a value for the CE of zero. However, Gundersen and Jensen (1987) have calculated that below a CE of 0.1 the fraction of the structure used for counting is no longer a factor in the reliability of the estimate. Therefore, to increase the fraction used by further sampling would be inefficient. All the CE values in our counts were below 0.1 indicating that the estimated totals for TH+ve cells within the SN were reliable.

West and Gundersen (1990) suggest that the value of CE^2 should be less than half the value of CV^2. If this is the case it indicates that the major contribution to the variability seen in the data comes from the inherent biological variability and not to errors in counting. In these experiments for both the three weeks and six weeks post lesion data this was not always the case. On the ipsilateral side the CE^2 was less than half the OCV^2 indicating that most of the variability was due to biological variation and not counting error. However, on the contralateral side the CE^2 was approximately three-quarters of the OCV^2 indicating that counting error played a greater role in the total variability that was seen on this side. The CE on the contralateral side was generally similar to the CE in the ipsilateral side. This shows that the reason for CE^2 not being less than half of OCV^2 was most likely to be due to the small size of the biological variability on the contralateral side and not a large counting error. That the variability in the counts on the contralateral side was this small suggests that the counts were accurate despite the CE^2 not being half the size of the OCV^2.

These indicators of the validity of the TH+ve cell counts suggest that the differences in the estimated total cell numbers on the ipsilateral versus the contralateral side are real differences. The question of the source of this discrepancy between the estimated total numbers of TH+ve cells on the sides ipsilateral and contralateral to the lesioned GP needs addressed. There are three ways that such a difference could have come about. It could be that the numbers of TH+ve cells on the contralateral side has increased. It would be very difficult to explain how a GP lesion could lead to an increase in the number of TH+ve cells in the contralateral SN but such a possibility needs to be considered. Alternatively, the numbers of TH+ve cells on the ipsilateral side could be reduced. Such a reduction could come about through cell death, but it is also possible to explain it through changes in gene expression.

Although it has been shown that in some cases neurones can be produced *de novo* in adulthood this is generally not the case. It is possible however that an increase in the numbers of TH+ve cells in the contralateral SN could come about if the non-dopaminergic cells within the nucleus that had not previously expressed TH started to express it. However, it is difficult to envisage how such changes in gene expression could be restricted to the side contralateral to the GP lesion.

More likely is the possibility that there has been a loss of TH+ve cells on the side ipsilateral to the GP lesion. This is supported by the TH+ve cell counts in the rats that had had a failed STN lesion. The estimated total numbers of TH+ve cells in the SN of these rats was 10483, this compares with 8777 for the contralateral side at three weeks following the GP lesion. This is suggestive that both ipsilateral and

contralateral sides have reduced numbers of TH+ve cells (the possibility of bilateral damage will be discussed below). It should not be automatically assumed that this loss of TH+ve cells represents the death of dopaminergic neurones. In the MPTP models of PD it has been suggested that apparent losses of dopaminergic cells can in certain circumstances be due to a temporary, and reversible, cessation of TH expression (Tatton *et al.*, 1990; Jackson-Lewis *et al.*, 1995). For example, mice receiving 30 mg/kg of MPTP a day for 5 or 10 consecutive days showed a dose related disappearance of TH+ve retinal amacrine cells at 20 days and five months following the exposure. However, the numbers of TH+ve cells had returned to the same levels as in age-matched controls by 9 - 11 months following the exposure (Tatton *et al.*, 1990). Monkeys receiving 0.5 mg/kg of MPTP for three or four days showed a greater loss of TH+ve cells than they did Nissl stained cells (Kitt *et al.*, 1986). The authors suggest that this be because dopaminergic neurones suffer axonal damage as a result of the MPTP and stop expressing TH as a consequence. Some of these neurones go on to die but some could recover. However, the smaller loss of Nissl-stained cells could simply reflect the fact that the GABAergic cells in the SNc were unaffected by the MPTP. Support for the author's hypothesis comes from evidence that axonal damage can lead to reversible changes in gene expression. Electrolytic lesions of the rat caudate nucleus, which destroy nigrostriatal axon terminals, can lead to a 40% reduction in TH activity in the SN at 7 days following the lesion that is almost entirely reversed by 21 days (Reis *et al.*, 1978). Similar effects have been seen in neurones using transmitters other than dopamine. For example cholinergic neurones (Lams *et al.*, 1988; Hagg *et al.*, 1989) and noradrenergic neurones (Ross & Reis, 1981) stop expressing CHAT or dopamine-β-

hydroxylase respectively in a reversible manner after axotomy. Although our data does not allow us to rule out this possibility completely, it is of note that all the studies that show reversible changes in TH expression point out that this reduced expression is a precursor to cell death and that recovery comes only if the initial insult is small. Evidence that cell death is likely to be the cause of the reduced numbers of TH+ve cells in the present experiments comes from the staining for GFAP and OX42. Levels of both of these markers were increased on the ipsilateral side at three weeks following the GP lesion. GFAP is a protein that is expressed mainly in astrocytes (Brenner *et al.*, 1994). When astrocytes are activated by local damage their expression of GFAP increases (Predy *et al.*, 1988). OX42 is an antibody against the type-3 complement receptor that is expressed by microglia (Kato *et al.*, 1995). Increases in OX42 staining are suggestive of activation of the microglia and invasion of the area by microglia from elsewhere (Kato *et al.*, 1995). Such activation usually occurs when neurones are dying and peaks at around three days following an insult. Activation of astrocytes and microglia is part of an inflammatory response that occurs to remove debris from areas where cells have died. That levels of both of these markers showed activation in the SN three weeks after the GP lesions suggests that there were indeed degenerative processes occurring at this time.

In conclusion the data from the present experiments shows that at three and six weeks following a GP lesion there is a reduction in the number of TH+ve cells on the ipsilateral side when compared to the contralateral side. This change represents a true

reduction in the numbers of cells in the ipsilateral SN that is most likely to be due to cell death.

6.4.3 The Cause of Dopamine Cell Death

There are a number of possible mechanisms by which cell death in the SN may follow an ibotenic acid lesion of the GP. A simple explanation is that the ibotenic acid injected to lesion the GP was able somehow to travel to the SN.

In the present experiments the most likely explanation would be that the internal capsule had provided a channel along which ibotenic acid injected into the GP had travelled into the SN lesioning the cells there along with the GP cells. If this were the case then it would be expected that the other nuclei through which the ibotenic acid would pass *en route* would also exhibit cell loss. The two nuclei that the ibotenic acid would have to pass to get to the SN are the EP and the STN. Neither of these nuclei show any obvious signs of cell loss at three or six weeks following the GP lesion. Coupled with this is the lack of any evidence for unilateral loss of cells in the SN following injections of ibotenic acid into the STN. If the ibotenic acid were able to flow along the internal capsule from the GP to the SN then it should be able to travel the shorter distance from the STN to the SN with ease. Taken together these two pieces of evidence suggest that ibotenic acid travelling along the internal capsule from the GP is unlikely to be the source of the cell death in the SN.

Another route for the ibotenic acid to travel to the dopaminergic cells in the SN would be through the striatum. In the present experiments all of the ibotenic acid lesions of the GP included a small part of the striatum. It is possible that some ibotenic acid may have been taken up by dopaminergic axon terminals in the striatum and transported retrogradely to the SN. There are two lines of evidence to suggest that this is not the case. Firstly, it is widely believed that ibotenic acid is not taken up by axon terminals or by axons of passage. Ibotenic acid may indirectly cause some damage to axons of passage but this is due to the inflammatory response and not the take-up of the toxin by these axons (Coffey *et al.*, 1990). Secondly, in the present series of experiments there was one rat in which the ibotenic acid lesion was entirely confined to the striatum. This rat showed no side-to-side difference in TH+ve cell numbers in the SN. This suggests that in this rat there had been no retrograde transport of the ibotenic acid and casts doubt on whether retrograde transport would occur in rats which had had a much smaller part of their striatum exposed to the toxin.

If the ibotenic acid injected into the GP had not been the direct cause of the loss of TH+ve cells in the SN then there must be an indirect cause.

As has already been raised above, there is evidence that ibotenic acid can cause damage to axons of passage (Coffey *et al.*, 1990). It is thought that this damage is mediated through the inflammatory response that usually accompanies tissue damage. It is possible that the inflammatory response in the GP damaged the dopaminergic fibres that pass through this nucleus. As we have seen, axonal damage

to dopaminergic cells can cause the cell to stop expressing TH and eventually to die (Reis *et al.*, 1978). However, most of the damage to axons of passage involves demyelination. Dopaminergic fibres are unmyelinated and so would not be damaged by any mechanism that involved demyelination. Another possible mechanism for the loss of the TH+ve nigral cells would be if the GP were an important source of growth factors to these neurones. Lesioning the GP may have destroyed the source of these growth factors thus causing the subsequent death of any cells that relied on them. However, the GP is not a major target of the nigral dopaminergic cells (Hauber & Fuchs, 2000) and so it would be surprising to find that it was their main source of growth factors.

The remaining explanation is that the lesions of the GP rendered the STN hyperactive such that its neurone's resting firing rates were increased and their response to cortical stimulation amplified. Such hyperactivity in the STN would lead to an increased level of glutamate release in its target nuclei, which includes the SN. These increases in glutamate release could cause cell death in these structures through excitotoxicity.

In the present experiments it was not verified that the GP lesions had actually resulted in hyperactivity in the STN. However many authors have consistently found a small (20%) but prolonged increase in the basal firing rate of STN neurones (Hassani *et al.*, 1996) and also an amplification of their response to cortical stimulation (Fujimoto & Kita, 1993) following GP lesions. Such increases, though small, may cause a slowly mounting level of excitotoxic damage to the dopaminergic

neurones of the SN over time. The STN is the prime candidate as the source of excitotoxicity in the SN following GP lesions but the PPN may also be involved.

Exactly which groups of cells constitute the PPN is the subject of much disagreement (for example, see Rye, *et al.* (1987)). This debate is beyond the scope of this thesis, so for simplicity the definition of the PPN used here will be as it is delineated in the atlas of Paxinos and Watson (1986). This group of neurones in the brainstem can be roughly divided into two components, a cholinergic and a non-cholinergic (midbrain extrapyramidal area; MEA (Rye *et al.*, 1987)) component. These two components show some separation but also a degree of overlap. The non-cholinergic component consists mostly of glutamatergic neurones (Rye *et al.*, 1987). The PPN sends projections to the dopaminergic neurones of the SNc (Jackson & Crossman, 1981a). It is unclear whether this projection is from the cholinergic cells or the non-cholinergic cells. Cells in the SNc that were activated orthodromically by electrical stimulation of the PPN were also excited by microiontophoretic administration of glutamate. The effects of both the orthodromic activation and administration of glutamate were reversibly blocked by administration of glutamatergic antagonists. These same cells were unaffected by acetylcholine or cholinergic antagonists (Scarnati *et al.*, 1986). These data suggest that this projection is glutamatergic. Rye, *et al* (1987) also assert that the projection to the SNc is from the non-cholinergic component of the PPN (the area that they call MEA). However axons and boutons stained for choline acetyl transferase (ChAT; an immunohistochemical marker of cholinergic neurones) have been seen in the SNc (Henderson & Greenfield, 1987). These cholinergic fibres formed asymmetrical synaptic specialisations onto TH+ve

neurones in the SNc (Bolam *et al.*, 1991). Intracellular labelling of PPN neurones showed both ChAT+ve and ChAT-ve cells with axon collaterals that terminated in the SNc (Takakusaki *et al.*, 1996). Contrary to the findings of Scarnati, *et al* (1986) other authors have found that acetylcholine acting at postsynaptic nicotinic (Calabresi *et al.*, 1989; Sorenson *et al.*, 1998) and presynaptic muscarinic receptors (Grillner *et al.*, 2000) depolarises dopaminergic neurones and increases their firing rate (Sorenson *et al.*, 1998). Both of these groups of neurones have dendritic trees that overlap with the other groups and axon collaterals that terminate within the nucleus (Takakusaki *et al.*, 1996). This means that there is a possibility of interactions between the cholinergic and non-cholinergic components within the nucleus.

The PPN also has connections with the STN (Canteras *et al.*, 1990). Injections of HRP into the PPN gave rise to retrogradely labelled neurones within the STN whereas injections into the STN produced terminal labelling in the PPN (Jackson & Crossman, 1981b). In a similar series of experiments neuronal cell bodies were labelled in the PPN following injections of WGA-HRP into the STN and labelled terminals were seen in the STN following injections of WGA-HRP into the PPN (Canteras *et al.*, 1990). In this second set of experiments the projection from the PPN to the STN was found to be bilateral. It should be noted however that the WGA-HRP injections used in these experiments (but not in Jackson & Crossman, 1981b) often included part of the zona incerta, a structure that also receives input from the PPN (Rye *et al.*, 1987). The projection from the STN to the PPN is presumed to be glutamatergic as there is no evidence for non-glutamatergic neurones in the rat STN

(Shink *et al.*, 1996). The projection from the PPN to the STN has been found to include cholinergic and glutamatergic fibres both of which form asymmetrical terminals in the STN (Bevan & Bolam, 1995). The glutamatergic component of the PPN also receives a GABAergic projection from the GP (Rye *et al.*, 1987).

Thus the GP, STN, SNc, and PPN form a very tightly interconnected network of nuclei. Following a lesion of the GP the resting firing rate of neurones in the STN is increased to approximately 20% greater than control levels (Hassani *et al.*, 1996). The response of the STN to cortical stimulation is also amplified (Fujimoto & Kita, 1993). The PPN will also be receiving less inhibitory input from the GP. Alongside this the PPN will be receiving extra excitatory inputs from the STN. It is reasonable therefore to conclude that resting firing rates of the neurones in the PPN may also be increased. Both the PPN and the STN send glutamatergic projections to the dopaminergic neurones of the SNc. However, although both nuclei are capable of increasing the activity of these dopaminergic neurones (Overton *et al.*, 1999; Lokwan *et al.*, 1999; Windels *et al.*, 2000b) this action is mostly through different receptor mechanisms. Glutamate released from the terminals of STN projections acts mainly through NMDA receptors (Chergui *et al.*, 1993; Chergui *et al.*, 1994), whilst glutamate released from the terminals of PPN projections acts mainly through AMPA receptors (Di Loreto *et al.*, 1992). Excitotoxicity is a consequence of increased intracellular Ca^{+} levels. Ca^{+} enters neurones through NMDA but not most AMPA receptor channels. This suggests that any excitotoxicity that occurred in the TH+ve neurones of the SNc in these experiments will primarily be due to the hyperactivity of the STN neurones.

NMDA receptors require binding of the ligand (glutamate) and post-synaptic depolarisation to occur simultaneously in order to open. Both the cholinergic and non-cholinergic projections from the PPN are capable of causing depolarisation of the dopaminergic neurones of the SNc so the involvement of the PPN in the excitotoxicity may be to work synergistically with the STN (figure 6.10). Depolarisation of the dopaminergic neurones caused by activation of the PPN may sensitise these neurones to the actions of the STN enabling the NMDA receptors to open more readily (Kitai *et al.*, 1999).

At six weeks following the GP lesions there was evidence that the loss of TH+ve cells was bilateral. This is in agreement with studies showing that, following electrical stimulation of the STN there is a bilateral increase in glutamate levels in the SNc (Windels *et al.*, 2000a). There is no evidence that the GP sends projections bilaterally to either the STN or the PPN. Also there is no evidence for bilateral projections from either the STN or the PPN to the SNc. The projection from the PPN to the STN is bilateral (Canteras *et al.*, 1990). This bilateral projection seems to provide the only possibility for downstream activation following a unilateral GP lesion having bilateral consequences (figure 6.10).

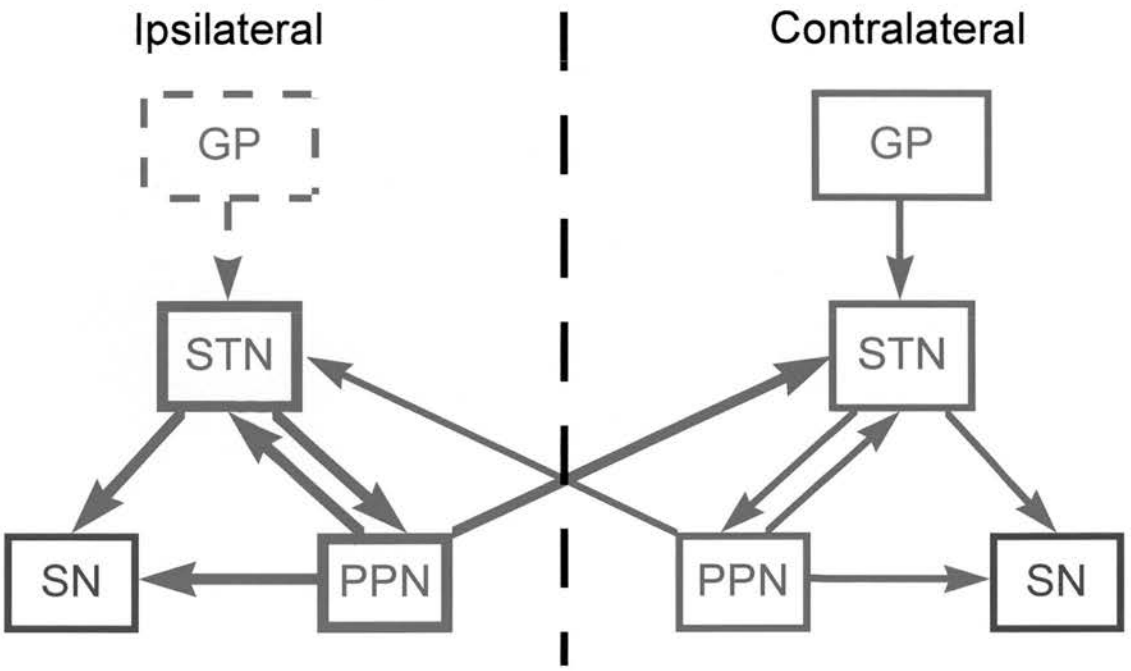

Figure 6.10 Diagram showing the possible route from an unilateral lesion of the globus pallidus (GP) to bilateral dopamine cell death in the substantia nigra (SN). Hyperactivity in the ipsilateral subthalamic nucleus (STN) is passed on to the ipsilateral pedunculopontine nucleus (PPN). These two nuclei both send excitatory projections to the ipsilateral SN and consequently cause the excitotoxic death of the dopaminergic neurones in the SN. A bilateral projection from the PPN to the STN could pass the hyperactivity to the contralateral side resulting in the same process occuring there too.

That the GP lesions did have bilateral consequences for the TH+ve cells leads us to question the use of the contralateral SN as a control. For this reason a full set of data from age-matched controls should be collected. These rats should be in two groups, each having sham lesions consisting of injections of vehicle (PBS) into the GP, one group left for three weeks post-surgery and the other six. In the absence of this data it is interesting to compare the data from the rats with sham STN lesions with that from the rats at three weeks post GP lesion. As there is only data from four animals with sham STN lesions it would be nonsensical to make this comparison statistically but a qualitative assessment is possible. The rats with sham STN lesions averaged 10780 ± 1311 TH+ve cells on the ipsilateral side and 10185 ± 1462 contralaterally. This compares with an average of 7433 ± 842 TH+ve cells ipsilateral and 8777 ± 626 contralateral to the GP lesion at three weeks post-lesion. There were 13.82% less cells on the contralateral side at three weeks post GP lesion than there were at four weeks after the sham STN lesions. This suggests that even at three weeks there has been bilateral damage. This being the case, then the 15.35% difference between the ipsilateral and contralateral sides at three weeks does not represent the actual loss of cells on the ipsilateral side. The control data presented here suggests that the actual loss of TH+ve cells in the ipsilateral SN three weeks after the GP lesion may be much greater. A comparison of the numbers of TH+ve cells on the ipsilateral side at three weeks post GP lesion compared with the same side in the rats with sham STN lesions gives a loss of 31.05%.

In summary, there is a substantial bilateral loss of dopaminergic cells in the SNc three weeks after a unilateral ibotenic acid lesion of the GP. This cell loss appears to be even greater at six weeks post-lesion. The most likely mechanism through which this loss of cells could occur is through excitotoxicity as a consequence of the GP lesion rendering the neurones in the STN hyperactive. There is however, strong evidence for an involvement of the PPN too. The consequences of these findings for research into PD will be discussed in chapter seven.

7 General Discussion

The STN has been attributed with a wide range of functions from vision (Cajal, 1911) through to cardiorespiratory control (Angyán & Angyán, 1999) and the selection of movement sequences (Redgrave *et al.*, 1999b). Dysfunction of the STN has been implicated in the genesis of the symptoms of an equally wide range of disorders, including absence epilepsy (Deransart *et al.*, 1998a; Deransart *et al.*, 1998b), ballism, Huntington's disease, and PD (Albin *et al.*, 1989). The experiments described in this thesis aimed to investigate one of the most notable features of STN neurones; their ability to achieve and maintain high frequencies of action potential firing (Nakanishi *et al.*, 1987). The first experiments investigated how this is possible, as previous modelling data had indicated that the normal range for the kinetics of NaCh and KCh were insufficient. The second experiments looked at how, when the neurones are excited to fire at higher rates, their firing patterns might be affected by the proposed network formed by the intranuclear axon collaterals, such that activity within the nucleus as a whole might achieve some degree of co-ordination. The final experiments aimed to look at a real situation where firing in the STN might be disrupted in such a way as to cause pathological levels of hyperactivity. The results of these experiments have been individually discussed. Here we will look at the implications of these experiments for the functioning of the basal ganglia as a whole, can they tell us anything new about the STN, it's normal functioning and it's role in the basal ganglia?

The conclusions from the experiments described in this thesis are that: (1) The ability of STN neurones to achieve high firing frequencies is due to alterations in the NaCh kinetics; (2) At higher firing frequencies actions of intranuclear axon collaterals are revealed; (3) Hyperactivity of STN neurones may play a role in the dopamine cell death seen in Parkinson's Disease.

7.1 High Frequency Firing of Subthalamic Nucleus Neurones

The experiments described in chapter 4 were devised to investigate the ability of STN neurones to achieve firing rates that were higher than could be achieved in model STN neurones. We wanted to see what features it was that the model was missing that enabled the neurones to fire action potentials at up to 500 Hz. We chose to investigate the rate of recovery from depolarisation block as this would give an estimate of the inactivation kinetics of NaCh. Surprisingly STN neurones were remarkably slow to recover from depolarisation block suggesting that NaCh inactivation in STN neurones is a slow process. Following this result we hypothesised that a method for achieving high firing rates might be to slow NaCh inactivation to the extent that very little inactivation occurs during the course of a single action potential. The NaCh β subunits are thought to be involved in the modulation of inactivation kinetics. Immunostaining against the β_1 and β_2 subunits revealed that the β_2 subunit was very poorly expressed in the STN. This therefore provides a possible mechanism for the slowing of inactivation. For neurones to be

able to fire action potentials in the absence of NaCh inactivation would require the presence of a fast and large potassium current. A possible candidate for the source of such a current was the voltage-gated potassium channel Kv3.1. This channel is expressed in many areas of the brain where neurones are able to achieve high firing rates, including the STN (Perney *et al.*, 1992; Weiser *et al.*, 1994; Gan & Kaczmarek, 1998). Indeed, experiments with mouse auditory neurones have revealed that these neurones lose their capacity for high frequency firing when Kv3.1 is inhibited (Wang *et al.*, 1998). Recently data has been published showing that blockade of Kv3.1 increases the duration of action potentials, slows firing, and increases the rate at which depolarisation block occurs in STN neurones (Wigmore & Lacey, 2000). From this data we hypothesised that it is a combination of slow NaCh inactivation and the presence of Kv3.1 that enables high frequency firing in the STN.

7.2 Intranuclear Axon Collaterals

Computer modelling had revealed the potential importance of interconnections between STN neurones for the way in which these neurones behave. Therefore, we performed experiments designed to look for evidence of the presence of such interconnections. In brain slices the resting firing of STN neurones is independent of any excitatory inputs to the neurones (Bevan & Wilson, 1999), a result that we were able to replicate in these experiments. However, following predictions made using the computer models, we hypothesised that actions mediated through the intranuclear collaterals may be revealed by the depolarisation of STN neurones. Increasing the concentration of potassium ions in the aCSF with which brain slices were perfused

increased the firing rate of STN neurones and changed their firing pattern from an extremely regular pattern to a more irregular one. The glutamatergic antagonist CNQX did not block the increase in firing rate, but it did attenuate the change in firing pattern. This confirms the predictions from the computer modelling and suggests that these neurones are indeed functionally connected to each other.

7.3 The Role of the Subthalamic Nucleus in Dopamine Cell Death

A nucleus which contains only excitatory neurones that are capable of high firing rates and have a high degree of interconnectivity with each other would need a lot of controls to stop the constituent neurones from becoming hyperactive. If a pathological situation occurred that caused these controls to break down it might be expected that the neurones would pass this hyperactivity on to neurones in their target nuclei. In the STN one such situation where the neurones become hyperactive is Parkinson's Disease. Previous authors had speculated that hyperactivity of STN neurones might contribute to the pathology of PD through excitotoxicity at their target neurones, which include the dopaminergic neurones of the SNc (Rodriguez *et al.*, 1998b).

The experiments described in chapter 6 aimed to investigate whether dopaminergic cell death in the SN could be induced by artificially increasing the levels of activity in the STN. To this end unilateral lesions of the GP were made and the numbers of TH+ve cells in the SN counted three or six weeks later. These experiments revealed a

progressive loss of TH+ve cells that was most prominent on the side ipsilateral to the GP lesion but also occurred on the contralateral side. This indicated that hyperactivity of STN neurones alone could be responsible for death of dopaminergic cells in the SN. The PPN was also implicated in this cell death due to its bilateral projections to the STN and SN.

7.4 The Functioning of the Subthalamic Nucleus

The direct/indirect pathway hypothesis (Albin *et al.*, 1989; Alexander & Crutcher, 1990) emphasised the role of the subthalamic nucleus as a relay in the indirect pathway. In this role, the subthalamic nucleus neurones exist solely to convert the inhibitory output from the striatum into excitatory input into the EP/SNr. Despite its lowly position in this scheme, attention was shifted to the STN because it became clear that changes in the balance of activity in the two pathways were an important feature of basal ganglia disorders. In particular the STN would become hyperactive in PD and hypoactive in Huntington's Disease and ballism. Surgical approaches aimed at altering levels of activity in the STN have been successful in the alleviation of the symptoms of PD (Bergman *et al.*, 1990; Guridi & Obeso, 1997; Krack *et al.*, 1998).

Recent authors have emphasised the importance of the cortical input to the STN, its close relationship with the GP and the influence of dopamine on STN neurones (Chesselet & Delfs, 1996; Hassani *et al.*, 1997; Urbain *et al.*, 2000; Ni *et al.*, 2000). In showing that the neurones of the STN are functionally interconnected we have

added a further level to the complexity of what is now often called the 'indirect network'.

Information flow through the basal ganglia has been regarded as travelling through many parallel channels (Albin & Tagle, 1995; Redgrave *et al.*, 1999b). Indeed the cortical projections to the STN maintain a degree of topography (Bevan *et al.*, 1995). However, if the neurones of the STN were connected together, this topographical organisation of information flow would break down. Why would the cortical projection to the STN maintain this topographical organisation if the interconnections in the STN were to make it irrelevant? The present experiments provide a possible answer to this problem. When the neurones of the STN were at rest we were unable to find any evidence for the presence of interconnections. This result is not only in agreement with the results of previous authors (Ryan *et al.*, 1992; Bevan & Wilson, 1999), but it was also fully predicted by the modelling data of Gillies and Willshaw (Gillies & Willshaw, 1998b). In this model, despite the level of interconnectivity that existed between the units, these units showed no correlation with each other when they were at rest. It was only when the neurones in the model received excitatory input that non-synchronous correlations began to emerge. If this input was strong enough then all the units could be driven into a persistent hyperactive state. A similar phenomenon was observed in the experimental data. When the STN neurones were depolarised the glutamatergic antagonist CNQX began to have a discernible effect on their firing pattern. As discussed in chapter 5, the most likely source of this effect is the intranuclear axon collaterals. This means that, whilst the topographic nature of the cortical projection to the STN may be maintained at

low levels of activity, when the neurones of the STN are driven to higher levels of activity this topography might break down. In effect the neurones of the STN form a network where the levels of activity of the neurones that make up this network can modulate the level of interconnectivity.

Gillies (1995) speculated that this two state property of the STN network would enable switch-like behaviour. Inputs to the STN would move the whole network (or at least parts of it) between these two states. The STN sends excitatory, glutamatergic projections to the output nuclei of the basal ganglia (EP/SNr). From this, the Albin *et al.* (1995) hypothesis would suggest that the high activity state would lead to a widespread suppression of voluntary movement. Gillies (1995) compared this with a break, suggesting that the STN neurones may produce pulses of activity at the end of movements to terminate them and allow the next movement, or sequence of movements, to proceed. From the present data we can propose a modification to this hypothesis. Depending on their membrane potential, the amount that individual neurones in the STN contribute to the interconnectivity can be varied. This means that in certain circumstances groups of neurones may act together to provide a wash of excitation to their targets. This collaboration between neurones may cross the functional divisions that are maintained by the inputs to the STN allowing the simultaneous excitation of neurones in multiple channels. On the other hand neurones in the STN can still act as individuals maintaining the functional segregation of information flow through the basal ganglia.

Redgrave *et al.* (1999b) propose a model of basal ganglia function in which the basal ganglia is responsible for action selection. This model requires clean switching between different actions. They suggest that the STN fulfil this role in a way that requires the STN to behave in the manner described above. Specifically, switching requires the STN to produce a co-ordinated pulse of activity followed by the suppression of STN activity in a particular channel. The data from the present experiments provides a possible mechanism through which this could happen. Increased excitatory input to the STN would allow the co-ordinated activation of many neurones through the intranuclear axon collaterals. If transmission of activity through the axon collaterals had a constant level of influence on the target neurones, it would be difficult to suppress this activity in a small area. However, focussed inhibition from the GP directed at that small area could hyperpolarise these neurones, which would effectively cut them off the STN network, stopping any crossover to these neurones from the neurones of other channels. In this way information flow through a single channel could be allowed whilst information flow through all other channels was blocked.

7.5 The Subthalamic Nucleus in Parkinson's Disease

This hypothesis for the functioning of the STN has interesting consequences for the way in which PD would affect STN neurones.

Following the Albin *et al.* (1989) model we find that the death of dopaminergic neurones would lead to the loss of inhibitory inputs to STN neurones. At the same

time there is evidence of increased cortical activity in animal models of PD. Hassani *et al.* (1996) showed that 6-OHDA lesions of the dopaminergic neurones in the SNc led to a greater increase in STN activity than ibotenic acid lesions of the GP. This means that, contrary to the predictions of the Albin *et al.* (1989) model, the increases in STN activity seen in 6-OHDA lesioned rats can occur independently of changes in GP activity. Hassani *et al.* (1996) propose this as evidence for a direct influence of dopamine on STN neurones. However, experimental data gained following the infusion by microiontophoresis of dopamine into the STN (Campbell *et al.*, 1985) calls this into question. These experiments showed that dopamine induced a decrease in the levels of activity in only about a half of the STN neurones that recordings were attained from. Assuming that lesioning the dopamine neurones that project to the STN has the opposite effect of applying dopamine to the STN then this would only account for the increases in activity seen in half of the STN cells. In this same study haloperidol, a dopaminergic antagonist, was found to either have little effect on the activity levels of STN neurones or to inhibit them. Taken together these data suggest that the increases in STN neuronal activity seen following 6-OHDA lesions cannot be fully explained either by decreases in inhibition from the GP or by the direct effects of DA on the STN neurones. Thus, it is possible that in these animal models of PD there is increased input to the neurones of the STN from the cortex. Whether through decreased GP activity, increased cortical activity, or a combination of the two there will be a tendency for STN neurones to be depolarised following dopamine cell death in the SN.

Such depolarisation would make it more difficult to keep STN neurones functionally isolated from each other. The consequences of this are two-fold. Firstly, there may be unwanted crossover between channels, which could result in the failure to open the desired channel. Secondly, the neurones in the nucleus will exist at a membrane potential that is closer to the point were runaway excitation would lead to the generation of a co-ordinated pulse of activity in the STN. The effects of excessive depolarisation of STN neurones then could lead to difficulty in selecting the correct movements combined with termination of movements occurring at inappropriate times. These consequences of increased interconnectivity between STN neurones correlate with some of the symptoms seen in PD patients, who have difficulty initiating voluntary movements and also suffer from the premature termination of movement sequences.

It has been suggested that in PD patients the cause of resting tremor is an oscillation that might develop between the STN and the GPe (Magariños-Ascone *et al.*, 2000; Levy *et al.*, 2000). Such oscillations were observed in experiments using cultures containing the STN and GP (Plenz *et al.*, 1998). Modelling experiments have shown that such oscillations cannot occur in a model system where the neurones in the STN are not connected together (Gillies & Willshaw, 1998a). Indeed, *in vivo* experiments in both anaesthetised rats (Urbain *et al.*, 2000), and in restrained conscious rats (Magill *et al.*, 2000), have failed to show evidence for correlated oscillations between the two nuclei. This again confirms that, at rest the neurones of the STN do not form a network with each other. However, under conditions were neurones in the STN become hyperactive (in PD patients for example) the interconnectivity of STN

neurones would be increased. This suggests that oscillations between the GPe and STN may be more likely to form in the PD brain than they are under normal circumstances.

The experiment described in chapter 4 aimed to investigate the mechanisms that underlie the ability of STN neurones to fire at high frequencies. The results of these experiments led to the suggestion that the NaCh in the STN may have differences from NaCh that have been characterised elsewhere in the brain to date. If these NaCh were confirmed to be new and restricted to the STN, or even just a small number of other nuclei, then there is the potential to modulate the firing of STN neurones therapeutically. It may be possible to develop a drug that can modulate the inactivation kinetics of the NaCh in the STN. If I_{Na} could be made to inactivate more quickly then this inactivation may occur between action potentials. This would limit the maximum firing rate of STN neurones and possibly change the nature of the relationship between membrane potential and firing rate. Such changes in the behaviour of STN neurones would make it less likely that the neurones could generate the co-ordinated pulses of the kind predicted by Gillies and Willshaw (1996; 1998b). Of the two changes to STN network activity that are predicted to occur in PD the inappropriate production of co-ordinated pulses of activity may then be treatable by such a drug. This might help PD patients by preventing the inappropriate termination of movement sequences before the entire sequence has been performed. It is worth noting that, should expression of a novel NaCh, be found to be confined to the STN this also opens the door to the development of 'gene

therapy' treatments for PD using the expression of proteins that could be confined to the STN.

Another potential strategy would be to develop a drug that could modulate the level of interconnectivity between the neurones in the STN. We have seen that excessive levels of interconnectivity due to the depolarisation of STN neurones could be responsible for the problems that PD patients have with the initiation of movements, premature termination of movements, and resting tremor. If a drug could be developed that targeted the interconnections between STN neurones and blocked synaptic transmission, this may help in the alleviation of all three of these motor problems. Such a drug would be difficult to develop as the interconnections are glutamatergic and blocking glutamatergic transmission in a non-selective manner would have disastrous side effects. However, it might be possible to find proteins whose expression is confined to the terminals of these interconnections. One possibility for such a target is the metabotropic glutamate receptor family (mGluR). Eight subtypes of mGluR have been classified and there are several splice variants (Kearney & Albin, 2000). Of these the group I receptors mGluR1 and mGluR5, and the group II receptors mGluR 2 and mGluR3 are expressed in the STN (Ohishi *et al.*, 1993a; Ohishi *et al.*, 1993b; Testa *et al.*, 1994). Intrasubthalamic nucleus injections of mGluR group II agonists induced an increase in STN activity whilst group III agonists induced a decrease in STN activity (Kearney & Albin, 2000). Experiments using injections of a subtype non-specific antagonist of mGluRs into the STN showed that this augmented STN activity levels (Miwa *et al.*, 2000). Combined, these data suggest that mGluRs may be involved in the modulation of glutamatergic

synaptic transmission in STN neurones. This could be either through presynaptic receptors that change the amount of glutamate released or through postsynaptic receptors that can change the neurones response through modulation of AMPA or NMDA receptor opening. The large number of splice variants of mGluRs means that it may be possible to use agonists or antagonists that are relatively selective for STN neurones. The mGluRs provide a possible receptor that may be differentially expressed at the glutamatergic inputs to the STN and the intranuclear axon collaterals. If this were the case then a drug could be developed that could modulate synaptic transmission at the terminals of the intranuclear collaterals in such a way as to reduce the overall interconnectivity of the nucleus.

The experiments described in chapter 6 pointed to another possible consequence of the changes in activity levels of STN neurones in PD. A higher resting level of firing combined with an increased likelihood of producing widespread pulses of activity could contribute to the progression of PD. These experiments showed that a different treatment that leads to hyperactivity of STN neurones was capable of causing a large amount of dopamine cell death in the SN over a relatively short period of time. This suggests that only small increases in the basal levels of activity of STN neurones, if they were persistent, could also lead to dopamine cell death.

Piallat *et al.* (1998) showed that a prior lesion of the STN was protective against the effects of 6-OHDA on dopaminergic neurones. Glutamatergic antagonists are also neuroprotective against the effects of both 6-OHDA and MPTP. Thus there is reason to suspect that hyperactivity of STN neurones may be responsible for the progressive

nature of PD. That our experiments showed that STN hyperactivity can kill previously healthy dopamine cells suggests, not only that could STN hyperactivity be responsible for the progression of PD but that it could also be a primary cause of the disease. Whether or not this is the case, treatments that alleviate the symptoms of PD by reducing hyperactivity in the STN might have the positive side effect that they also halt the progression of the disease.

References

AFSHARPOUR, S. (1985). Light microscopic analysis of golgi impregnated rat subthalamic neurons. *Journal of Comparative Neurology* **236**, 1-13.

ALBIN, R.L. & TAGLE, D.A. (1995). Genetics and molecular biology of Huntington's disease. *Trends in Neurosciences* **18**, 11-14.

ALBIN, R.L., YOUNG, A.B. & PENNEY, J.B. (1989). The functional anatomy of basal ganglia disorders. *Trends in Neurosciences* **12**, 366-375.

ALEXANDER, G.E. & CRUTCHER, M.D. (1990). Functional architecture of basal ganglia circuits: neural substrates of parallel processing. *Trends in Neurosciences* **13**, 266-271.

ANGYÁN, L. & ANGYÁN, Z. (1999). Subthalamic influences on the cardiorespiratory functions in the cat. *Brain Research* **847**, 130-133.

ARBUTHNOTT, G.W., BROWN, J.R., KAPOOR, V. & WHALE, D. (1984). Presynaptic actions of dopamine in the neostriatum. In *The Basal Ganglia - Structure and Function.*, eds. MCKENZIE, J.S., KEMM, R.E. & WILCOCK, L.N., pp. 173-203. New York: Plenum Press.

AUGOOD, S.J., WALDVOGEL, H.J., MÜNKLE, M.C., FAULL, R.L. & EMSON, P.C. (1999). Localization of calcium-binding proteins and GABA transporter (GAT-1) messenger RNA in the human subthalamic nucleus. *Neuroscience* **88**, 521-534.

BARNÉOUD, P., MAZADIER, M., MIQUET, J.-M., PARMENTIER, S., DUBÉDAT, P., DOBLE, A. & BOIREAU, A. (1996). Neuroprotective effects of riluzole on a model of Parkinson's disease in the rat. *Neuroscience* **74**, 971-983.

BAUNEZ, C. & ROBBINS, T.W. (1999a). Effects of dopamine depletion of the dorsal striatum and further interaction with subthalamic nucleus lesions in an attentional task in the rat. *Neuroscience* **92**, 1343-1356.

BAUNEZ, C. & ROBBINS, T.W. (1999b). Effects of transient inactivation of the subthalamic nucleus by local muscimol and APV infusions on performance on the five choice serial reaction time task in rats. *Psychopharmacology* **141**, 57-65.

BEJJANI, B.P., GERVAIS, D., ARNULF, I., PAPADOPOULOS, S., DEMERET, S., BONNET, A.M., CORNU, P., DAMIER, P. & AGID, Y. (2000). Axial parkinsonian symptoms can be improved: the role of levodopa and bilateral subthalamic stimulation. *Journal of Neurology, Neurosurgery and Psychiatry* **68**, 595-600.

BENABID, A.L., BENAZZOUZ, A., LIMOUSIN, P., KOUDSIE, A., KRACK, P., PIALLAT, B. & POLLAK, P. (2000). Dyskinesias and the subthalamic nucleus. *Annals of Neurology* **47**, S189-S192

BENAZZOUZ, A., BORAUD, T., DUBÉDAT, P., BOIREAU, A., STUTZMANN, J.M. & GROSS, C. (1995). Riluzole prevents MPTP-induced parkinsonism in the rhesus monkey: A pilot study. *Eur.J.Pharmacol.* **284**, 299-307.

BENAZZOUZ, A., GAO, D.M., NI, Z.G. & BENABID, A.L. (2000). High frequency stimulation of the STN influences the activity of dopamine neurons in the rat. *NeuroReport* **11**, 1593-1596.

BERGMAN, H., WICHMANN, T. & DELONG, M.R. (1990). Reversal of experimental parkinsonism by lesions of the subthalamic nucleus. *Science* **249**, 1436-1438.

BEURRIER, C., BIOULAC, B. & HAMMOND, C. (2000). Slowly inactivating sodium current (I_{NaP}) underlies single-spike activity in rat subthalamic neurons. *Journal of Neurophysiology* **83**, 1951-1957.

BEURRIER, C., CONGAR, P., BIOULAC, B. & HAMMOND, C. (1999). Subthalamic nucleus neurons switch from single-spike activity to burst-firing mode. *Journal of Neuroscience* **19**, 599-609.

BEVAN, M.D. & BOLAM, J.P. (1995). Cholinergic, GABAergic, and glutamate-enriched inputs from the mesopontine tegmentum to the subthalamic nucleus in the rat. *Journal of Neuroscience* **15**, 7105-7120.

BEVAN, M.D., CLARKE, N.P. & BOLAM, J.P. (1997). Synaptic integration of functionally diverse pallidal information in the entopeduncular nucleus and subthalamic nucleus in the rat. *Journal of Neuroscience* **17**, 308-324.

BEVAN, M.D., CROSSMAN, A.R. & BOLAM, J.P. (1994). Neurons projecting from the entopeduncular nucleus to the thalamus receive convergent synaptic inputs from the subthalamic nucleus and the neostriatum in the rat. *Brain Research* **659**, 99-109.

BEVAN, M.D., FRANCIS, C.M. & BOLAM, J.P. (1995). The glutamate-enriched cortical and thalamic input to neurons in the subthalamic nucleus of the rat: Convergence with GABA- positive terminals. *Journal of Comparative Neurology* **361**, 491-511.

BEVAN, M.D. & WILSON, C.J. (1999). Mechanisms underlying spontaneous oscillation and rhythmic firing in rat subthalamic neurons. *Journal of Neuroscience* **19**, 7617-7628.

BEVAN, M.D., WILSON, C.J., BOLAM, J.P. & MAGILL, P.J. (2000). Equilibrium potential of $GABA_A$ current and implications for rebound burst firing in rat subthalamic neurons in vitro. *Journal of Neurophysiology* **83**, 3169-3172.

BOIREAU, A., DUBÉDAT, P., BORDIER, F., PENY, C., MIQUET, J.-M., DURAND, G., MEUNIER, M. & DOBLE, A. (1994). Riluzole and experimental parkinsonism: Antagonism of MPTP- induced decrease in central dopamine levels in mice. *NeuroReport* **5**, 2657-2660.

BOLAM, J.P., FRANCIS, C.M. & HENDERSON, Z. (1991). Cholinergic input to dopaminergic neurons in the substantia nigra: a double immunocytochemical study. *Neuroscience* **41**, 483-494.

BRENNER, M., KISSEBERTH, W.C., SU, Y., BESNARD, F. & MESSING, A. (1994). GFAP promoter directs astrocyte-specific expression in transgenic mice. *Journal of Neuroscience* **14**, 1030-1037.

BRUET, N., WINDELS, F., POUPARD, A., BERTRAND, A., VERNA, J.M. & SAVASTA, M. (2000). Increase of striatal dopamine induced by high frequency stimulation of the subthalamic nucleus induces a concomitant decrease of striatal glutamate involving DA D2 receptors. *Society for Neuroscience Abstracts* **26**, 246-246.(Abstract)

CAJAL, R. (1911). *Histology of the nervous system.* Oxford University Press.

CALABRESI, P., LACEY, M.G. & NORTH, R.A. (1989). Nicotinic excitation of rat ventral tegmental neurones *in vitro* studied by intracellular recording. *British Journal of Pharmacology* **98**, 135-140.

CAMPBELL, G.A., ECKARDT, M.J. & WEIGHT, F.F. (1985). Dopaminergic Mechanisms in Subthalamic Nucleus of Rat: Analysis Using Horseradish Peroxidase and Microiontophoresis. *Brain Research* **333**, 261-270.

CANTERAS, N.S., SHAMMAH-LAGNADO, S.J., SILVA, B.A. & RICARDO, J.A. (1990). Afferent connections of the subthalamic nucleus: a combined retrograde and anterograde horseradish peroxidase study in the rat. *Brain Research* **513**, 43-59.

CARLSON, J.D., PEARLSTEIN, R.D., BUCHHOLZ, J., IACONO, R.P. & MAEDA, G. (1999). Regional metabolic changes in the pedunculopontine nucleus of unilateral 6-OHDA Parkinson's model rats. *Brain Research* **828**, 12-19.

CATTERALL, W.A. (1992). Cellular and molecular biology of voltage-gated sodium channels. *Physiological Reviews* **72**, S15-S48

CELADA, P., PALADINI, C.A. & TEPPER, J.M. (1999). Gabaergic control of rat substantia nigra dopaminergic neurons: Role of globus pallidus and substantia nigra pars reticulata. *Neuroscience* **89**, 813-825.

CHATHA, B.T., BERNARD, V., STREIT, P. & BOLAM, J.P. (2000). Synaptic localization of ionotropic glutamate receptors in the rat substantia nigra. *Neuroscience* **101**, 1037-1051.

CHERGUI, K., AKAOKA, H., CHARLÉTY, P.J., SAUNIER, C.F., BUDA, M. & CHOUVET, G. (1994). Subthalamic nucleus modulates burst firing of nigral dopamine neurones via NMDA receptors. *NeuroReport* **5**, 1185-1188.

CHERGUI, K., CHARLÉTY, P.J., AKAOKA, H., SAUNIER, C.F., BRUNET, J.-L., BUDA, M., SVENSSON, T.H. & CHOUVET, G. (1993). Tonic activation of NMDA receptors causes spontaneous burst discharge of rat midbrain dopamine neurons *in vivo*. *European Journal of Neuroscience* **5**, 137-144.

CHESSELET, M.-F. & DELFS, J.M. (1996). Basal ganglia and movement disorders: an update. *Trends in Neurosciences* **19**, 417-422.

CLARKE, N.P. & BOLAM, J.P. (1998). Distribution of Glutamate Receptor Subunits at Neurochemically Characterized Synapses in the Entopeduncular Nucleus and Subthalamic Nucleus of the Rat. *Journal of Comparative Neurology* **397**, 403-420.

COFFEY, P.J., PERRY, V.H. & RAWLINS, J.N. (1990). An investigation into the early stages of the inflammatory response following ibotenic acid-induced neuronal degeneration. *Neuroscience* **35**, 121-132.

COGGESHALL, R.E. (1992). A consideration of neural counting methods. *Trends in Neurosciences* **15**, 9-13.

COOPER, A.J. & STANFORD, I.M. (2000). Electrophysiological and morphological characteristics of three subtypes of rat globus pallidus neurone *in vitro*. *Journal of Physiology* **527**, 291-304.

COYLE, J.T. (1983). Neurotoxic Action of Kainic Acid. *Journal of Neurochemistry* **41**, 1-11.

CRILL, W.E. (1996). Persistent sodium current in mammalian central neurons. *Annual Reviews in Physiology* **58**, 349-362.

CRITZ, S.D., WIBLE, B.A., LOPEZ, H.S. & BROWN, A.M. (1993). Stable expression and regulation of a rat brain K^+ channel. *Journal of Neurochemistry* **60**, 1175-1478.

CROSSMAN, A.R. (2000). Functional anatomy of movement disorders. *Journal of Anatomy* **196**, 519-525.

DENIAU, J.M., KOLOMIETS, B.P., GLOWINSKI, J. & THIERRY, A.M. (2000). Do Inputs Originating from Functionally Distinct Cortical Areas Segregate or Converge in the Subthalamic Nucleus. *Society for Neuroscience Abstracts* **26**, 961(Abstract)

DERANSART, C., LÊ, B.T., MARESCAUX, C. & DEPAULIS, A. (1998a). Role of the subthalamo-nigral input in the control of amygdala-kindled seizures in the rat. *Brain Research* **807**, 78-83.

DERANSART, C., VERCUEIL, L., MARESCAUX, C. & DEPAULIS, A. (1998b). The role of basal ganglia in the control of generalized absence seizures. *Epilepsy Research* **32**, 213-223.

DI LORETO, S., FLORIO, T. & SCARNATI, E. (1992). Evidence that non-NMDA receptors are involved in the excitatory pathway from the pedunculopontine region to nigrostriatal dopaminergic neurons. *Experimental Brain Research* **89**, 79-86.

EVANS, R.H., FRANCIS, A.A., HUNT, K., OAKES, D.J. & WATKINS, J.C. (1979). Antagonism of excitatory amino acid-induced responses and of synaptic excitation in the isolated spinal cord of the frog. *British Journal of Pharmacology* **67**, 591-603.

FEGER, J. & ROBLEDO, P. (1991). The Effects of Activation or Inhibition of the Subthalamic Nucleus on the Metabolic and Electrophysiological Activities Within the Pallidal Complex and Substantia Nigra in the Rat. *European Journal of Neuroscience* **3**, 947-952.

FÉGER, J., BEVAN, M.D. & CROSSMAN, A.R. (1994). The projections from the parafascicular thalamic nucleus to the subthalamic nucleus and the striatum arise from separate neuronal populations: A comparison with the corticostriatal and corticosubthalamic efferents in a retrograde fluorescent double- labelling study. *Neuroscience* **60**, 125-132.

FLEIDERVISH, I.A. & GUTNICK, M.J. (1996). Kinetics of slow inactivation of persistent sodium current in layer V neurons of mouse neocortical slices. *Journal of Neurophysiology* **76**, 2125-2130.

FLORES, G., ROSALES, M.G., HERNÁNDEZ, S., SIERRA, A. & ACEVES, J. (1995). 5-Hydroxytryptamine increases spontaneuos activity of subthalamic neurons in the rat. *Neuroscience Letters* **192**, 17-20.

FLORES, G., VALENCIA, J., ROSALES, M.G., SIERRA, A. & ACEVES, J. (1993). Appearance of EMG activity and motor asymmetry after unilateral lesions of the dopaminergic innervation to the subthalamic nucleus. *Neuroscience Letters* **162**, 153-156.

FUJIMOTO, K. & KITA, H. (1993). Response characteristics of subthalamic neurons to the stimulation of the sensorimotor cortex in the rat. *Brain Research* **609**, 185-192.

FUTAMI, T., TAKAKUSAKI, K. & KITAI, S.T. (1995). Glutamatergic and cholinergic inputs from the pedunculopontine tegmental nucleus to dopamine neurons in the substantia nigra pars compacta. *Neurosci.Res.* **21**, 331-342.

GAN, L. & KACZMAREK, L.K. (1998). When, where, and how much? Expression of the Kv3.1 potassium channel in high-frequency firing neurons. *Journal of Neurobiology* **37**, 69-79.

GAO, D.M., BENAZZOUZ, A., PIALLAT, B., BRESSAND, K., ILINSKY, I.A., KULTAS-ILINSKY, K. & BENABID, A.L. (1898). High-frequency stimulation of the subthalamic nucleus suppresses experimental resting tremor in the monkey. *Neuroscience* **88**, 201-212.

GILLIES, A. & ARBUTHNOTT, G. (2000). Computational models of the basal ganglia. *Movement Disorders* **15**, 762-770.

Gillies, A. J. The role of the subthalamic nucleus in the basal ganglia. 1995. (GENERIC) Ref Type: Thesis/Dissertation

GILLIES, A.J. (1996). Electrical properties of subthalamic nucleus projection neurons. In *Computational Neuroscience*, ed. BOWER, J., New York: Academic Press.

GILLIES, A.J., ATHERTON, J.F., ARBUTHNOTT, G.W. & WILLSHAW, D.J. (2000). The nature of glutamatergic interactions between neurons in the subthalamic nucleus. *European Journal Neuroscience.* **12**, 507(Abstract)

GILLIES, A.J. & WILLSHAW, D. (1998a). A Model of the interaction between the globus pallidus and the subthalamic nucleus. *European Journal of Neuroscience* **10**, S301-S301

GILLIES, A.J. & WILLSHAW, D.J. (1998b). A massively connected subthalamic nucleus leads to the generation of widespread pulses. *Proceedings of the Royal Society of London.B:Biological Sciences* **265**, 2101-2109.

GOOD, P.F., HSU, A., WERNER, P., PERL, D.P. & OLANOW, C.W. (1998). Protein nitration in Parkinson's disease. *Journal of Neuropathology and Experimental Neurology* **57**, 338-342.

GRAYBIEL, A.M. (1990). Neurotransmitters and neuromodulators in the basal ganglia. *Trends in Neurosciences* **13**, 244-254.

GREENE, J. & D'OLIVEIRA, M. (1982). *Learning to use statistical tests in psychology.* Milton Keynes: Open University Press.

GRILLNER, P., BERRETTA, N., BERNARDI, G., SVENSSON, T.H. & MERCURI, N.B. (2000). Muscarinic receptors depress GABAergic synaptic transmission in rat midbrain dopamine neurons. *Neuroscience* **96**, 299-307.

GUNDERSEN, H.J.G. & JENSEN, E.B. (1987). The efficiency of systematic sampling in stereology and its prediction. *Journal of Microscopy* **147**, 229-263.

GURIDI, J. & OBESO, J.A. (1997). The role of the subthalamic nucleus in the origin of hemiballism and parkinsonism: New surgical perspectives. *Advances in Neurology* **74**, 235-247.

HAGG, T., FASSHOLMES, B., VAHLSING, H.L., MANTHORPE, M., CONNER, J.M. & VARON, S. (1989). Nerve growth-factor (NGF) reverses axotomy-induced decreases in choline-acetyle transferase, NGF receptor and size of medial septum cholinergic neurons. *Brain Research* **505**, 29-38.

HAMMOND, C., DENIAU, J.M., RIZK, A. & FEGER, J. (1978). Electrophysiological demonstration of an excitatory subthalamonigral pathway in the rat. *Brain Research* **151**, 235-244.

HAMMOND, C. & YELNIK, J. (1983). Intracellular labelling of rat subthalamic neurones with horseradish peroxidase: Computer analysis of dendrites and characterization of axon arborization. *Neuroscience* **8**, 781-790.

HASSANI, O.-K., FRANCOIS, C., YELNIK, J. & FEGER, J. (1997). Evidence for a dopaminergic innervation of the subthalamic nucleus in the rat. *Brain Research* **749**, 88-94.

HASSANI, O.-K., MOUROUX, M. & FEGER, J. (1996). Increased subthalamic neuronal activity after nigral dopaminergic lesion independent of disinhibition via the globus pallidus. *Neuroscience* **72**, 105-115.

HAUBER, W. (1998). Blockade of subthalamic dopamine D_1 receptors elicits akinesia in rats. *NeuroReport* **9**, 4115-4118.

HAUBER, W. & FUCHS, H. (2000). Dopamine release in the rat globus pallidus characterised by in vivo microdialysis. *Behavioural Brain Research* **111**, 39-44.

HENDERSON, J.M. & DUNNETT, S.B. (1998). Targeting the subthalamic nucleus in the treatment of Parkinson's disease. *Brain Research Bulletin* **46**, 467-474.

HENDERSON, Z. & GREENFIELD, S.A. (1987). Does the substantia nigra have a cholinergic innervation? *Neuoscience Letters* **73**, 109-113.

HÉDOU, G., CHASSEROT-GOLAZ, S., KEMMEL, V., GOBAILLE, S., ROUSSEL, G., ARTAULT, J.C., ANDRIAMAMPANDRY, C., AUNIS, D. & MAITRE, M. (2000). Immunohistochemical studies of the localization of neurons containing the enzyme that synthesizes dopamine, GABA, or γ-hydroxybutyrate in the rat substantia nigra and striatum. *Journal of Comparative Neurology* **426**, 549-560.

HILLE, B. (1992). *Ionic Channels of Excitable Membranes.* Massachusetts: Sinauer Associates.

HINES, M.L. & CARNEVALE, N.T. (1997). The NEURON simulation environment. *Neural Computation* **9**, 1179-1209.

HINES, M.L. & CARNEVALE, N.T. (2000). Expanding NEURON's repertoire of mechanisms with NMODL. *Neural Computation* **12**, 995-1007.

HONORÉ, T., DAVIES, S.N., DREJER, J., FLETCHER, E.J., JACOBSEN, P., LODGE, D. & NIELSEN, F.E. (1988). Quinoxalinediones: potent competative non-NMDA glutamate receptor antagonists. *Science* **241**, 701-703.

HUMPHRIES, M.D. & GURNEY, K. (2000). A computational model of action selection in the basal ganglia: Thalamic and cortical interactions. *European Journal of Neuroscience* **12**, 508-508.(Abstract)

INGHAM, C.A., HOOD, S.H., TAGGART, P. & ARBUTHNOTT, G.W. (1998). Plasticity of synapses in the rat neostriatum after unilateral lesion of the nigrostriatal dopaminergic pathway. *Journal of Neuroscience* **18**, 4732-4743.

ISOM, L.L., DE JONGH, K.S., PATTON, D.E., REBER, B.F.X., OFFORD, J., CHARBONNEAU, H., WALSH, K., GOLDIN, A.L. & CATTERALL, W.A. (1992). Primary structure and functional expression of the β_1 subunit of the rat brain sodium channel. *Science* **256**, 839-842.

ISOM, L.L., RAGSDALE, D.S., DE JONGH, K.S., WESTENBROEK, R.E., REBER, B.F.X., SCHEUER, T. & CATTERALL, W.A. (1995). Structure and function of the β2 subunit of brain sodium channels, a transmembrane glycoprotein with a CAM motif. *Cell* **83**, 433-442.

JACKSON-LEWIS, V., JAKOWEC, M., BURKE, R.E. & PRZEDBORSKI, S. (1995). Time course and morphology of dopaminergic neuronal death caused by the

neurotoxin 1-methyl-4-phenyl-1,2,3,6-tetrahydropyridine. *Neurodegeneration* **4**, 257-269.

JACKSON, A. & CROSSMAN, A.R. (1981a). Basal ganglia and other afferent projections to the peribrachial region in the rat: a study using retrograde and anterograde transport of horseradish peroxidase. *Neuroscience* **6**, 1537-1549.

JACKSON, A. & CROSSMAN, A.R. (1981b). Subthalamic projection to nucleus tegmenti pedunculopontinus in the rat. *Neuroscience Letters* **22**, 17-22.

JACKSON, A. & CROSSMAN, A.R. (1983). Nucleus tegmenti pedunculopontinus: Efferent connections with special reference to the basal ganglia. Studied in the rat by anterograde and retrograde transport of horseradish peroxidase. *Neuroscience* **10**, 725-765.

JARNOT, M.D. & CORBETT, A.M. (1995). High titer antibody to mammalian neuronal sodium channels produces sustained channel block. *Brain Research* **674**, 159-162.

JONES-HUMBLE, S.A., MORGAN, P.F. & COOPER, B.R. (1994). The novel anticonvulsant lamotrigine prevents dopamine depletion in C57 black mice in the MPTP animal model of Parkinson's disease. *Life Sciences* **54**, 245-252.

JUNG, H.Y., MICKUS, T. & SPRUSTON, N. (1997). Prolonged sodium channel inactivation contributes to dendritic action potential attenuation in hippocampal pyramidal neurons. *Journal of Neuroscience* **17**, 6639-6646.

KANEMASA, T., GAN, L., PERNEY, T.M., WANG, L.-Y. & KACZMAREK, L.K. (1995). Electrophysiological and pharmacological characterization of a mammalian *shaw* channel expressed in NIH 3T3 fibroblasts. *Journal of Neurophysiology* **74**, 207-217.

KANG, Y. & FUTAMI, T. (1999). Arrhythmic Firing in Dopamine Neurons of Rat Substantia Nigra Evoked by Activation of Subthalamic Neurons. *Journal of Neurophysiology* **82**, 1632-1637.

KATO, H., KOGURE, K., ARAKI, T. & ITOYAMA, Y. (1995). Graded expression of immunomolecules on activated microglia in the hippocampus following ischemia in a rat model of ischemic tolerance. *Brain Research* **694**, 85-93.

KEARNEY, J.A.F. & ALBIN, R.L. (2000). Intrasubthalamic nucleus metabotropic glutamate receptor activation: A behavioural, fos immunohistochemical and [^{14}C]2-deoxyglucose autoradiographic study. *Neuroscience* **95**, 409-416.

KEMP, J.M. & POWELL, T.P.S. (1971). The structure of the caudate nucleus of the cat: light and electron microscopy. *Phil.Trans.R.Soc.Lond.B.* **262**, 383-401.

KITA, H., CHANG, H.T. & KITAI, S.T. (1983a). Pallidal inputs to subthalamus: intracellular analysis. *Brain Research* **264**, 255-265.

KITA, H., CHANG, H.T. & KITAI, S.T. (1983b). The morphology of intracellularly labeled rat subthalamic neurons: A light microscope analysis. *Journal of Comparative Neurology* **215**, 245-257.

KITA, H. & KITAI, S.T. (1987). Efferent Connections of the Subthalamic Nucleus in the Rat: Light and Electron Microscopic Analysis With the PHA-L Method. *Journal of Comparative Neurology* **260**, 435-452.

KITAI, S.T. & KITA, H. (1986). Anatomy and Physiology of the Subthalamic Nucleus: A Driving Force of the Basal Ganglia. In *The Basal Ganglia II: Structure and Function - Current Concepts.*, eds. CARPENTER, M.B. & JAYARAMAN, A., pp. 357-373. New York: Plenum Press.

KITAI, S.T., SHEPARD, P.D., CALLAWAY, J.C. & SCROGGS, R. (1999). Afferent modulation of dopamine neuron firing patterns. *Current Opinion in Neurobiology* **9**, 690-697.

KITT, C.A., CORK, L.C., EIDELBERG, F., JOH, T.H. & PRICE, D.L. (1986). Injury of nigral neurons exposed to 1-methyl-4-phenyl-1,2,3,6- tetrahydropyridine: a tyrosine hydroxylase immunocytochemical study in monkey. *Neuroscience* **17**, 1089-1103.

KRACK, P., BENAZZOUZ, A., POLLAK, P., LIMOUSIN, P., PIALLAT, B., HOFFMANN, D., XIE, J. & BENABID, A.L. (1998). Treatment of tremor in Parkinson's disease by subthalamic nucleus stimulation. *Movement Disorders* **13**, 907-914.

KREISS, D.S., MASTROPIETRO, C.W., RAWJI, S.S. & WALTERS, J.R. (1997). The response of subthalamic nucleus neurons to dopamine receptor stimulation in a rodent model of Parkinson's disease. *Journal of Neuroscience* **17**, 6807-6819.

KRIMER, L.S. & GOLDMAN-RAKIC, P.S. (1997). An interface chamber for anatomical and physiological studies of living brain slices. *Journal of Neuroscience Methods* **75**, 55-58.

LAMS, B.E., ISACSON, O. & SOFRONIEW, M.V. (1988). Loss of transmitter-associated enzyme staining following axotomy does not indicate death of brainstem cholinergic neurons. *Brain Research* **475**, 401-406.

LANGSTON, J.W., FORNO, L.S., TETRUD, J., REEVES, A.G., KAPLAN, J.A. & KARLUK, D. (1999). Evidence of active nerve cell degeneration in the substantia nigra of humans years after 1-methyl-4-phenyl-1,2,3,6-tetrahydropyridine exposure. *Annals of Neurology* **46**, 598-605.

LARSEN, K.D. & SUTIN, J. (1978). Output organization of the feline entopeduncular and subthalamic nuclei. *Brain Research* **157**, 21-31.

LEVY, R., HUTCHISON, W.D., LOZANO, A.M. & DOSTROVSKY, J.O. (2000). High-frequency synchronization of neuronal activity in the subthalamic nucleus of parkinsonian patients with limb tremor. *Journal of Neuroscience* **20**, 7766-7775.

LIMOUSIN, P., KRACK, P., POLLAK, P., BENAZZOUZ, A., ARDOUIN, C., HOFFMANN, D. & BENABID, A.L. (1998). Electrical stimulation of the subthalamic nucleus in advanced Parkinson's disease. *New England Journal of Medicine* **339**, 1105-1111.

LOKWAN, S.J., OVERTON, P.G., BERRY, M.S. & CLARK, D. (1999). Stimulation of the pedunculopontine tegmental nucleus in the rat produces burst firing in A9 dopaminergic neurons. *Neuroscience* **92**, 245-254.

LUCAS, D.R. & NEWHOUSE, J.P. (1957). The toxic effect of sodium L-glutamate on the inner layers of the retina. *Arch.Opthal.* **58**, 193-201.(Abstract)

LUNEAU, C.J., WILLIAMS, J.B., MARSHALL, J., LEVITAN, E.S., OLIVA, C., SMITH, J.S., ANTANAVAGE, J., FOLANDER, K., STEIN, R.B., SWANSON, R., KACZMAREK, L.K. & BUHROW, S.A. (1991). Alternative splicing contributes to the generation of K^+ channel diversity in the mammalian central nervous system. *Proceedings of the National Academy of Sciences of the United States of America* **88**, 3932-3936.

LUYS, J. (1865). *Recherches sur le système nerveux cérébrospinal, sa structure, ses functions et ses maladies.* Paris: J.B. Ballière et Fils.

MAGARIÑOS-ASCONE, C.M., FIGUEIRAS-MENDEZ, R., RIVA-MEANA, C. & CÓRDOBA-FERNÁNDEZ, A. (2000). Subthalamic neuron activity related to tremor and movement in Parkinson's disease. *European Journal of Neuroscience* **12**, 2597-2607.

MAGILL, P.J., BOLAM, J.P. & BEVAN, M.D. (2000). Relationship of activity in the subthalamic nucleus-globus pallidus network to cortical electroencephalogram. *Journal of Neuroscience* **20**, 820-833.

MAGNIN, M., MOREL, A. & JEANMONOD, D. (2000). Single-unit analysis of the pallidum, thalamus and subthalamic nucleus in parkinsonian patients. *Neuroscience* **96**, 549-564.

MAURICE, N., DENIAU, J.M., GLOWINSKI, J. & THIERRY, A.-M. (1998). Relationships between the prefrontal cortex and the basal ganglia in the rat: Physiology of the corticosubthalamic circuits. *Journal of Neuroscience* **18**, 9539-9546.

MCQUEEN, J., WRIGHT, A.K., ARBUTHNOTT, G.W. & FINK, G. (1990). Glial fibrillary acidic protein (GFAP)-immunoreactive astrocytes are increased in the hypothalamus of androgen-insensitive testicular feminized (Tfm) mice. *Neuroscience Letters* **118**, 77-81.

MIWA, H., NISHI, K., FUWA, T. & MIZUNO, Y. (2000). Effects of blockade of metabotropic glutamate receptors in the subthalamic nucleus on haloperidol-induced Parkinsonism in rats. *Neuroscience Letters* **282**, 21-24.

MONTES-GONZALEZ, F.M., PRESCOTT, T.J., GURNEY, K. & REDGRAVE, P. (2000). The robot basal ganglia: Control of robot action selection by an embodied model of the mammalian basal ganglia. *European Journal of Neuroscience* **12**, 134-134.(Abstract)

MOUROUX, M., HASSANI, O.-K. & FEGER, J. (1997). Electrophysiological and fos immunohistochemical evidence for the excitatory nature of the parafascicular projection to the globus pallidus. *Neuroscience* **81**, 387-397.

MULLEN, R.J., BUCK, C.R. & SMITH, A.M. (1992). NeuN, A neuronal specific nuclear-protein in vertebrates. *Development* **116**, 201-211.

MULLER, D., JOLY, M. & LYNCH, G. (1988). Contributions of quisqualate and NMDA receptors to the induction and expression of LTP. *Science* **242**, 1694-1697.

MURER, M.G. & PAZO, J.H. (1993). Circling behaviour induced by activation of $GABA_A$ receptors in the subthalamic nucleus. *NeuroReport* **4**, 1219-1222.(Abstract)

NAKANISHI, H., KITA, H. & KITAI, S.T. (1987). Electrical membrane properties of rat subthalamic neurons in an in vitro slice preparation. *Brain Research* **437**, 35-44.

NARAHASHI, T., MOORE, J.W. & SCOTT, W.R. (1964). Tetrodotoxin blockage of sodium conductance increase in lobster giant axons. *Journal of General Physiology* **47**, 965-974.

NAUTA, H.J.W. & CUENOD, M. (1982). Perikaryal cell labeling in the subthalamic nucleus following the injection of ^{3}H-γ-aminobutyric acid into the pallidal complex: an autoradiographic study in cat. *Neuroscience* **7**, 2725-2734.

NI, Z.G., BOUALI-BENAZZOUZ, R., GAO, D.M., BENABID, A.-L. & BENAZZOUZ, A. (2000). Changes in the firing pattern of globus pallidus neurons after the degeneration of nigrostriatal pathway are mediated by the subthalamic nucleus in the rat. *European Journal Neuroscience.* **12**, 4338-4344.

OBESO, J.A., RODRÍGUEZ-OROZ, M.C., RODRÍGUEZ, M., LANCIEGO, J.L., ARTIEDA, J., GONZALO, N. & OLANOW, C.W. (2000). Pathophysiology of the basal ganglia in Parkinson's disease. *Trends in Neurosciences* **23**, S8-S19

OHISHI, H., SHIGEMOTO, R., NAKANISHI, S. & MIZUNO, N. (1993a). Distribution of the messenger RNA for a metabotropic glutamate receptor, mGluR2, in the central nervous system of the rat. *Neuroscience* **53**, 1009-1018.

OHISHI, H., SHIGEMOTO, R., NAKANISHI, S. & MIZUNO, N. (1993b). Distribution of the mRNA for a metabotropic glutamate receptor (mGluR3) in the rat brain: an *in situ* hybridisation study. *Journal of Comparative Neurology* **335**, 252-266.

OLANOW, C.W. & TATTON, W.G. (1999). Etiology and pathogenesis of Parkinson's disease. *Annual Review of Neuroscience* **22**, 123-144.

OLNEY, J.W., HO, O.L. & RHEE, V. (1971). Cytotoxic effects of acidic and sulphur containing amino acids on the infant mouse central nervous system. *Exp.Br.Res.* **14**, 61-76.(Abstract)

OORSCHOT, D.E. (1996). Total number of neurons in the neostriatal, pallidal, subthalamic, and substantia nigral nuclei of the rat basal ganglia: a stereological study using the cavalieri and optical disector methods. *Journal of Comparative Neurology* **366**, 580-599.

ORIEUX, G., FRANCOIS, C., FÉGER, J., YELNIK, J., VILA, M., RUBERG, M., AGID, Y. & HIRSCH, E.C. (2000). Metabolic activity of excitatory parafascicular

and pedunculopontine inputs to the subthalamic nucleus in a rat model of Parkinson's disease. *Neuroscience* **97**, 79-88.

OVERTON, P., RICHARDS, C.D., BERRY, M.S. & CLARK, D. (1999). Long-term potentiation at excitatory amino acid synapses on midbrain dopamine neurons. *NeuroReport* **10**, 221-226.

OVERTON, P.G., O'CALLAGHAN, J.F. & GREENFIELD, S.A. (1995). Possible intermixing of neurons from the subthalamic nucleus and substantia nigra pars compacta in the guinea-pig. *Experimental Brain Research* **107**, 151-165.

OXFORD, G.S. (1981). Some kinetic and steady-state properties of sodium channels after removal of inactivation. *Journal of General Physiology* **77**, 1-22.

PARENT, A. & HAZRATI, L.-N. (1995). Functional anatomy of the basal ganglia. II. The place of teh subthalamic nucleus and external pallidum in basal ganglia circuitry. *Brain Research Reviews* **20**, 128-154.

PARKINSON, J. (1817). *An essay on the shaking palsy*. London: Sherwood, Neely and Jones.

PATLAK, J. (1991). Molecular kinetics of voltage-dependent Na^+ Channels. *Physiological Reviews* **71**, 1047-1080.

PAXINOS, G. & WATSON, C. (1986). *The Rat Brain in Stereotaxic Coordinates*. New York: Academic Press.

PERKINS, M.N. & STONE, T.W. (1980). Subthalamic projections to the globus pallidus: an electrophysiological study in the rat. *Experimental Neurology* **68**, 500-511.

PERNEY, T.M., MARSHALL, J., MARTIN, K.A., HOCKFIELD, S. & KACZMAREK, L.K. (1992). Expression of the mRNAs for the Kv3.1 potassium channel gene in the adult and developing rat brain. *Journal of Neurophysiology* **68**, 756-766.

PÉRIER, C., AGID, Y., HIRSCH, E.C. & FÉGER, J. (2000). Ipsilateral and contralateral subthalamic activity after unilateral dopaminergic lesion. *NeuroReport* **11**, 3275-3278.

PHILLIPS, J.M., LATIMER, M.P., GUPTA, S., WINN, P. & BROWN, V.J. (1998). Excitotoxic lesions of the subthalamic nucleus ameliorate asymmetry induced by striatal dopamine depletion in the rat. *Behavioural Brain Research* **90**, 73-77.

PIALLAT, B., BENAZZOUZ, A. & BENABID, A.-L. (1998). Subthalamic nucleus lesion in rats prevents dopaminergic nigral neuron degeneration after striatal 6-OHDA injection: Behavioural and immunohistochemical studies. *European Journal of Neuroscience* **8**, 1408-1414.

PICKEL, V.M., JOH, T.H., FIELD, P.M., BECKER, C.G. & REIS, D.J. (1975). Cellular localization of tyrosine hydroxylase by immunohistochemistry. *Journal of Histochemistry & Cytochemistry* **23**, 1-12.

PICKEL, V.M., JOH, T.H. & REIS, D.J. (1976). Monoamine-synthesizing enzymes in central dopaminergic, noradrenergic and serotonergic neurons. Immunocytochemical

localization by light and electron microscopy. *Journal of Histochemistry & Cytochemistry* **24**, 792-306.

PLENZ, D., HERRERA-MARSCHITZ, M. & KITAI, S.T. (1998). Morphological organization of the globus pallidus-subthalamic nucleus system studied in organotypic cultures. *Journal of Comparative Neurology* **397**, 437-457.

PLENZ, D. & KITAI, S.T. (1999). A basal ganglia pacemaker formed by the subthalamic nucleus and external globus pallidus. *Nature* **400**, 677-682.(Abstract)

PONGRÁZ, F., POOLOS, N., KOCSIS, J. & SHEPHERD, G. (1992). A model of NMDA receptor-mediated activity in dendrites of hippocampal CA1 pyramidal neurones. *Journal of Neurophysiology* **68**, 2248-2259.

PREDY, R., MALHOTRA, S.K. & DAS, G.D. (1988). Enhanced expression of a protein antigen (J1-31 antigen, 30 kilodaltons) by reactive astrocytes in lacerated spinal cord. *Journal of Neuroscience Research* **19**, 397-404.

RAGSDALE, D.S., SCHEUER, T. & CATTERALL, W.A. (1991). Frequency and voltage-dependent inhibition of type IIA Na^+ channels, expressed in a mammalian cell line, by local anaesthetic, antiarrhythmic, and anticonvulsant drugs. *Molecular Pharmacology* **40**, 756-765.

REDGRAVE, P., PRESCOTT, T.J. & GURNEY, K. (1999a). Is the short-latency dopamine response too short to signal reward error? *Trends in Neurosciences* **22**, 146-151.

REDGRAVE, P., PRESCOTT, T.J. & GURNEY, K. (1999b). The basal ganglia: A vertebrate solution to the selection problem? *Neuroscience* **89**, 1009-1023.

REIS, D.J., GILAD, G., PICKEL, V.M. & JOH, T.H. (1978). Reversible changes in the activities and amounts of tyrosine hydroxylase in dopamine neurons of the substantia nigra in response to axonal injury as studied by immunochemical and immunocytochemical methods. *Brain Res* **144**, 325-342.

ROBINSON, A.P., WHITE, T.M. & MASON, D.W. (1986). Macrophage heterogeneity in the rat as delineated by two monoclonal antibodies MRC OX41 and MRC OX42, the latter recognising the complement receptor type 3. *Immunology* **57**, 239-247.(Abstract)

ROBLEDO, P. & FEGER, J. (1990). Excitatory influence of rat subthalamic nucleus to substantia nigra pars reticulata and the pallidal complex: electrophysiological data. *Brain Research* **518**, 47-54.

RODRIGUEZ, M.C., GURIDI, O.J., ALVAREZ, L., MEWES, K., MACIAS, R., VITEK, J., DELONG, M.R. & OBESO, J.A. (1998a). The subthalamic nucleus and tremor in Parkinson's disease. *Movement Disorders* **13**, 111-118.

RODRIGUEZ, M.C., OBESO, J.A. & OLANOW, C.W. (1998b). Subthalamic nucleus-mediated excitotoxicity in Parkinson's disease: A target for neuroprotection. *Annals of Neurology* **44**, S175-S188

ROSS, R.A. & REIS, D.J. (1981). Reversible changes in the activities of tyrosine-hydroxylase and dopamine-β-hydroxylase in neurons of the nucleus locus coeruleus after experimental stroke. *Experimental Neurology* **73**, 571-575.

ROUZAIRE-DUBOIS, B., HAMMOND, C., HAMON, B. & FEGER, J. (1980). Pharmacological blockade of the globus pallidus-induced inhibitory response of subthalamic cells in the rat. *Brain Research* **200**, 321-329.

ROUZAIRE-DUBOIS, B., HAMMOND, C., YELNIK, J. & FEGER, J. (1984). Anatomy and neurophysiology of the subthalamic efferent neurones. In *The Basal Ganglia: Structure and Function*, ed. MCKENZIE, J.S., pp. 205-234. New York: Plenum.

ROUZAIRE-DUBOIS, B., SCARNATI, E., HAMMOND, C., CROSSMAN, A.R. & SHIBAZAKI, T. (1983). Microiontophoretic studies on the nature of the neurotransmitter in the subthalamo-entopeduncular pathway of the rat. *Brain Research* **271**, 11-20.

RYAN, L.J., SANDERS, D.J. & CLARK, K.B. (1992). Auto- and cross-correlation analysis of subthalamic nucleus neuronal activity in neostriatal- and globus pallidal-lesioned rats. *Brain Research* **583**, 253-261.

RYE, D.B., SAPER, C.B., LEE, H.J. & WAINER, B.H. (1987). Pedunculopontine tegmental nucleus of the rat: Cytoarchitecture, cytochemistry. and some extrapyrmaidal connections of the mesopontine tegmentum. *Journal of Comparative Neurology* **259**, 483-528.

SAVASTA, M., BRUET, N., WINDELS, F. & POUPARD, A. (2000). High Frequency Stimulation of Subthalamic Nucleus Increases Striatal Dopamine Release in Normal and Partially Dopaminergic Denervated Rats. *European Journal of Neuroscience* **12**, 114(Abstract)

SCARNATI, E., PROIA, A., CAMPANA, E. & PACITTI, C. (1986). A microiontophoretic study on the nature of the putative synaptic neurotransmitter involved in the pedunculopontine-substantia nigra pars compacta excitatory pathway in the rat. *Experimental Brain Research* **62**, 470-478.

SCHMITT, O. & SCHMIDT, H. (1972). Influences of calcium ions on the ionic currents of nodes of Ranvier treated with scorpion venom. *Pflugers Archiv European Journal of Physiology* **333**, 51-61.

SCHULTZ, W. (1997). Dopamine neurons and their role in reward mechanisms. *Current Opinion in Neurobiology* **7**, 191-197.

SHINK, E., BEVAN, M.D., BOLAM, J.P. & SMITH, Y. (1996). The subthalamic nucleus and the external pallidum: two tightly interconnected structures that control the output of the basal ganglia in the monkey. *Neuroscience* **73**, 335-357.

SMITH, Y., BEVAN, M.D., SHINK, E. & BOLAM, J.P. (1998). Microcircuitry of the direct and indirect pathways of the basal ganglia. *Neuroscience* **86**, 353-387.

SMITH, Y. & PARENT, A. (1988). Neurons of the subthalamic nucleus in primates display glutamate but not GABA immunoreactivity. *Brain Research* **453**, 353-356.

SORENSON, E.M., SHIROYAMA, T. & KITAI, S.T. (1998). Postsynaptic nicotinic receptors on dopaminergic neurons in the substantia nigra pars compacta of the rat. *Neuroscience* **87**, 659-673.

STANDAERT, D.G., TESTA, C.M., YOUNG, A.B. & PENNEY, J.B., Jr. (1994). Organization of N-methyl-D-aspartate glutamate receptor gene expression in the basal ganglia of the rat. *Journal of Comparative Neurology* **343**, 1-16.

SU, M.T., DUNWIDDIE, T.V. & GERHARDT, G.A. (1990). Combined electrochemical and electrophysiological studies of monoamine overflow in rat hippocampal slices. *Brain Research* **518**, 149-158.

SURI, R.E. & SCHULTZ, W. (1998). Learning of sequential movements by neural network model with dopamine-like reinforcement signal. *Experimental Brain Research* **121**, 350-354.

SURI, R.E. & SCHULTZ, W. (1999). A neural network model with dopamine-like reinforcement signal that learns a spatial delayed response task. *Neuroscience* **91**, 871-890.

TAKAKUSAKI, K., SHIROYAMA, T., YAMAMOTO, T. & KITAI, S.T. (1996). Cholinergic and noncholinergic tegmental pedunculopontine projection neurons in rats revealed by intracellular labeling. *Journal of Comparative Neurology* **371**, 345-361.

TASKER, R.R., LANG, A.E. & LOZANO, A.M. (1997). Pallidal and thalamic surgery for Parkinson's disease. *Experimental Neurology* **144**, 35-40.

TATTON, W.G., KWAN, M.M., VERRIER, M.C., SENIUK, N.A. & THERIAULT, E. (1990). MPTP produces reversible disappearance of tyrosine hydroxylase-containing retinal amacrine cells. *Brain Res* **527**, 21-31.

TESTA, C.M., STANDAERT, D.G., YOUNG, A.B. & PENNEY, J.B., Jr. (1994). Metabotropic glutamate receptor mRNA expression in the basal ganglia of the rat. *Journal of Neuroscience* **14** , 3005-3018.

UNGERSTEDT, U. & ARBUTHNOTT, G.W. (1970). Quantitative recording of rotational behaviour in rats after 6- hydroxy-dopamine lesions of the nigrostriatal dopamine system. *Brain Research* **24**, 485-493.

URBAIN, N., GERVASONI, D., SOULIÈRE, F., LOBO, L., RENTÉRO, N., WINDELS, F., ASTIER, B., SAVASTA, M., FORT, P., RENAUD, B., LUPPI, P.H. & CHOUVET, G. (2000). Unrelated course of subthalamic nucleus and globus pallidus neuronal activities across vigilance states in the rat. *European Journal of Neuroscience* **12**, 3361-3374.

VILA, M., PÉRIER, C., FÉGER, J., YELNIK, J., FAUCHEUX, B., RUBERG, M., RAISMAN-VOZARI, R., AGID, Y. & HIRSCH, E.C. (2000). Evolution of changes in neuronal activity in the subthalamic nucleus of rats with unilateral lesion of the substantia nigra assessed by metabolic and electrophysiological measurements. *European Journal of Neuroscience* **12**, 337-344.

VIRGINIO, C. & CHERUBINI, E. (1995). Functional expression of voltage dependent sodium channels in *Xenopus* oocytes injected with mRNA from neonatal or adult rat brain. *Developmental Brain Research* **87**, 153-159.

VITEK, J.L. & BAKAY, R.A. (1997). The role of pallidotomy in Parkinson's disease and dystonia. *Current Opinion in Neurology* **10**, 332-339.

VOLGUSHEV, M., VIDYASAGAR, T.R., CHISTIAKOVA, M., YOUSEF, T. & EYSEL, U.T. (2000). Membrane properties and spike generation in rat visual cortical cells during reversible cooling. *Journal of Physiology* **522**, 59-76.

WANG, L.-Y., GAN, L., FORSYTHE, I.D. & KACZMAREK, L.K. (1998). Contribution of the Kv3.1 potassium channel to high-frequency firing in mouse auditory neurones. *J.Physiol* **509**, 195-209.

WEISER, M., BUENO, E., SEKIRNJAK, C., MARTONE, M.E., KER, H., HILLMAN, D., CHEN, S., THORNHILL, W., ELLISMAN, M. & RUDY, B. (1995). The potassium channel subunit Kv3.1b is localized to somatic and axonal membranes of specific populations of CNS neurons. *Journal of Neuroscience* **15**, 4298-4314.

WEISER, M., VEGA-SAENZ DE MIERA, E., KENTROS, C., MORENO, H., FRANZEN, L., HILLMAN, D., BAKER, H. & RUDY, B. (1994). Differential expression of *Shaw*-related K^+ channels in the rat central nervous system. *Journal of Neuroscience* **14**, 949-972.

WEST, M.J. & GUNDERSEN, H.J.G. (1990). Unbiased Stereological Estimation of the Number of Neurons in the Human Hippocampus. *Journal of Comparative Neurology* **296**, 1-22.

WEST, M.J., SLOMIANKA, L. & GUNDERSEN, H.J.G. (1991). Unbiased Stereological estimation of the total number of neurons in the subdivisions of the rat hippocampus using the optical fractionator. *Anatomical Record* **231**, 482-497.

WESTBY, G.W.M., MANA, S., CHEVALIER, G. & REDGRAVE, P. (2000). Electrophysiological activation of ventral midbrain dopamine cells by chemical stimulation of the superior colliculus in the rat. *European Journal of Neuroscience* **12**, 506-506.(Abstract)

WHIM, M.D. & KACZMAREK, L.K. (1998). Heterologous expression of the $K_v3.1$ potassium channel eliminates spike broadening and the induction of a depolarizing afterpotential in the peptidergic bag cell neurons. *Journal of Neuroscience* **18**, 9171-9180.

WHITTIER, J.R. & METTLER, F.A. (1949a). Studies on the Subthalamic Nucleus of the Rhesus Monkey. I. Anatomy and Fiber Connections of the Subthalamic Nucleus of Luys. *Journal of Comparative Neurology* **90**, 281-317.

WHITTIER, J.R. & METTLER, F.A. (1949b). Studies on the Subthalamic Nucleus of the Rhesus Monkey. II. Hyperkinesia and Other Physiologic Effects of Subthalamic Lesions, with Special Reference to the Subthalamic Nucleus of Luys. *Journal of Comparative Neurology* **90**, 319-372.

WICKENS, J.R., MCKENZIE, D., COSTANZO, E. & ARBUTHNOTT, G.W. (1998). Effects of potassium channel blockers on synaptic plasticity in the corticostriatal pathway. *Neuropharmacology* **37**, 523-533.

WIGMORE, M.A. & LACEY, M.G. (2000). Kv3-like persistent, outwardly rectifying, Cs^+-permeable, K^+ current in raf subthalamic nucleus neurones. *Journal of Physiology* **527**, 493-506.

WINDELS, F., BRUET, N., POUPARD, A. & SAVASTA, M. (2000a). High Frequency Stimulation of Subthalamic Nucleus Increases Extracellular Contents of Glutamate in Substantia Nigra and External Pallidum. *European Journal of Neuroscience* **12**, 214(Abstract)

WINDELS, F., BRUET, N., POUPARD, A., URBAIN, N., CHOUVET, G., FEUERSTEIN, C. & SAVASTA, M. (2000b). Effects of high frequency stimulation of subthalamic nucleus on extracellular glutamate and GABA in the substantia nigra and globus pallidus in the normal rat. *European Journal of Neuroscience* **12**, 4141-4146.

WOLF, H.K., BUSLEI, R., SCHMIDTKASTNER, R., SCHMIDTKASTNER, P.K., PIETSCH, T., WIESTLER, O.D. & BLUMCKE, I. (1996). NeuN - A useful neuronal marker for diagnostic histopathology. *Journal of Histochemistry & Cytochemistry* **44**, 1167-1171.

Appendix A – Recipes

Recipe 1 – Articifial Cerebrospinal Fluid (aCSF1)

	mM	MW	g/2000 ml
KCl	3.3	74.56	0.50
$MgSO_4$	2.4	246.47	1.18
$NaHCO_3$	25.7	84.01	4.32
KH_2PO_4	1.25	136.09	0.34
D-Glucose	11.0	180.16	3.96

Mix the above in 2000 ml of distilled H_2O, then split into proportions of 1750 ml and 250 ml.

aCSF1^N

Add the following to the 1750 ml portion of the above mixture:

Sucrose	248	342.3	21.33

aCSF1^S

With the 250 ml portion add the fluid to the following, ensuring a final volume of 250 ml:

NaCl	124	58.44	12.68
$CaCl_2.6H_2O$	3.5	219.08	1.34

Recipe 2 – Articifial Cerebrospinal Fluid (aCSF2)

Make up stock solutions to the following recipes.

10× Artificial CSF Component

	MM	MW	g/1000 ml
NaCl	126.0	58.4	73.63
KCl	2.5	74.6	1.86
$NaH_2PO_4.H_2O$	1.25	138.0	1.73
$CaCl_2.2H_2O$	2.0	219.08	4.38
$MgSO_4.7H_2O$	2.0	246.5	4.93
***D*-Glucose**	10.0	180.1	18.01

10× Bicarbonate Component

$NaHCO_3$	26.0	84.0	21.84

10× Sucrose Component

KCl	2.5	74.6	1.86
$NaH_2PO_4.H_2O$	1.25	138.0	1.73
$CaCl_2.2H_2O$	0.5	219.08	1.1
$MgSO_4.7H_2O$	10.0	246.5	24.65
***D*-Glucose**	10.0	180.01	18.01

Stock solutions can be stored in the fridge for up to a week before use. When needed they should be diluted and mixed as follows:

aCSF2^N

Take 200 ml of the 10× artificial CSF component, add 200 ml of distilled H_2O and mix well. Then add 200 ml of the 10× bicarbonate component and make up to 2000 ml with distilled H_2O.

aCSF2^S

Take 20 ml of the 10× sucrose component, add 20 ml of distilled H_2O and mix well. Then add 20 ml of the 10× bicarbonate component and make up to 200 ml with distilled H_2O. 15.74 g of sucrose should then be added to this and the solution mixed well.

Recipe 3 – Avertin

Stock Solution

Dissolve 100 g of 2-2-2-tribromoethanol (Sigma-Aldrich Company Ltd., Poole, UK) in 62.5 ml of amyl alcohol (Sigma).

Freeze in 1 ml aliquots for use when needed.

Avertin Solution

Dissolve one aliquot of stock solution in 5 ml of ethanol and mix well. Then add 45 ml of sterile saline (0.9% NaCl). Store in the fridge and inject at 1 ml/100 g.

Appendix B – Published Abstracts

1998 Forum of European Neuroscience, Berlin

Abstract Number 118.05

European Journal of Neuroscience 10(S10): 300

The Relationship Between Voltage-Gated Sodium Channel Inactivation and Firing Frequency in the Subthalamic Nucleus Projection Neuron.

J.F. Atherton, A.J. Gillies, A.M. Corbett & G.W. Arbuthnott

A single cell computer model of the subthalamic nucleus (STN) projection neuron was constructed. During this process it was discovered that the currently known kinetics of voltage-gated sodium channels (NaCh) are insufficient to account for the high firing rates of these neurons (500Hz). The inactivation properties of STN neuronal NaChs were investigated using intracellular recordings from STN neurons in parasagittal rat brain slices at 37°C. NaCh inactivation in these cells was found to be very slow; reaching 50% recovery at 30ms. This result mimics the effect of administration of inhibitors of NaCh inactivation on NaChs in other preparations. No correlation was found between NaCh inactivation and firing frequency.
These results suggested that the high firing rates seen in STN projection neurons might be achieved by modifications of their NaCh subunit composition such that the inactivation curve is slowed. One such modification could be the lack of NaCh $ß_1$ subunits, but when rat brains were stained with antibodies for both $ß_1$ and $ß_2$ subunits both were found to be present in STN neurons at levels comparable with other brain areas.

1999 The Physiological Society, Glasgow Meeting

The Journal of Physiology 521(P): 48P

Depolarisation Changes Neuronal Activity Patterns in the Isolated Rat Subthalamic Nucleus Through Glutamatergic Interconnections

J.F. Atherton, A.J. Gillies, and G.W. Arbuthnott

The subthalamic nucleus (STN) is now the focus of much of the clinical research aimed towards the alleviation of Parkinson's Disease. However, little is known about how the

neurones within the STN process information. Up to 50% of the axons of STN neurones produce intranuclear axon collaterals (Kita *et al.* 1983). A network model of the STN (Gillies & Willshaw, 1998) showed that, even if these collaterals only made a small number of active connections, the effect on the behaviour of the nucleus as a whole could be massive. The model highlighted the need to investigate the nature of these interconnections. Although the interactions between the firing of neurones at rest should be small, the model suggested that some degree of interaction between unit responses should occur at higher levels of activity. To test this, extracellular recordings were made from single STN neurones *in vitro*. Male Sprague-Dawley rats (200-400g) were anaesthetised with Avertin (1 ml $(100g)^{-1}$ I.P.) and decapitated. The brain was rapidly dissected and placed in ice-cold artificial cerebrospinal fluid (ACSF) in which the NaCl had been replaced by 230 mM sucrose. Single unit extracellular recordings were made from 400 μm sagittal slices bathed in ACSF at 35°C using glass microelectrodes (50-70 MΩ) filled with 1 M NaCl.

The inter-spike interval (ISI) of STN neurones under control conditions was 81.98 ± 75.23 ms (mean ± S.D.). Coefficient of variation (CV) of the ISI was 0.20 + 0.21. Depolarisation with potassium gluconate caused a decrease in ISI to 63.36 ± 23.56% of control levels (Student's *t* test; $P < 0.01$, n = 14), and an increase in CV to 199.85 ± 113.41 % ($P < 0.05$, n = 8). 6-Cyano-7-nitroquinoxaline-2,3-dione (CNQX; 10 μM) had no effect on ISI in either of the experimental conditions but, when added in the presence of potassium gluconate, it reduced the increase in CV that was seen in its absence (159.51 ± 108.22% of control levels; n.s., n = 6).

The regular firing of STN neurones at rest may be the result of intrinsic membrane properties but with increased activity the neuronal firing pattern is influenced by incoming glutamatergic activity, perhaps from neighbouring neurones.

Gillies, A.J. & Willshaw, D.J. (1998). *Proc. R. Soc.* B **265**, 2101-2109.
Kita, H., Chang, H.T. & Kitai, S.T. (1983). *J. Comp. Neurol.* **215**, 245-257.

2000 Forum of European Neuroscience, Brighton

Abstract Number 62.20

European Journal of Neuroscience 12(S11): 136

Evidence for the Presence of Glutamatergic Interconnections Between Neurones in the Rat Subthalamic Nucleus.

J.F. Atherton, A.J. Gillies & G.W. Arbuthnott

The Subthalamic Nucleus (STN) has emerged as an important target for novel therapeutic strategies towards the alleviation of Parkinson's disease. A valuable route to

increasing our understanding of the role of the STN in the diseased state is to try to elucidate what, if any, information processing occurs in the normal STN. Up to 50% of STN neurones posses intranuclear axon collaterals (1). Computer modelling has revealed that, even if these collaterals contacted only a small number of cells, the behaviour of the nucleus could be massively affected (2). We have investigated whether STN neurones are indeed functionally interconnected. Extracellular recordings were obtained using slices of rat brain that contained the STN physically isolated from all its known external inputs. The firing pattern of STN neurones was measured both under control conditions and after the cells had been depolarised by changing the perfusion medium to one containing 10mM potassium gluconate. Depolarisation led to a decrease in interspike interval (ISI) to 63.36 ± 23.56% of control levels and an increase in coefficient of variation (CV) to 199.85 ± 113.41% of control levels. Under control conditions the presence of the glutamatergic antagonist 6-cyano-7-nitroquinoxaline-2,3-dione (10μM) had little effect on either ISI or CV. However, the increase in CV seen when the cells were depolarised was attenuated. As the neurones of the STN had been isolated from their known external inputs, this attenuation must be mediated through a glutamatergic mechanism that is intrinsic to the nucleus. The main candidate for such a mechanism is the intranuclear axon collateral system.

(1) Kita *et al.* (1983) J. Comp. Neurol. 215: 245-257
(2) Gillies & Willshaw (1998) Proc. R. Soc. B. 265: 2101-2109

Abstract Number 226.03

European Journal of Neuroscience 12(S11): 507

The Nature of Glutamatergic Interactions Between Neurons in the Subthalamic Nucleus

A. Gillies, J. Atherton, G. Arbuthnott, D. Willshaw

Computer modelling studies and mathematical analysis suggest that functional intranuclear axon collaterals within the subthalamic nucleus (STN) play an important role in basal ganglia function and dysfunction [1,2]. However, there is only limited anatomical evidence for the existence of such collaterals in the rat [3]. A recent *in vitro* electrophysiological experiment in rat provides evidence for functional interactions between STN neurons [4]. In tandem, we have constructed a detailed computer model of this experiment to both replicate the findings and examine the type of interconnectivity within the STN. A multi-compartmental model of single rat STN projection neurons including 6 channel types (sodium, potassium, calcium high and low voltage activated, sodium leak, and glutamatergic synaptic) is demonstrated to replicate single cell physiology. The behaviour of a network of these model neurons interconnected with glutamatergic synapses replicates the experimental results. This provides further evidence for the existence of functional intranuclear axon collaterals. Furthermore, examination of this model allows us to investigate the nature of the connectivity between

STN neurons providing insights into synaptic distribution and level of connectivity. It is predicted that synapses from other STN neurons are likely to be found over the soma and proximal areas of the dendritic tree.

[1] Gillies & Willshaw, (1998). Eur. J. Neurosci, 10: 301
[2] Gillies & Willshaw, (1998). Proc. R. Soc. Lond. B, 265: 2101-2109
[3] Kita *et al,* (1983). J. Comp. Neurol. 215: 245-257
[4] Atherton *et al,* (2000). FENS 2000 abst.

2000 Society for Neuroscience, New Orleans

Abstract Number 456.1

Society for Neuroscience Abstracts 26(1): 1223

Lesions of the Globus Pallidus Which Increase Subthalamic Nucleus Activity Cause Dopamine Cell Death

J.F. Atherton, K.E. McLaughlin, A.K. Wright, L. Norrie, G.W. Arbuthnott

Parkinson's Disease is a neurodegenerative disorder caused by the loss of dopaminergic (DA) neurones within the substantia nigra (SN). Studies, both in human patients and in animal models of the disease, have shown that the mean firing rate of neurones in the subthalamic nucleus (STN) is increased in the diseased state. As STN neurones send excitatory, glutamatergic projections to the SN, it is possible that this overactivity may result in excitotoxicity, leading to further DA cell loss. It has been shown that lesions of the STN can be neuroprotective against DA cell loss caused by injections of 6-hydroxydopamine into the rat striatum. However, it has not been shown that STN overactivity can cause such cell death. To address this question ibotenic acid lesions were made in the rat globus pallidus (GP), a treatment that has been shown to increase the firing rate of STN neurones. The animals were left for 3 weeks before being transcardially perfused, their brains removed and 50-micron sections cut on a freezing microtome. Sections were stained for OX-42, glial fibrillary acid protein (GFAP), and tyrosine hydroxylase (TH). OX-42 and GFAP staining showed a significant increase in microglial activity and astrocytic activation in the SN ipsilateral to the lesion, whilst unbiased stereological counting of DA neurones stained with TH showed a 23.7% loss. This data shows an ongoing loss of DA cells in the SN 3 weeks after a GP lesion which we believe will prove to be due to excitotoxicity related to increased firing of STN neurones.